

# **TUMOR TARGETING WITH B<sub>12</sub> SCAFFOLD**

## **A COORDINATION CHEMISTRY APPROACH**

---

**Dissertation**

zur

**Erlangung der naturwissenschaftlichen Doktorwürde**

**(Dr. sc. nat.)**

vorgelegt der

**Mathematisch-naturwissenschaftlichen Fakultät**

der

**Universität Zürich**

von

**TRAN THANH QUYNH MAI**

aus

**Vietnam**

**Promotionskomitee**

Prof. Dr. Roger Alberto (Vorsitz)

Prof. Dr. Roland K. O. Sigel

Zürich 2013

“The real voyage of discovery consists not in seeking new lands  
but in seeing with new eyes.”

Marcel Proust

... for my mother and my family ...

## **Acknowledgements**

I would like to express my gratitude to Prof. Dr. Roger Alberto for his supervision, constructive critiques, and detailed correction of my work. In addition, I truly appreciate the financial funding he maintained for the project.

I am thankful to Prof. Dr. Roland K. O. Sigel for the great support he offered, especially via CMSZH.

I would like to thank Dr. Pilar Ruiz Sánchez for her willingness to share experience of vitamin B<sub>12</sub> research.

It gives me a great pleasure in acknowledging Prof. Dr. Stefan Stürup, Prof. Dr. Ian Henry Lambert, and Dorthe Nielsen from Copenhagen University. Their kind welcome and full support made my stay productive and convenient.

I am truly grateful to Christiane König and Dr. Stefano Ferrari from the IMCR for their generous introduction of cell culture techniques.

Assistance provided by Dr. Robert Waibel, Dr. Evelyne Furger, and Susan Cohrs from the PSI was highly appreciated.

I wish to thank Dr. Thomas Fox, Dr. Fabio Zobi, Dr. Bernhard Spingler, Dr. Ferdinand Wild, Dr. Miguel Guttentag, Thomas Zehnder, and Nathalie Fichter for their availabilities and support.

I would like to extend my gratitude to colleagues at the ACI, especially to René Oetterli, Dr. Kai Zhou, Dr. Christine Männel-Croisé, Dr. Susmita Gupta, Majorie Sonnay, Lucas Prieto, Anna Leonidova, and Crisina Mari for the friendship and memories we have shared.

I wish to share the credit of my work with the kindest friends I have had during my stay in Switzerland: Andreas and his family, Esther, Van, Richard, Sara, Melanie, Thanh, Nhung, and Dung.

I am indebted to my beloved family and my friends in Vietnam and Sweden, who have been far but never away from my life for the last four years.

---

## Abstract

Based on vitamin B<sub>12</sub> demand for proliferation, several prodrugs were built on B<sub>12</sub> scaffold. These include the rising metallodrugs (mainly Pt and Ru-based) and the more traditional organic chemotherapeutic drugs. Coordination chemistry is the focus of the project. Drugs or fluorophores were conjugated to the B<sub>12</sub> scaffold either directly via CN<sup>-</sup>-bridge or indirectly via a [*trans*-Pt(NH<sub>3</sub>)<sub>2</sub>-CN]<sup>+</sup> bridge.<sup>1</sup> This strategy allowed B<sub>12</sub> to carry reasonably-sized molecules. The stability, reductive release and activity of these complexes were demonstrated. They remained high affinities with all cobalamin transport proteins. Their cellular accumulation was measured by attaching radioactive centers to their structures. Alternatively, the correlation of existing transition metals also reflected the cellular distribution of these complexes. It was found that charged complexes were preferably internalized into cells in a transcobalamin-independent pathway, which should be considered in future design of B<sub>12</sub>-prodrugs.

---

## **Zusammenfassung**

Vitamin B<sub>12</sub> ist essentiell für den Vorgang der Zellteilung. Das Ziel dieser Arbeit ist die Synthese von B<sub>12</sub> Derivativen, die die Zellteilung stark proliferierender Zellen, wie zum Beispiel Krebszellen, unterbinden oder verlangsamen. Diese Derivative beinhalten metallhaltige Pharmaka (hauptsächlich Pt- und Ru- basiert) sowie klassische organische Chemotherapeutika. Ein Schwerpunkt dieser Arbeit lag dabei auf der Entwicklung und Untersuchung der Koordinationschemie dieser B<sub>12</sub> Derivative. Pharmaka oder Fluorophore wurden direkt (CN<sup>-</sup>-Brücke) oder indirekt [*trans*-Pt(NH<sub>3</sub>)<sub>2</sub>-CN]<sup>+</sup> an das B<sub>12</sub> Gerüst koordiniert. Diese Strategie erlaubte es dem B<sub>12</sub> Derivat das entsprechende Molekül zu transportieren. Des Weiteren konnte gezeigt werden, dass die Koordinierten Pharmaka oder Fluorophore reaktiv freigesetzt werden können und dabei ihre biologische Aktivität nicht verlieren. Trotz der strukturellen Modifikationen behalten die synthetisierten B<sub>12</sub> Derivative ihre starken Affinitäten zu den Cobalamin-Transportproteinen. Das biologische Verhalten wurde durch eingefügte radioaktive Marker verfolgt, dabei wurde nachgewiesen, dass geladene Konjugate über einen Transcobalamin-unabhängigen Weg in die Zellen eingeschleust werden.

---

## Abbreviation list

ACN	acetonitrile
apo	(apo-protein) a protein whose cofactor is absent
Asp	aspartic acid
ATP	adenosyltriphosphate
bipy	2,2'-bipyridine
Boc	tert-butyloxycarbonyl
°C	degree Celsius
C <sub>18</sub>	an octadecyl type of hydrocarbon
ca.	circa (approximately)
CDI	1,1'-carbonyldiimidazole
cDNA	complementary DNA
CDT	1,1'-carbonyldi(1,2,4-triazole)
Ci	curie
COD	cyclooctadiene
Cp	cyclopentadiene
Cy	cyanide dye
CYP450	cytochrome P450
d	doublet
Da	Dalton
DEE	diethyl ether
DMF	N,N'-dimethyl formamide
DMSO	dimethyl sulfoxide
DNA	deoxyribonucleotide acid
D <sub>2</sub> O	deuterated water
DSF	Differential Scanning Fluorimetry
DTPA	diethylene triamine pentaacetic acid
EDTA	ethylenediaminetetraacetic acid
en	ethylenediamine
ESI	electron spray ionization
et al.	et alii (and others)
EtOAc	ethyl acetate

---

EtOH	ethanol
FCS	fetal calf serum
g	gravitational force unit
h	hour
HEPES	4-(2-hydroxyethyl)-1-piperazineethanesulfonic acid
His	histidine
holo	conjugate of apo-protein and its cofactor
HPLC	high performance liquid chromatography
HSA	human serum albumin
Hz	hertz
IC <sub>50</sub>	half maximal inhibitory concentration
ICP	inductively coupled plasma
IR	infrared (spectroscopy)
J	coupling constant (Hz)
LC <sub>50</sub>	lethal concentration, 50%
K	degree Kelvin
Lys	lysine
m	multiplet
MeOD	deuterated methanol
MeOH	methanol
MS	mass spectroscopy
m/z	mass to charge ratio
NBD-CO-Hz	4-(N-Hydrazinocarbonylmethyl-N-methylamino)-7-nitro-2,1,3-benzoxadiazole
NCBI	national center for biotechnology information
NMR	nuclear magnetic resonance (spectroscopy)
PAMA	picolylamine monoacetic acid
PBS	phosphate buffered saline
PCR	polymerase chain reaction
phen	phenanthroline
ppm	parts per million
R <sub>f</sub>	retardation factor

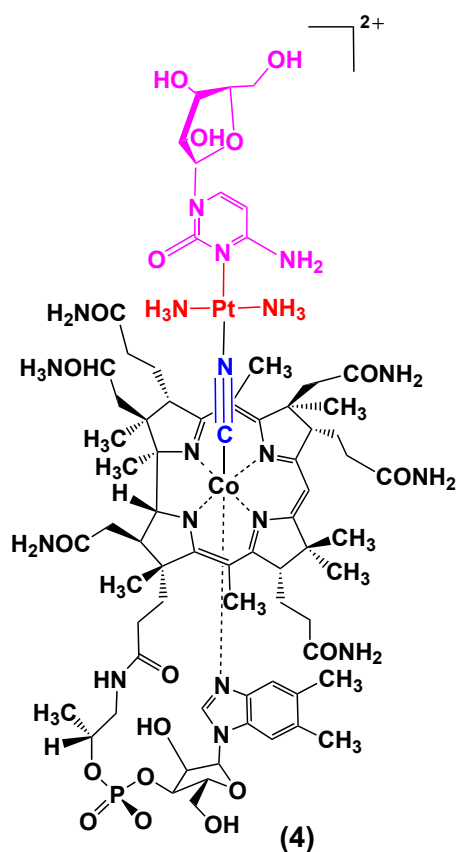
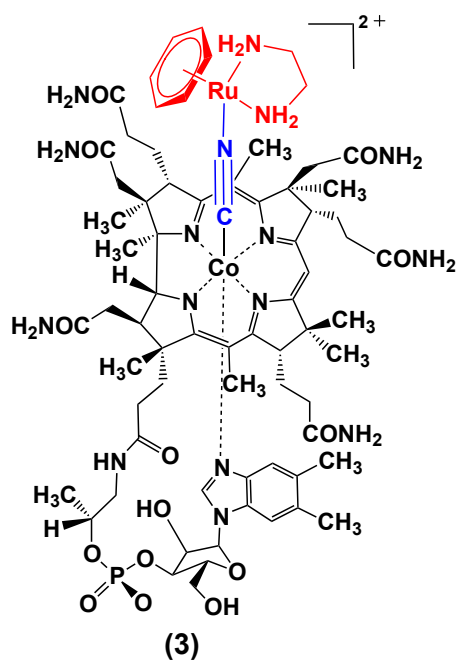
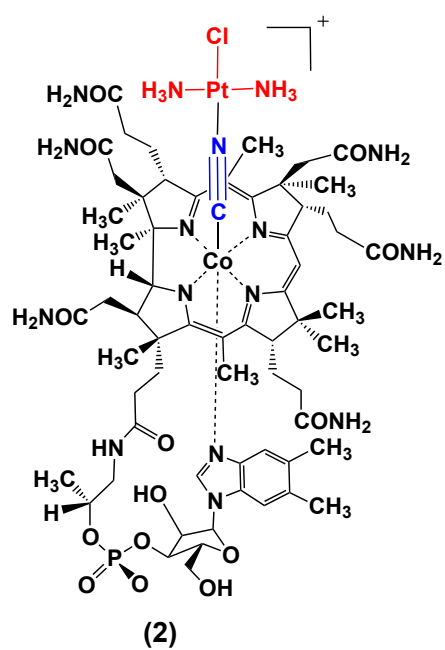
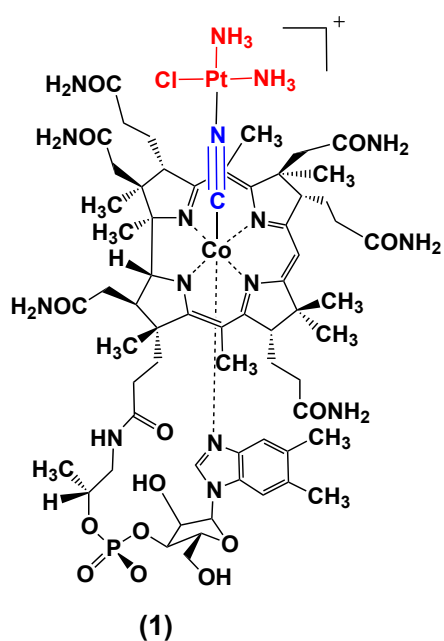
---

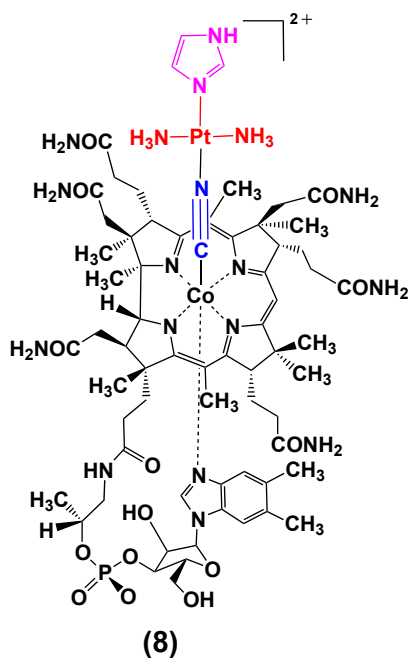
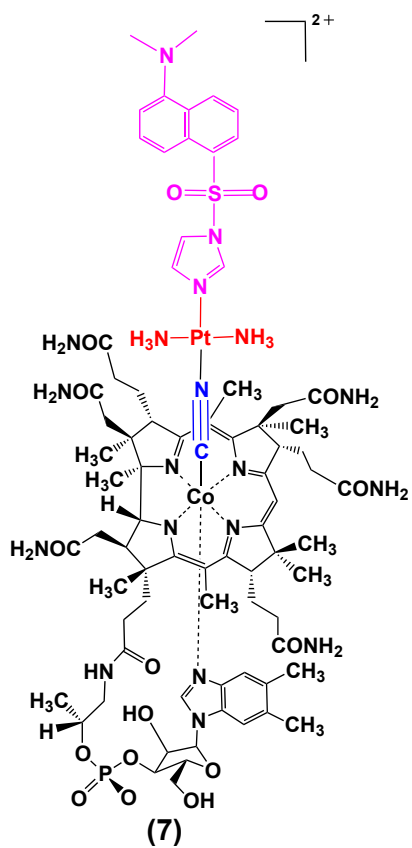
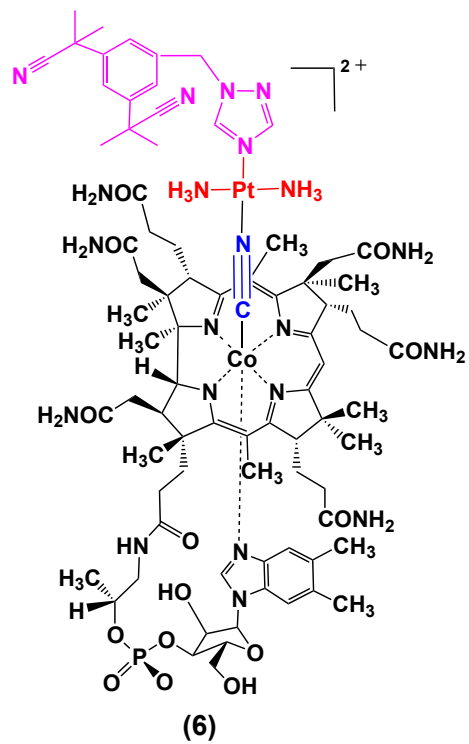
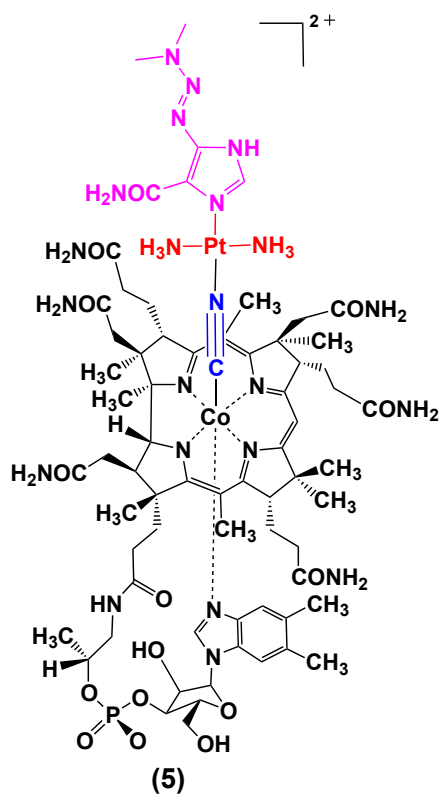


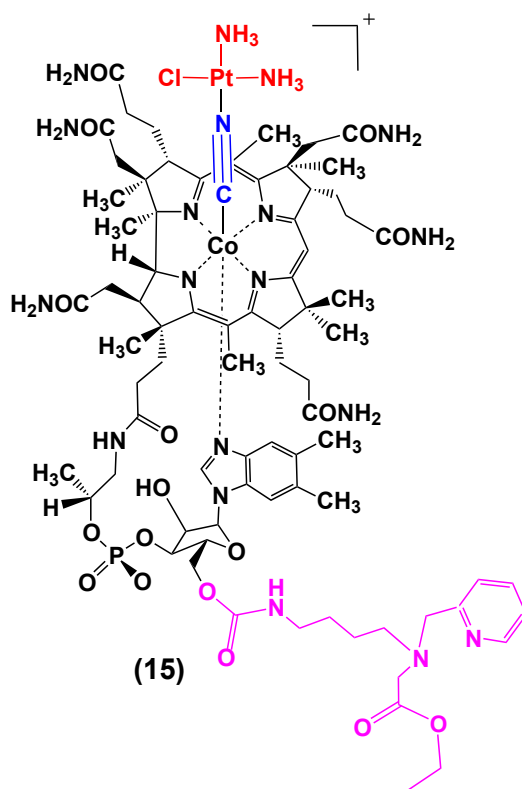
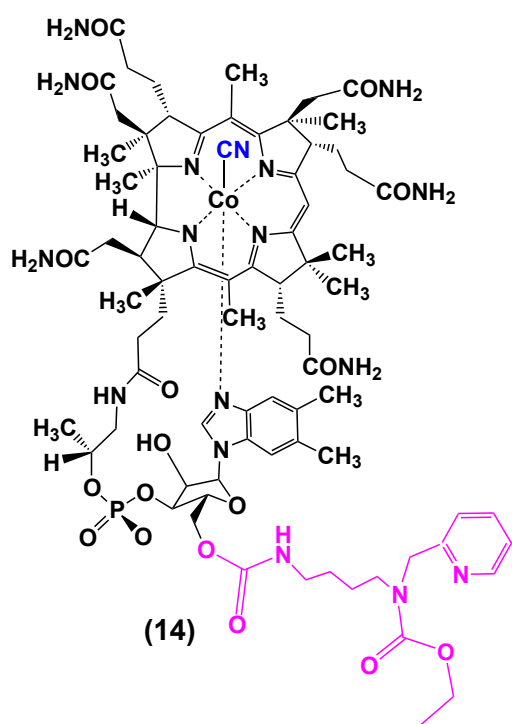
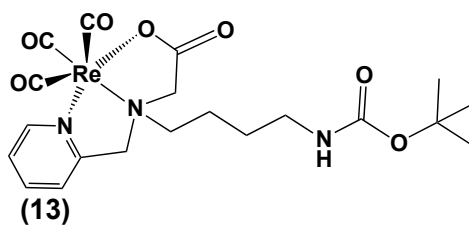
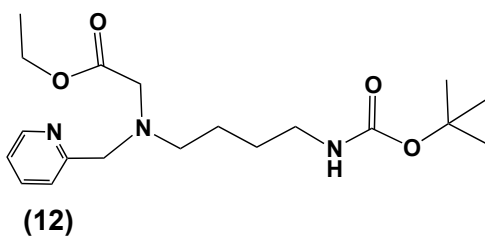
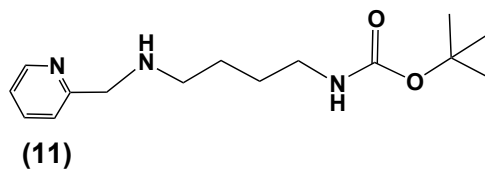
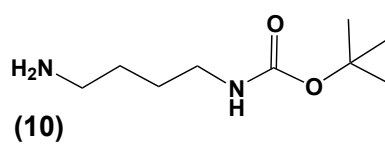
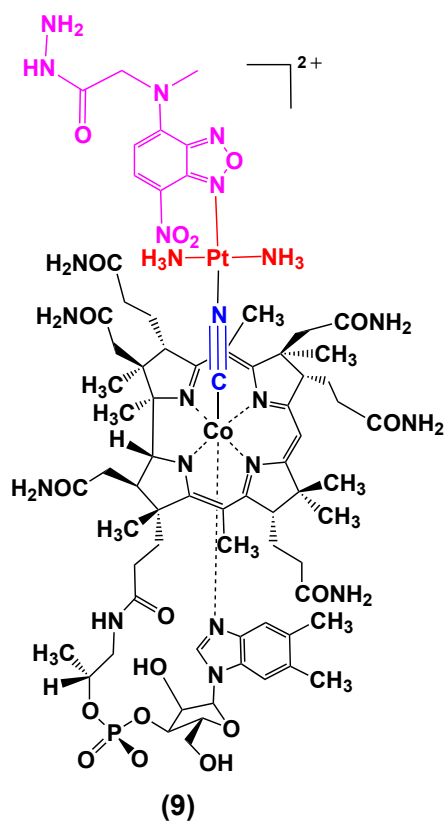
ROS	reactive oxygen species
RP	reverse phase
RPMI	Roswell Park Memorial Institute medium
r.t.	room temperature
s	singlet
SEC	size-exclusion chromatography
Ser	Serine
S <sub>N</sub> 2	bimolecular nucleophilic substitution
T	Temperature
TBTU	o-(benzotriazol-1-yl)-N,N,N',N'-tetramethyluronium
TEA	triethylamine
TEAP	Triethyammonium phosphate
terpy	terpyridine
TFA	trifluoroacetic acid
THA	tetrahydroanthracene
TrxR	thioredoxin reductase
U/ml	units/milliliter
vs.	versus

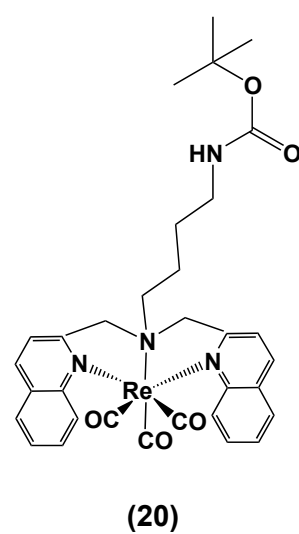
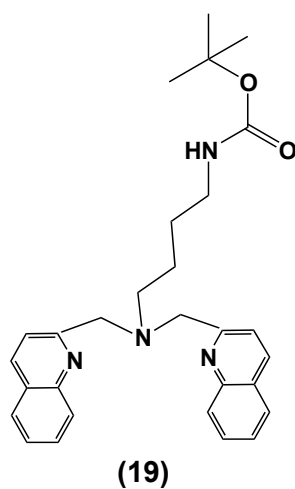
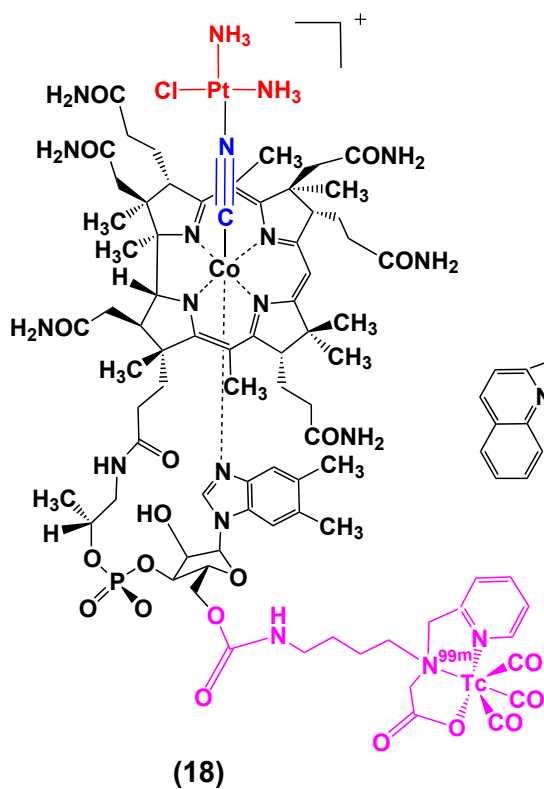
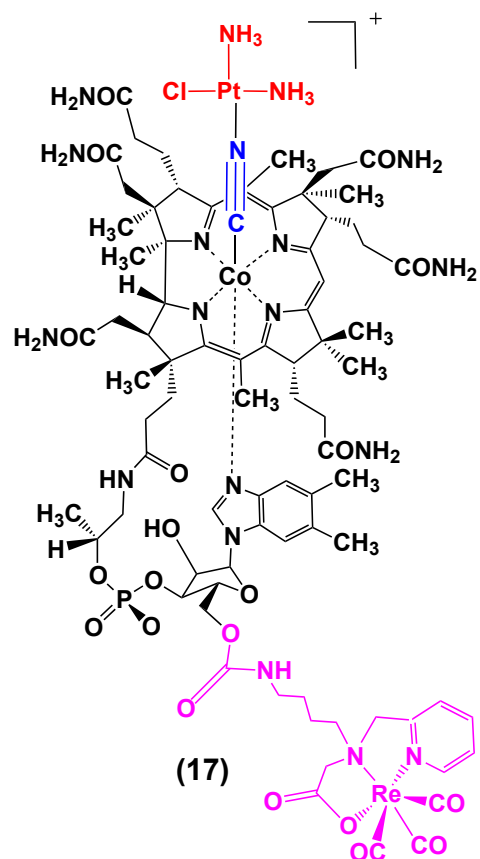
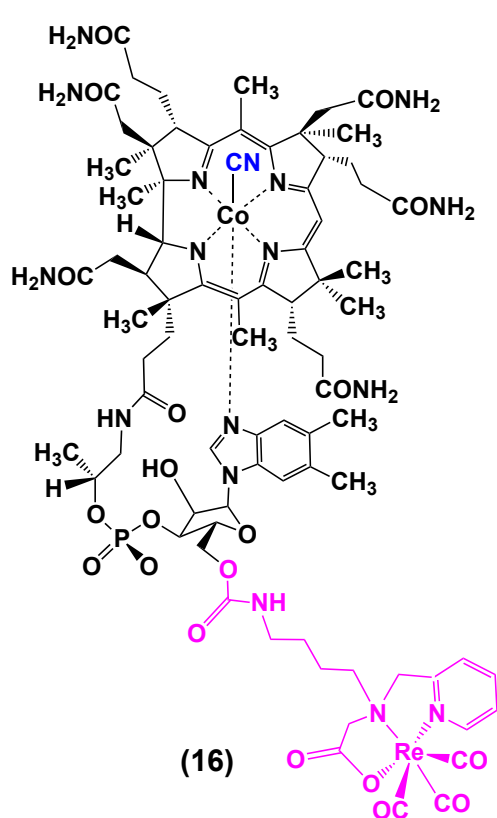
---

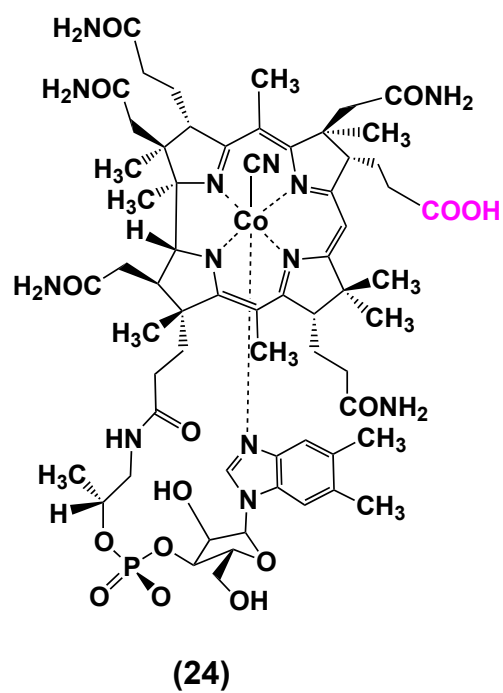
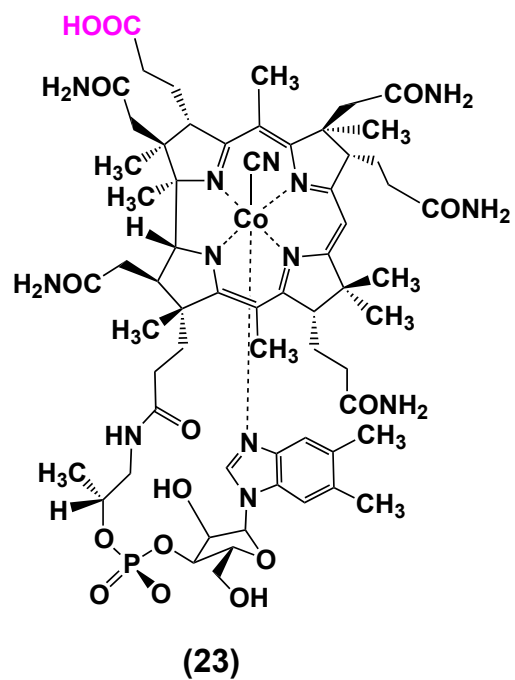
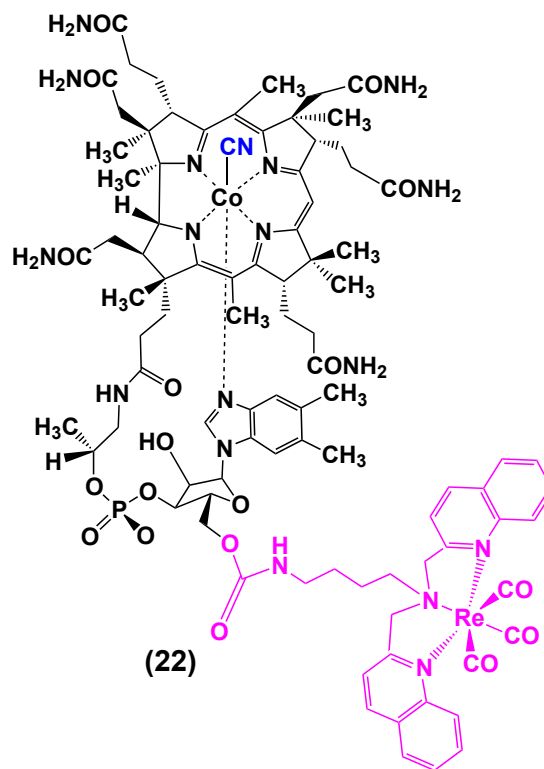
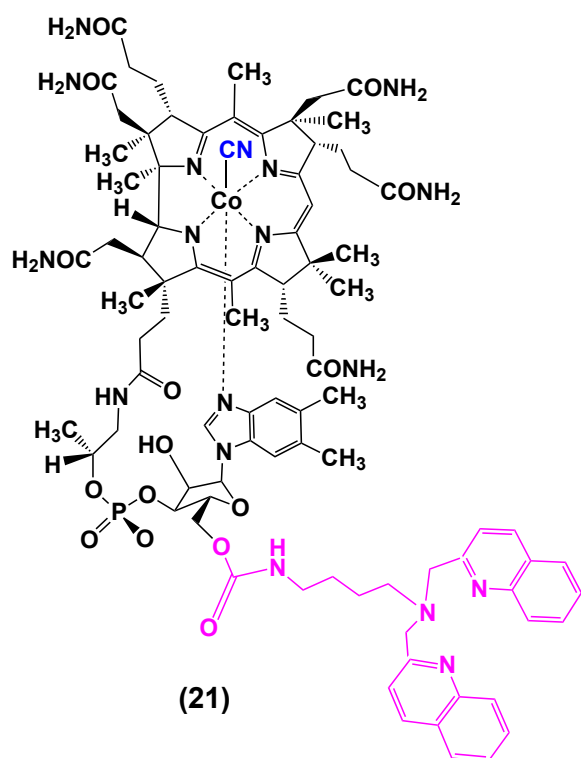
## Overview of structures

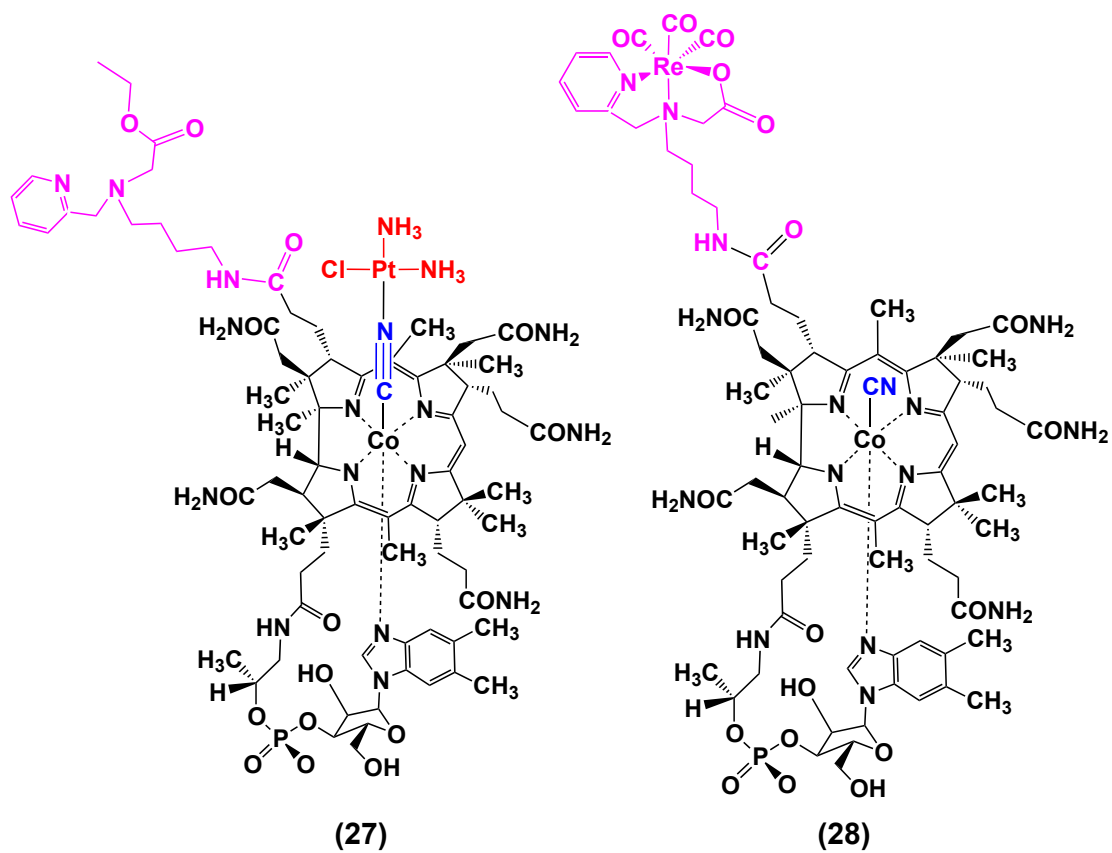
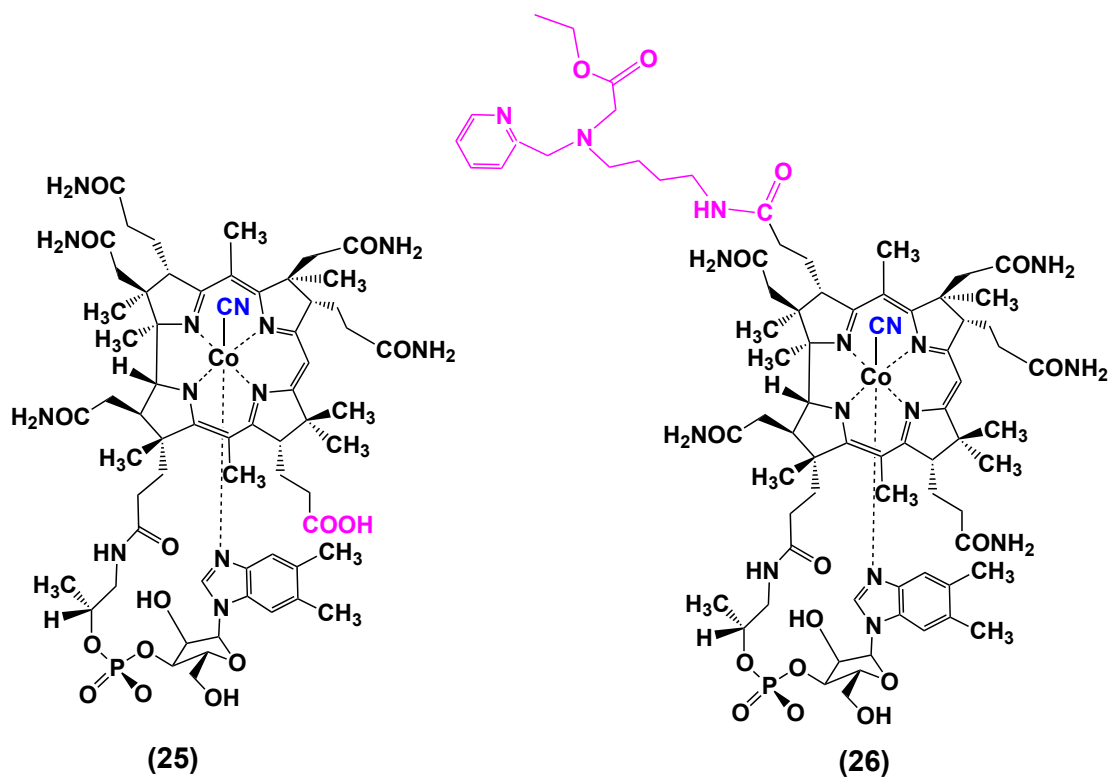


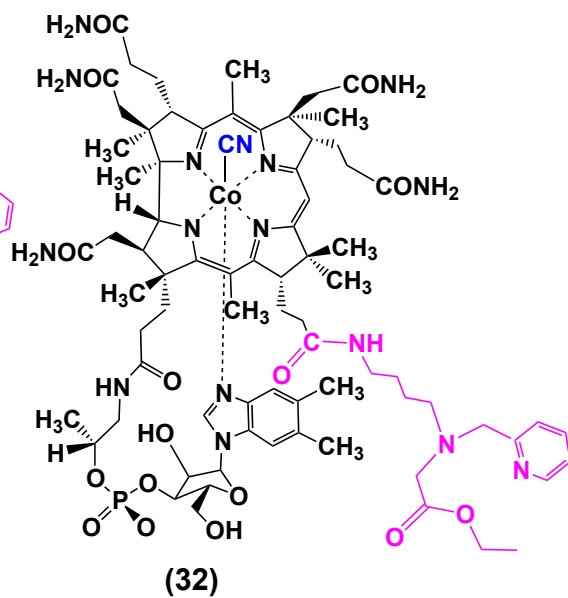
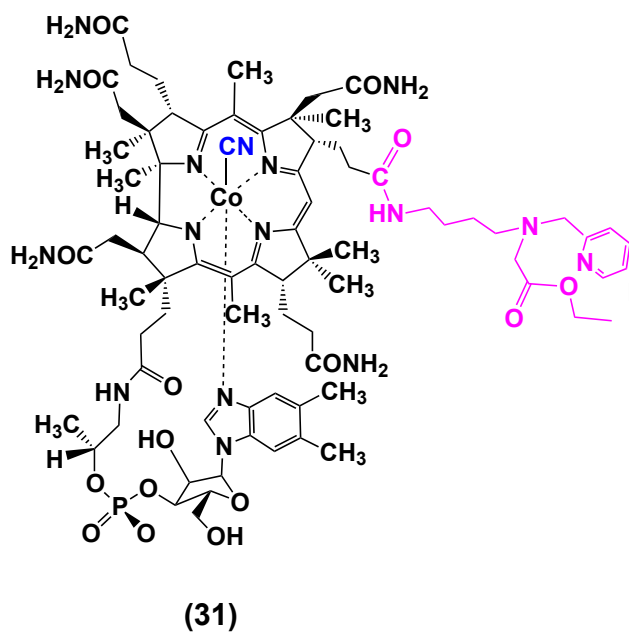
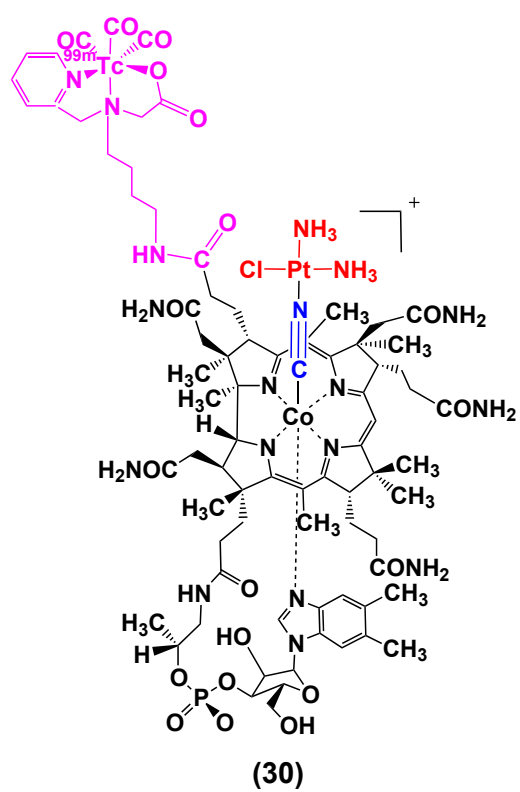
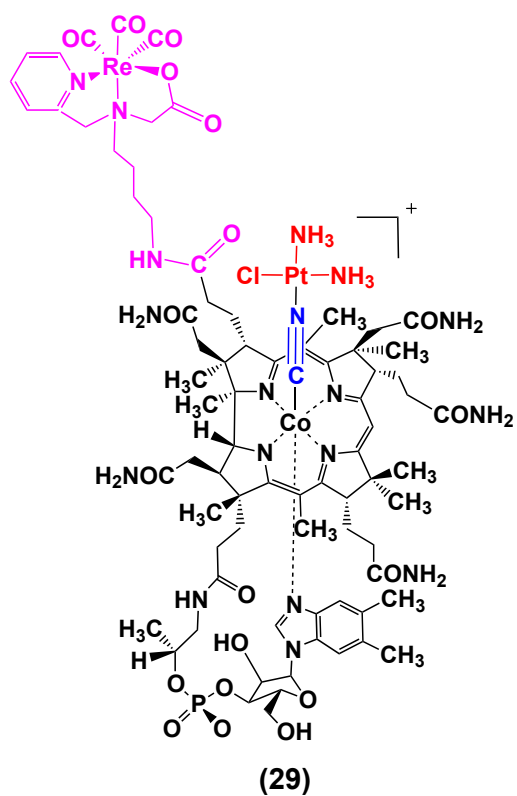




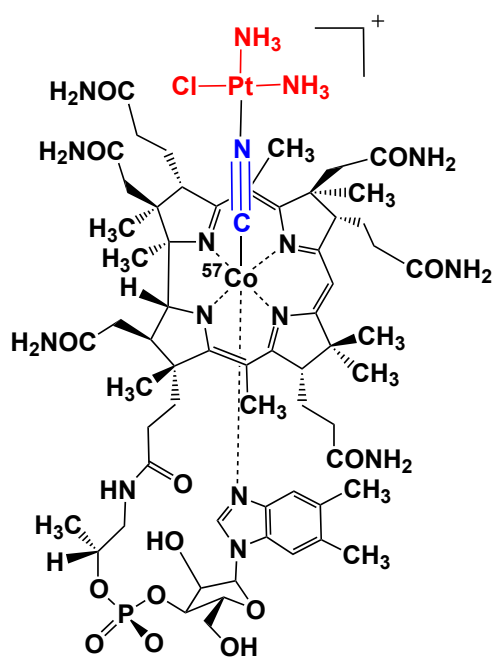












(33)

---

---

## Table of content

I	INTRODUCTION .....	1
I.1	A “Noble” history .....	1
I.2	B <sub>12</sub> coenzymes .....	3
I.3	Transport and metabolism of cobalamin.....	7
I.4	Structure of cobalamin .....	10
I.5	Cobalamin conjugates .....	12
I.6	Metal anticancer drugs .....	14
I.6.1	Gold anticancer drugs .....	14
I.6.2	Ruthenium anticancer drugs .....	15
I.7	Organic anticancer drugs .....	16
I.8	Imaging agents .....	18
II	OBJECTIVES .....	19
III	RESULTS AND DISCUSSION .....	20
III.1	{Metallodrug}-{B <sub>12</sub> } conjugates .....	20
III.1.1	{[Ru]-drug}-{B <sub>12</sub> } conjugate.....	21
III.1.2	{[Au]-drug}-{B <sub>12</sub> } conjugate .....	24
III.2	{Organic-drug}-{B <sub>12</sub> } double prodrugs.....	25
III.2.1	Synthesis of B <sub>12</sub> double prodrugs .....	25
III.2.2	Stability of B <sub>12</sub> double prodrugs .....	27
III.2.3	Affinity of B <sub>12</sub> double prodrugs to B <sub>12</sub> transport proteins .....	28
III.2.4	Reductive release of drugs from B <sub>12</sub> double prodrugs.....	30
III.2.5	In vitro cytotoxicity of B <sub>12</sub> double prodrug .....	32
III.3	{Imaging agent}-{B <sub>12</sub> } conjugates .....	33
III.3.1	Fluorescent B <sub>12</sub> derivatives .....	33
III.3.2	[ <sup>99m</sup> Tc]-labeled-B <sub>12</sub> prodrugs .....	36

---

---

III.3.2.1	Synthesis of B <sub>12</sub> prodrugs .....	36
III.3.2.2	Affinity of B <sub>12</sub> prodrugs to transcobalamin .....	38
III.3.2.3	Cell uptake of B <sub>12</sub> prodrugs .....	39
III.3.3	[ <sup>57</sup> Co]-labeled B <sub>12</sub> prodrug.....	44
IV	CONCLUSIONS.....	45
V	OUTLOOK .....	47
VI	BIBLIOGRAPHY .....	49
VII	EXPERIMENTAL SECTION .....	54
VII.1	Materials and methods .....	54
VII.2	Synthesis .....	55
VII.3	Reductive release of drug from double prodrug .....	66
VII.4	Biological study .....	67
VII.4.1	Binding of double prodrug <b>4</b> to human serum albumin .....	67
VII.4.2	Affinity of double prodrug <b>4</b> to Cbl transport proteins.....	67
VII.4.3	Cell viability assay .....	69
VII.4.4	Uptake measurement with [ <sup>99m</sup> Tc]-radiolabeling .....	70
VII.4.5	Uptake measurement with ICPMS.....	70
VIII	APPENDICES .....	71
IX	CURRICULUM VITAE.....	78

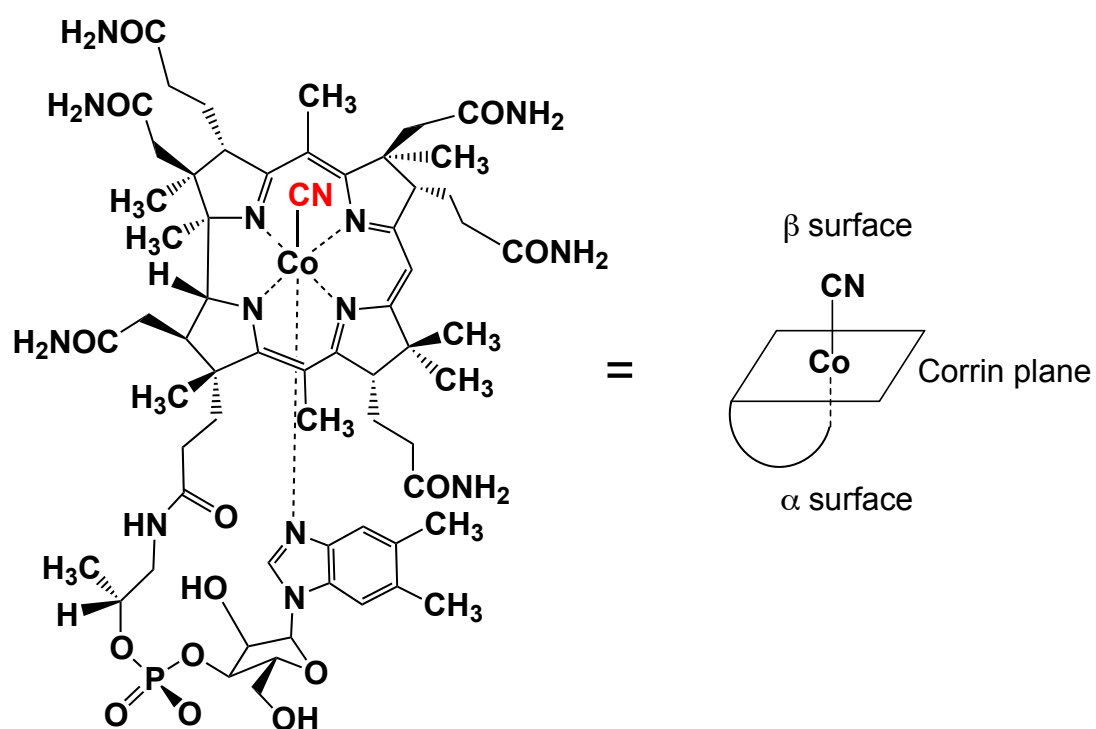
---

## I Introduction

### I.1 A “Noble” history

The 19<sup>th</sup> and 20<sup>th</sup> century witnessed remarkable achievements in vitamin-related research. More than 10 Nobel prizes were conferred to the discoveries, isolation, synthesis and structural elucidation of vitamins A, B<sub>1</sub>, B<sub>2</sub>, B<sub>6</sub>, B<sub>12</sub>, C, D, E, and K. The concept of “vitamins”, which means “vital amines”, was established only in 1911.<sup>2</sup> It turned out that not all vitamins contain “amines”. In fact, different from other organic nutrients (proteins, fats, starch, and sugar), all vitamins share no common structural unit. The most complex structure of all vitamins belongs to vitamin B<sub>12</sub>. “The renaissance in the field of B<sub>12</sub> research”, as described by Banerjee,<sup>3</sup> was highlighted with 3 Nobel prizes in a 30-year period (1934-1965). The discovery of B<sub>12</sub> (Scheme 1) was acknowledged with a shared Nobel Prize for Whipple, Minot, and Murphy in 1934. The studies with anaemic dog led Whipple to propose liver as a rich source of a haematopoietic material, which can cure pernicious anaemia. Minot and Murphy subsequently translated the success to human anaemia.<sup>4</sup> Concurrently, the isolation of pure “anti-pernicious anaemia factor” from liver was reported in 1948.<sup>5,6</sup> Its structure was resolved by Dorothy Hodgkin.<sup>7,8</sup> This success brought her a Nobel Prize in 1964. In 1965, a Nobel Prize was awarded to Woodward, who subsequently achieved the chemical synthesis of B<sub>12</sub> together with Eschenmoser in an effort involving more than a hundred scientists throughout 11 years.<sup>9</sup> Scientists desire hitherto to understand every chemical property and biochemical process of B<sub>12</sub>.<sup>3, 10, 11</sup> Remarkable efforts were made to discover and elucidate structures of every B<sub>12</sub>-related biomolecule. The gastric juice experiment allowed Castle to conclude that interaction between B<sub>12</sub> (extrinsic factor) and a gastric juice factor (intrinsic factor) was required to reverse haematopoiesis.<sup>12</sup> Following this discovery of intrinsic factor (IF), B<sub>12</sub> complex transport pathway was gradually revealed.<sup>11, 13</sup> The B<sub>12</sub> “Noble” history is advancing to “a new medicinal era of vitamin B<sub>12</sub>”, as Randaccio proposed.<sup>14</sup>

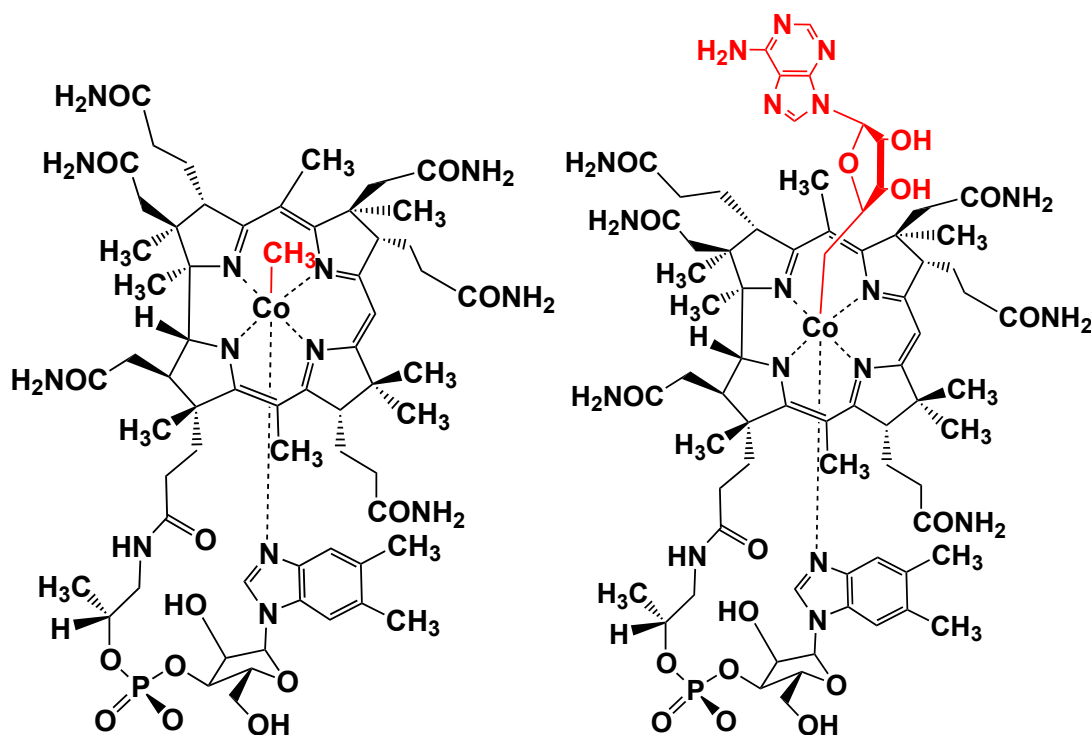
---



**Scheme 1:** Structure of B<sub>12</sub>.

## I.2 B<sub>12</sub> coenzymes

The coenzyme forms of B<sub>12</sub> are methylcobalamin (Me-Cbl) and adenosylcobalamin (Ado-Cbl) (Scheme 2). A list of enzymes requiring the assistance of these two coenzymes can be found in (Table 1). There are actually only two B<sub>12</sub>-dependent enzymes in mammals, methionine synthase (MetH) and methylmalonyl Co-A mutase (MMCM).



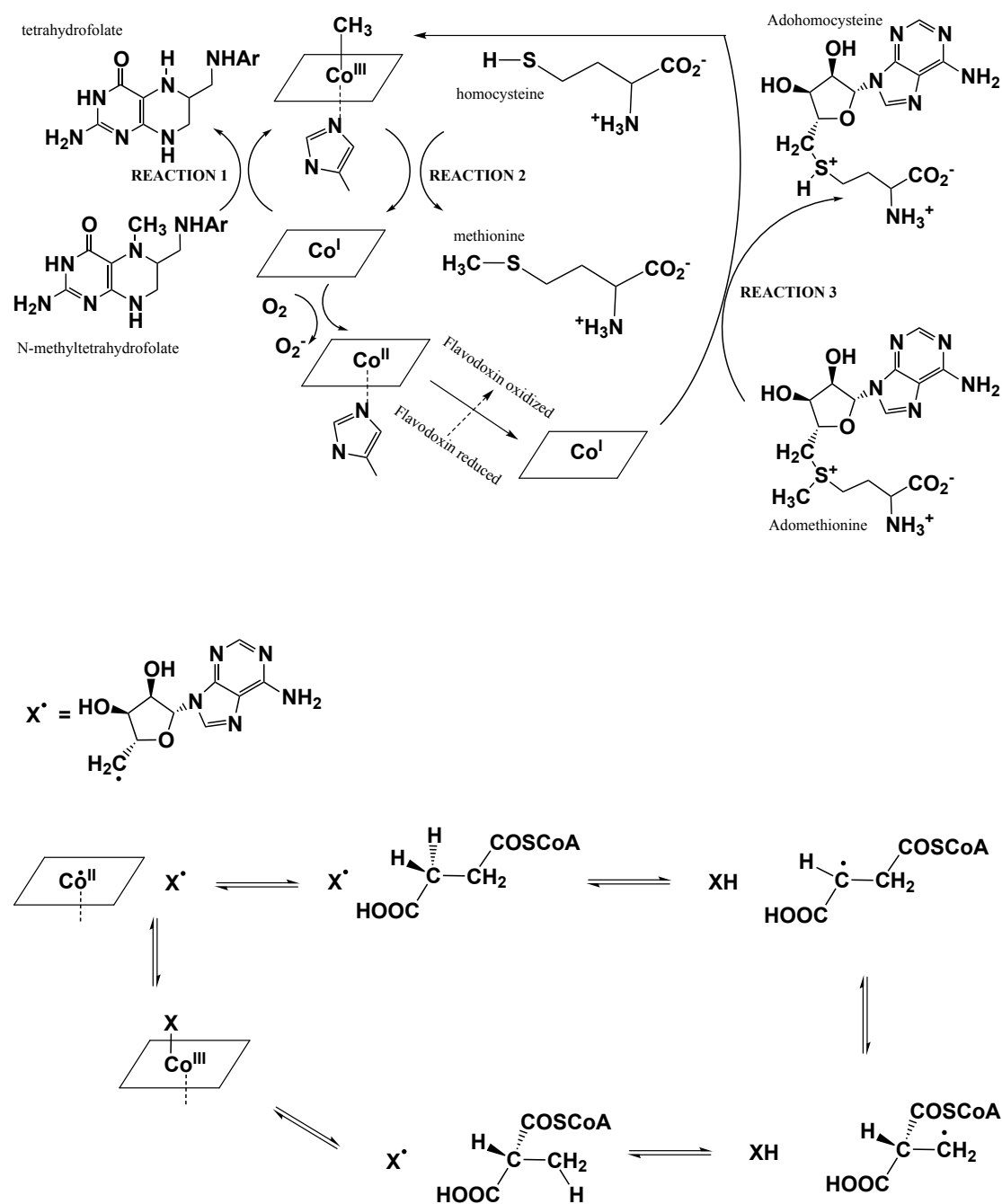
**Scheme 2:** Structure of coenzyme B<sub>12</sub>: Me-Cbl (left) and Ado-Cbl (right).

MetH is a modular protein with separate binding domains for homocysteine (Hcy), methyl tetrahydrofolate (Me-THF) (substrate regions), Me-Cbl (B<sub>12</sub> binding region), and AdoMet (activation region). It catalyzes the conversion of Hcy to methionine using Me-THF as the methyl-source (Scheme 3).<sup>15</sup> This process releases THF, which is required in DNA synthesis. Methionine is an essential amino acid. It can be converted to the methyl donor adenosyl methionine (AdoMet). The catalytic cycle of MetH involves two S<sub>N</sub>2 reactions. MetH accelerates the heterolytic cleavage of Co-C bond by a factor of 10<sup>5</sup>-fold.<sup>16</sup> Deprotonated Hcy acts as a nucleophile attacking on Me-Cbl to form methionine and Co(I)balamin. Me-THF is activated by protonation. The nucleophilic Co(I)balamin could, in theory, attack either proton or methyl group.

As Co(I)balamin is weakly basic ( $pK_a \sim 1$ ),<sup>17</sup> the latter is opted to regenerate Me-Cbl.<sup>18</sup> Oxidative inactivation occurs once per 2000 turnovers resulting in Co(II)balamin, which interacts with AdoMet and MetH-reductase to regenerate Me-Cbl.<sup>19</sup>

MMCM catalyzes the interchange between the carbonyl-CoA group and a hydrogen from the vicinal carbon (Scheme 3). MMCM requires homolysis of Co-C bond in Ado-Cbl. Though this bond is inherently weak with a bond dissociation energy of approximately 30 kCal/mol,<sup>20</sup> the enzyme even accelerates homolysis by a factor of ca.  $10^{12}$ . The enzyme binding probably creates strain in the structure of Ado-Cbl. Homolysis results in two radicals, deoxyadenosyl and Co(II)balamin.<sup>21</sup> The former abstracts hydrogen from the methyl group of methylmalonyl-CoA. The yielded radical undergoes 1,2-rearrangement with the neighbouring carbon, which subsequently reabstracts a hydrogen from 5'-deoxyadenosine. Ado-Cbl is reproduced by the combination of 5'-deoxyadenosyl and Co(II)balamin radicals.<sup>20</sup>

In the holo- forms of both enzymes, the lower  $\alpha$ -dimethylbenzimidazole ( $\alpha$ -DMB) was replaced by His, which forms ligand triad with another two amino acids via hydrogen bonds. In MetH, the ligand triad includes His759, Asp757, and Ser810<sup>22</sup> whereas His610, Asp608, and Lys604 form the ligand triad of MMCM.<sup>23</sup> Coordination of His to the cobalt center does not result in a stronger *trans*-effect on the  $\beta$ -ligand. The role played by the ligand triad indeed remains unclear and so is the mechanism, under which the enzymes determines the fate of Co-C bond.<sup>24</sup>



**Scheme 3:** Coenzymatic mechanism of Me-Cbl (above) and Ado-Cbl (below).



Coenzyme	Enzyme class	Enzyme	Required additional coenzyme	Coenzyme-enzyme binding mode
Me-Cbl	Methyl-transferases	MetH	Zn <sup>2+</sup>	Base-off/ His-on
		Enzymes involving in CO <sub>2</sub> fixing pathway	[Fe <sub>4</sub> S <sub>4</sub> ] cluster	
Ado-Cbl	Eliminases		K <sup>+</sup>	Base-on
	Mutases/ Isomerases	Ribonucleotide reductase (RNR)	K <sup>+</sup>	Base-on
		MMCM, isobutyryl-CoA mutase, glutamate mutase, methylene glutarate mutase, ethanolamine ammonia lyase, D-ornithine aminomutase, β-lysine mutase, diol dehydrase, glycerol dehydratase		Base-off/ His-on
	Reductive dehalogenases		[Fe <sub>4</sub> S <sub>4</sub> ], [Fe <sub>3</sub> S <sub>4</sub> ] clusters	

**Table 1:** List of B<sub>12</sub>-dependent enzymes.

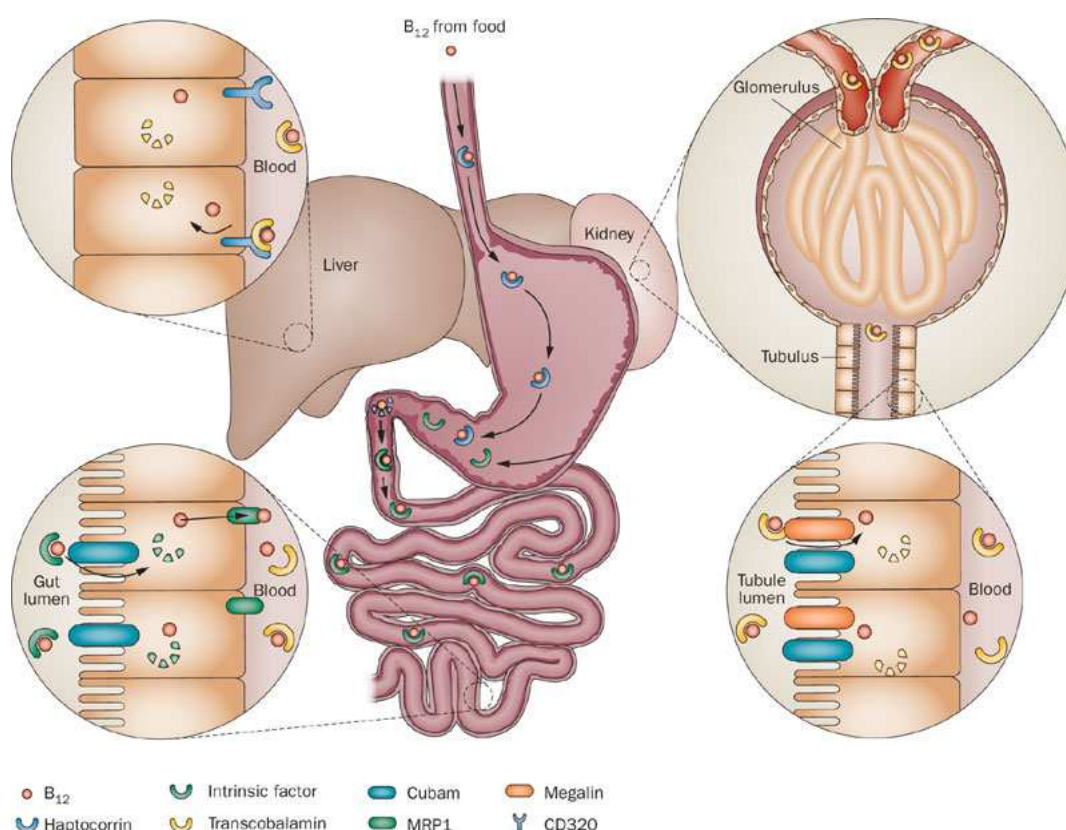
### I.3 Transport and metabolism of cobalamin

It is with great care that the body handles precious amounts of Cbl. Concerted involvement of many proteins in the extra- and intracellular journeys of Cbl was revealed. The former includes haptocorrin (HC), intrinsic factor (IF), and TC. The holo-proteins are recognized by corresponding receptors: asiaglycoprotein (ASGP-R) (41 or 46 kDa), cubilin (460 kDa), TC-receptor (TC-R) (58 kDa) and megalin (600 kDa) (Table 2).<sup>13</sup> Except for AGPR, other receptors recognize only holo-proteins. AGPR accepts both holo-and apo-HC and accounts for liver uptake of HC. Besides, it binds indeed to all glycoproteins with terminal galactose residues. Its absence does not result in B<sub>12</sub> deficiency.

Receptors	Expression sites
AGPR	Liver, intestine, colon carcinoma (HT-29, Caco-2) <sup>25, 26</sup>
Cubilin	Intestine mucosa, kidney proximal tubule, yolk sac, etc <sup>27, 28</sup>
TC-R	All tissues, <sup>29-31</sup> Overexpression: kidney, liver, placenta, intestine and fast-growing cells. <sup>31-34</sup>
Megalín	Renal proximal tubule epithelium, other absorptive epithelia (brain ependyma, yolk sac epithelium, placenta, lung). <sup>35</sup>

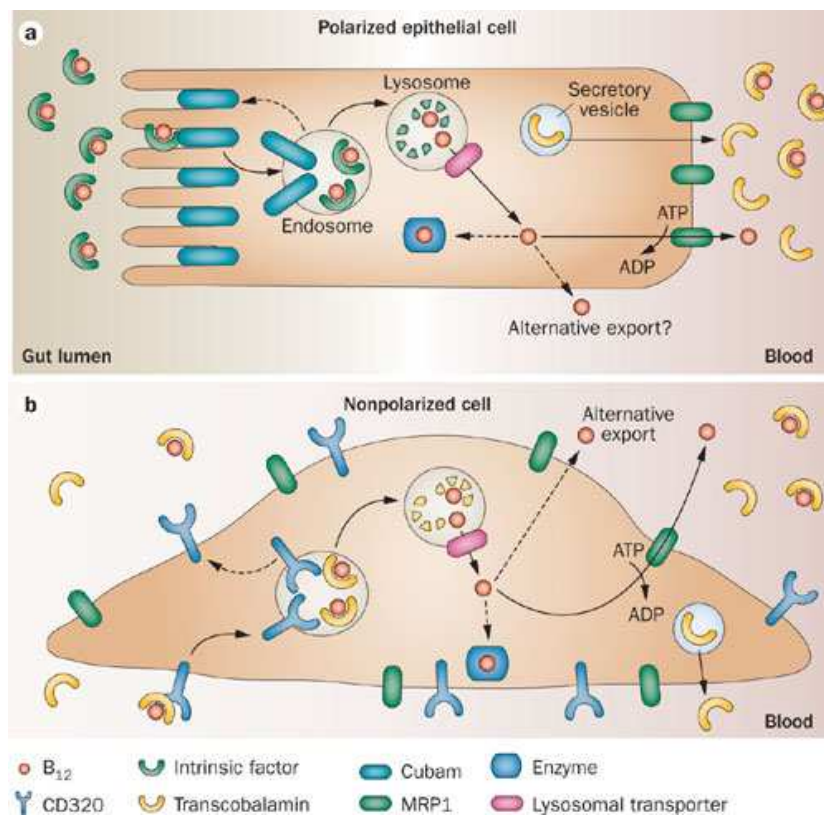
**Table 2:** Expression sites of receptors.

Following its oral intake, Cbl is associated with HC.<sup>36, 37</sup> Pancreatic enzyme degrades HC and Cbl is transferred to IF.<sup>38</sup> As Cbl-IF interaction is highly specific,<sup>39-42</sup> IF excludes unusual Cbl analogues from plasma entrance. Holo-IF crosses enterocytes, where IF is degraded and free Cbl is released to plasma (Scheme 4). In plasma, ca. 20% of Cbl is captured by TC.<sup>43, 44</sup> Holo-TC is then distributed to most of the tissues via TC-R. In addition, it is recycled from primary urine by megalin receptor. The major amount (80%) of plasma Cbl is, however, in complex with HC. HC possibly serves as a second filter to exclude analogous Cbls from tissue distribution. Also, it can mediate the storage of Cbl in liver. The exact role of HC remains to be elucidated.<sup>25, 45</sup>



**Scheme 4:** Uptake and transport of B<sub>12</sub>.<sup>11</sup>

Scheme 5 shows cellular import and export of Cbl in polarized vs. non-polarized cells. The two cell types share the same Cbl export mechanism (via MRP1). The cellular entrance of Cbl, however, is different. In both cases, the receptors (cubilin and TC-R) are recycled whilst the transport proteins (IF and TC) are degraded in lysosome. Free Cbl exits lysosome via LMBD1. Decyanation of B<sub>12</sub> and dealkylation of alkyl-Cbl occur through binding to MMACHC in cytosol. MMADHC subsequently drives Cbl to its mitochondrion and cytosol pathway. In cytosol, cob(II)alamin binds to MetH and MetH-reductase subsequently catalyzes the formation of Me-Cbl. In the mitochondrion, MMAB catalyzes the formation of Ado-Cbl, which is then transferred to MMCM.<sup>46</sup>



**Scheme 5:** Uptake and exit of B<sub>12</sub> in polarized (above) and non-polarized cells.<sup>11</sup>

## I.4 Structure of cobalamin

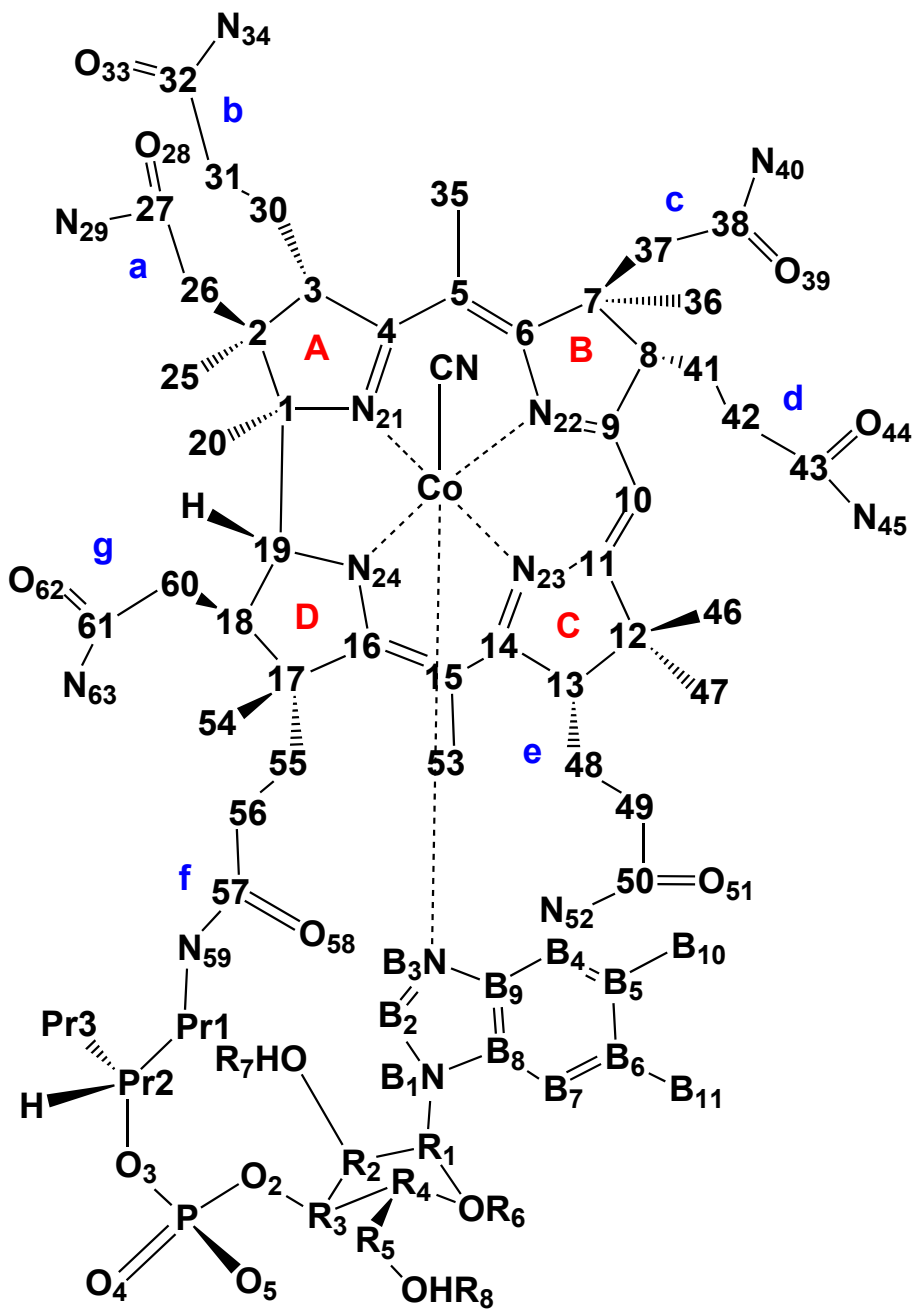
“B<sub>12</sub> turned out to be a substance of frightening complexity” (Lord Todd)

Cbl is an octahedral complex of Co<sup>III</sup> with a tetradentate corrin ring, an  $\alpha$ -nucleotide loop, and an exchangeable  $\beta$ -ligand.<sup>47</sup> The corrin consists of 4 reduced pyrrole rings with a direct connection between A and D rings (Scheme 6). It folds upward around the Co-C10 axis. The folding angle ranges from 1.9-23.9° (17.9°, 14.8°, and 10° in case of B<sub>12</sub>, Me-Cbl, and Ado-Cbl, accordingly). The bulk of  $\alpha$ -ligand and the Co-N( $\alpha$ ) bond length (2.19 and 2.21 Å in Me-Cbl and Ado-Cbl) regulate the corrin folding. The corrin, on the other hand, exerts a labilizing *cis*-effect on axial ligands. The trans-effect of the  $\beta$ -ligand indirectly influences the  $\alpha$ -ligand via Co-N( $\alpha$ ) bond length.

The semicovalent Co-C bond in B<sub>12</sub> coenzymes is unusually stable, which is attributed to the dominance of Co 4s (instead of 3d) orbital in ligand bonding.<sup>48</sup> Its coenzymatic function was triggered when the Co<sup>III</sup> center is reduced stepwise to form square pyramid cob(II)alamin and square planar cob(I)alamin.<sup>49, 50</sup> The latter is a supernucleophile. It involves in several S<sub>N</sub>2 reaction including attacking ATP to form Ado-Cbl or attacking Me-THF to form Me-Cbl.

The decrease in cobalt oxidation state is accompanied by the decrease in coordination number. The  $\beta$ -ligand is more susceptible to reductive cleavage than the  $\alpha$ -loop. Reoxidization recovers the octahedral geometry.<sup>17</sup> Coenzymes B<sub>12</sub> are formed by displacement of the  $\beta$ -ligand with either a methyl or an adenosyl group.<sup>51, 52</sup>

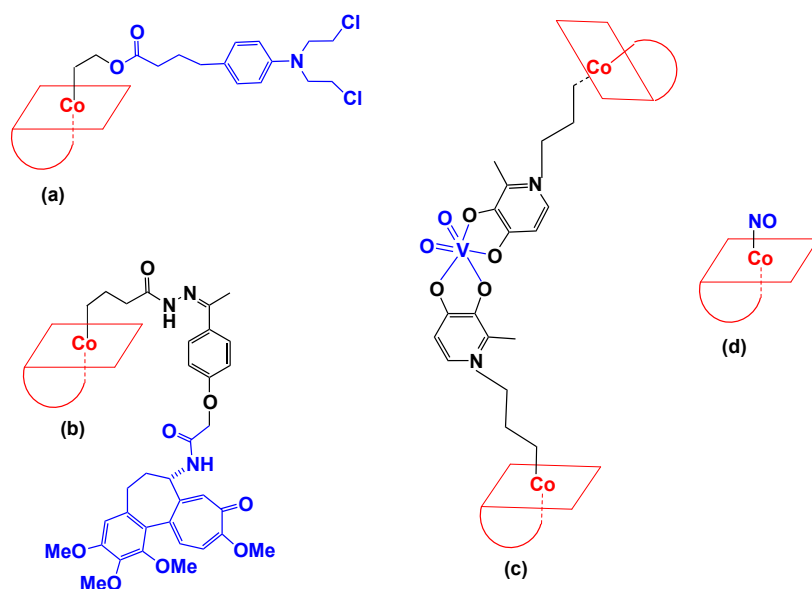
---



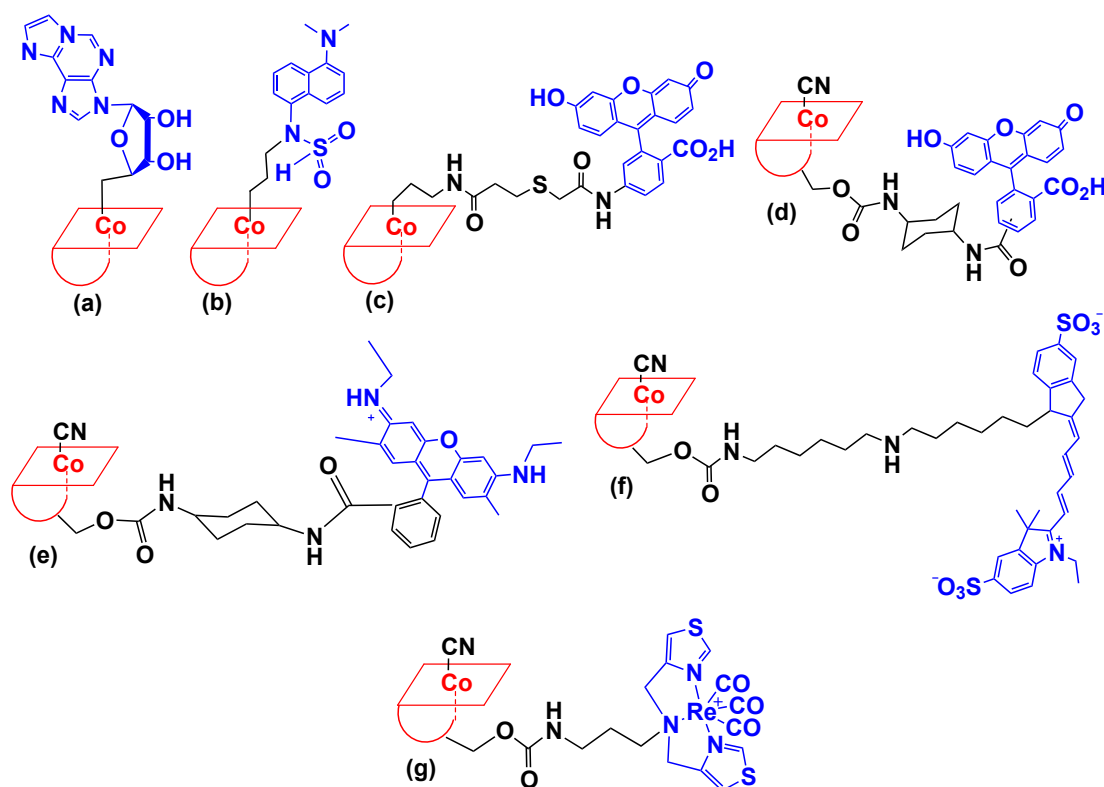
**Scheme 6:** B<sub>12</sub> numbering scheme.

## I.5 Cobalamin conjugates

The demand of Cbl in proliferation process was applied to cancer treatment in various strategies. Among those was the inactivation of B<sub>12</sub>-dependent MetH by N<sub>2</sub>O,<sup>53-56</sup> the inhibition of B<sub>12</sub> by its antagonists including B<sub>12</sub>-[c-lactam]<sup>57</sup> and B<sub>12</sub> with peptide backbone.<sup>58, 59</sup> The most common strategy is, however, to attach cytotoxic molecules to B<sub>12</sub> structure. Drugs and analytical probes were readily introduced to the B<sub>12</sub> structure through numerous functional groups on the corrin side chains.<sup>60</sup> Radioactive <sup>111</sup>In-DTPA and <sup>99m</sup>Tc-DTPA were coupled to B<sub>12</sub> via the b-side chain.<sup>61, 62</sup> [<sup>99m</sup>Tc(CO)<sub>3</sub>]<sup>+</sup> moiety was coupled to B<sub>12</sub> at b and d-positions.<sup>63</sup> Biotin was conjugated to B<sub>12</sub> at b, c, d, and e positions (Scheme 6).<sup>60</sup> In addition, the β-position is especially common owing to its ease-of-release in cellular reducing environment and its little involvement in protein binding (1 and Scheme 7). The ribose-OH group is another convenient derivatization site (Scheme 6) as its role in protein interaction is also not critical.<sup>64</sup> Indeed, fluorophores<sup>65, 66</sup> (Scheme 8), cytotoxic agents,<sup>67</sup> insulin,<sup>68</sup> and appetite suppressing peptide hPYY,<sup>69</sup> were coupled to B<sub>12</sub> via the ribose-hydroxyl. The increasing structural knowledge of Cbl and related proteins laid the background to fine-tune designs of B<sub>12</sub> derivatives. Tissue distribution was interfered by modifying B<sub>12</sub> structure at critical sites of protein interaction such as b- or d-side chain of the corrin.<sup>70</sup>



**Scheme 7:** Drugs conjugated to Cbl: (a) nitrogen mustard chlorambucil,<sup>71</sup> (b) colchicine,<sup>72</sup> (c) insulinomimetic vanadate (V) compound,<sup>73</sup> (d) nitric oxide.<sup>74</sup>



**Scheme 8:** Some fluorescent B<sub>12</sub> with: fluorescent nucleoside(a),<sup>75</sup> dansyl derivative (b),<sup>75</sup> fluorescein (c, d),<sup>76</sup> Rhodamin 6G (e),<sup>65</sup> Cy5 (f),<sup>77</sup> Re(I)-based-fluorophore(g).<sup>78</sup>

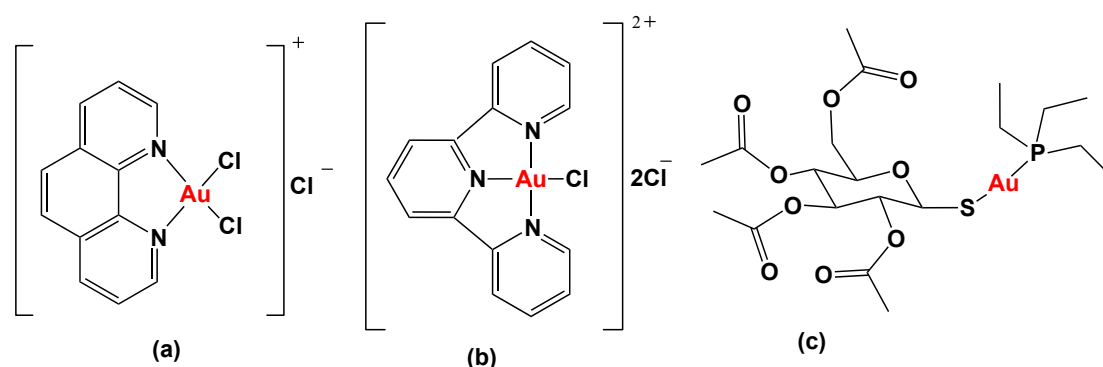
A great deal of researches was dedicated to discover and explore the correlation of B<sub>12</sub> demand and DNA synthesis. It should, however, be noted that B<sub>12</sub> can also lend other interesting properties to its conjugated molecules. Its excellent water solubility allowed convenient administration of the attached insoluble drugs.<sup>79</sup> B<sub>12</sub> protected protein-peptide drugs<sup>68, 69, 80</sup> from hydrolysis in the acidic condition of the gastrointestinal track.<sup>81</sup> The utilization of Cbl in transporting drugs appeared to be restrained by its cellular loading capacity.<sup>82</sup> Different strategies were applied to overcome this limitation. Minimization of competitive background B<sub>12</sub> was achieved in-vitro by depriving B<sub>12</sub> and folic acid from culture medium.<sup>83</sup> This corresponded to a B<sub>12</sub>-free diet in in-vivo experiments.<sup>70</sup> Besides, increase in TC-R expression was induced by interferon  $\beta$  (IFN- $\beta$ ).<sup>74</sup> A greater number of TC-R would endocytose a higher amount of Cbl. The addition of IFN- $\beta$  had a synergistic effect on both in-vitro and in-vivo cytotoxicity of nitrosyl-Cbl. B<sub>12</sub> overdosing was another treatment regime. A recent study showed that tissue accumulation of B<sub>12</sub> increased significantly (up to 350%) upon overdosing of the vitamin.<sup>84</sup>



## I.6 Metal anticancer drugs

### I.6.1 Gold anticancer drugs

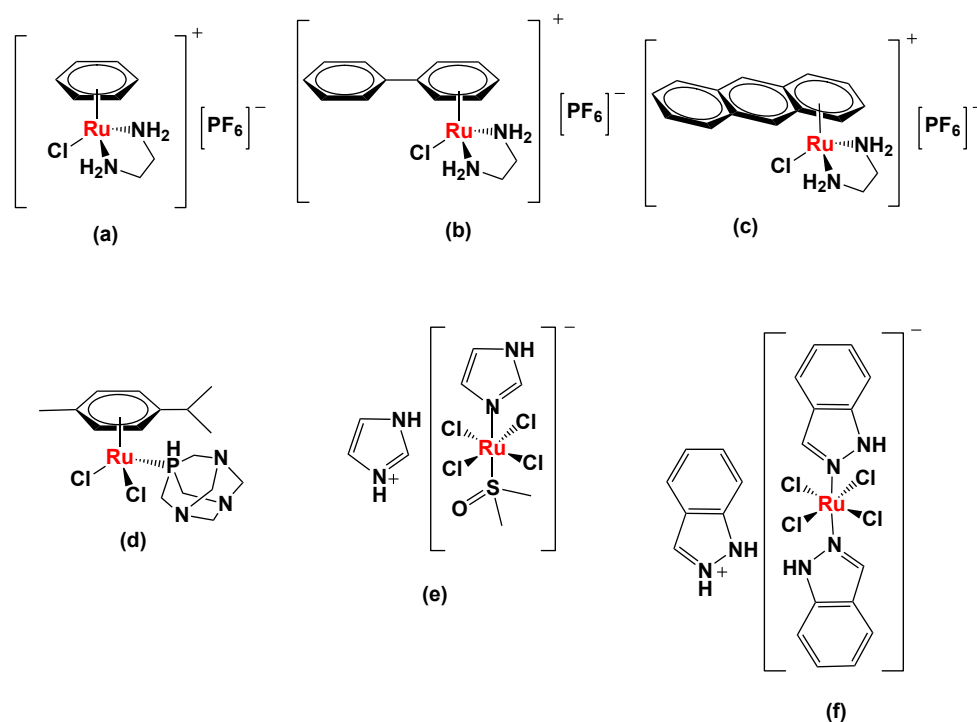
Gold found application in ancient medicine in China, India, and Egypt before any scientific rationalization was established in the 20<sup>th</sup> century. Both Au(I)- and Au(III)-complexes were widely studied for anticancer activity (Scheme 9).<sup>85</sup> "Soft" ligands with S and P as donor atoms are popular for Au(I)-complexes. "Hard" ligands with O, N, or C as donor atoms were more compatible to the highly oxidizing Au(III) as "soft ligands" are generally reducing. Failure in translation from in-vitro cytotoxicity to in-vivo antitumor profile hampered the development of Au(I)-complexes in cancer research as they were bound to serum proteins. Au(III)-complexes were expected to have interesting properties owing to the isoelectronic ( $d^8$ ) and isostructural (square planar) relation to Pt(II). Though interesting cytotoxic profiles were reported, Au(III)-complexes were found to act differently from cisplatin as DNA is not their primary target.<sup>86, 87</sup>



**Scheme 9:** Structures of some Au(III) and Au(I) complexes: (a) [Au(phen)Cl<sub>2</sub>]<sup>+</sup>Cl<sup>-</sup>, [Au(terpy)Cl<sub>2</sub>]<sup>2+</sup>2Cl<sup>-</sup>,<sup>88</sup> and Auranofin.<sup>89</sup>

## I.6.2 Ruthenium anticancer drugs

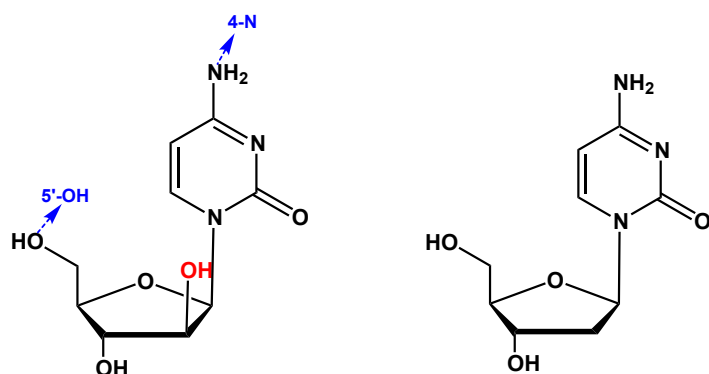
The most prominent non-Pt metal-based cancer drugs are probably Ru-complexes with novel properties: i) Ru various oxidation states (II, III, and IV), ii) tumor accumulation, iii) antimestatic effects, iv) slow ligand exchange kinetics, and v) good biocompatibility (owing to iron micmicking). The most interesting Ru(III)-complexes were the anti-metastatic NAMI-A and the cytotoxic KP1019 (Scheme 10) with established data from clinical phase-I study.<sup>90-92</sup> Even though Ru(II)-complexes were considered to be more active than Ru(III)-complexes, suitable ligand selection proved to enhance the stability. Most noticeable among Ru(II)-complexes were Ru(II)-arene compounds from Sadler's and Dyson's groups (Scheme 10), Ru(II)-half-sandwich and antimestatic Ru(II)-RAPTA-complexes, correspondingly.<sup>93, 94</sup> Despite similar structural aspects, they exert different effects on tumour via distinct modes of action.



**Scheme 10:** Structures of some Ru-drugs: (a)  $[\text{Ru}(\text{phen})(\text{en})\text{Cl}][\text{PF}_6]$ , (b)  $[\text{Ru}(\text{bipy})(\text{en})\text{Cl}][\text{PF}_6]$ , (c)  $[\text{Ru}(\text{THA})(\text{en})\text{Cl}][\text{PF}_6]$ ,<sup>95</sup> (d) RuRAPTA,<sup>96</sup> (e) NAMI-A, and (f) KP1019.<sup>97</sup>

## I.7 Organic anticancer drugs

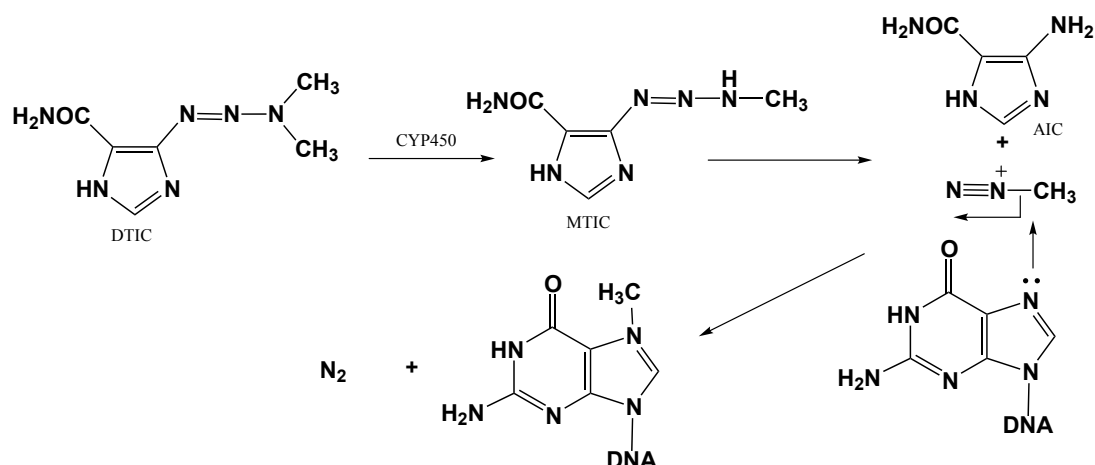
Cytarabine (Cyt), an analogue of the nucleoside deoxycytidine (Scheme 11), was approved for the treatment of myeloid leukemia and non-Hodgkin's lymphoma.<sup>98,99</sup> It is metabolized to its triphosphate form at 5'-OH position and respectively competes with deoxycytidine triphosphate in DNA synthesis. Cyt, however, represents a challenge for tumor targeting due to its short plasma half-life, low stability and limited bioavailability. Low membrane permeability and the ease to be inactivated by cytidine deaminase at the 4-N position limit its therapeutic efficiency.<sup>100</sup>



**Scheme 11:** Structure of Cyt (left) and deoxycytidine (right)

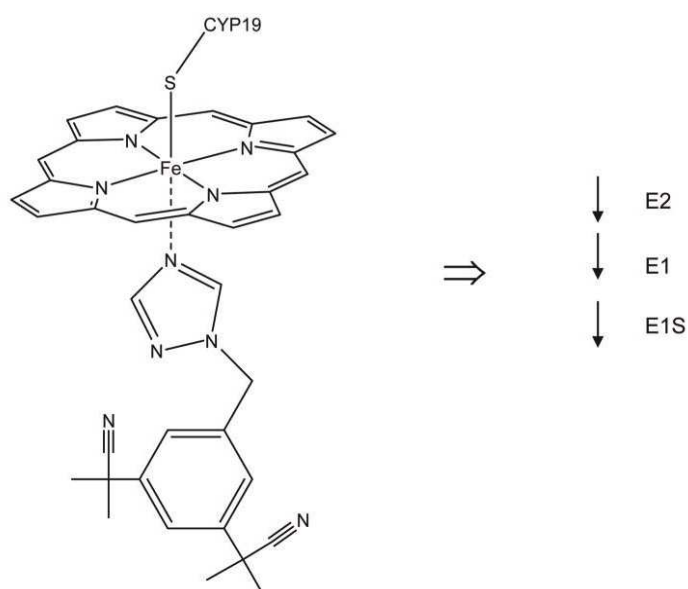
Extensive research on targeted delivery of Cyt includes conjugation with amino acids, fatty acids, and phosphates at either 4-N or 5'-OH site to prevent drug degradation and enhance membrane permeability. Among these formulations are hydrogels, liposomes and niosomes. Encapsulation maintains chemical integrity of the drug and enhances membrane transport. Nevertheless, it is the ability to liberate drugs, which determines success of such delivery system. Strong interactions of Cyt with hydrogels and niosomes lead to poor drug release. Only liposome, with its enhanced permeability and retention (EPR) effect, was shown to be a relevant delivery system for Cyt.<sup>101</sup>

Dacarbazine (Dac) is a melanoma and Hodgkin's disease drug. Several mechanisms of actions were suggested for Dac including methylating DNA, interacting with SH groups, and inducing ROS formation.<sup>102, 103</sup> Dac, however, is mostly referred as a DNA alkylation agent. It is activated to MTIC by the liver enzyme CYP450.<sup>104</sup> The electrophilic methyl group is attacked by the nucleophilic N-7 and O-6 of guanine (Scheme 12).<sup>105, 106</sup>



**Scheme 12:** Methylating mechanism of Dac on N-7 of guanine.<sup>103</sup>

Anastrozole (Ana) is prescribed for post-menopausal women with hormone receptor positive early breast cancer. Ana binds reversibly to the heme iron of aromatase (Scheme 13) and, thus, inhibits the aromatase-dependent synthesis of estradiol (E2).<sup>107</sup> As hormone receptor positive breast tumors depend on E2 for their growth, the interference with E2 synthesis suppresses proliferation.<sup>108</sup>



**Scheme 13:** Mechanism of action of Ana.<sup>108</sup>

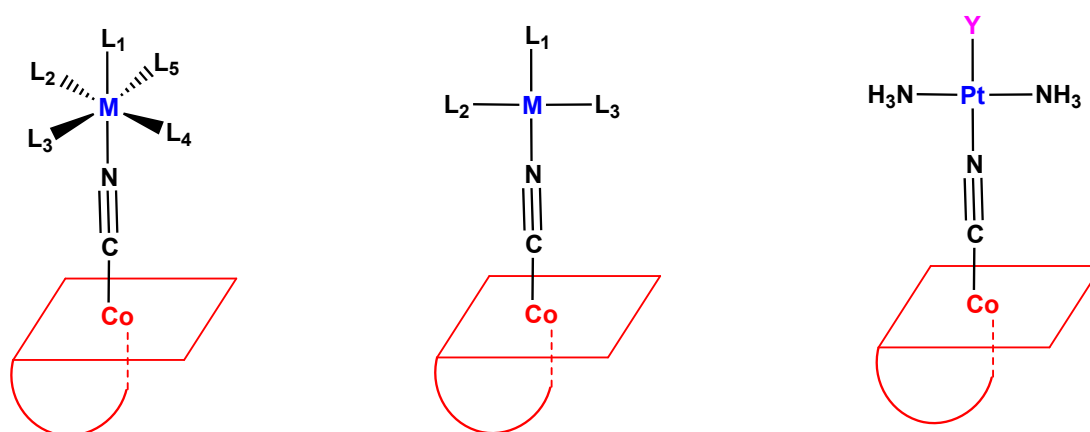
## I.8 Imaging agents

Several fluorophores were conjugated to B<sub>12</sub> via either Co-C bond or ribose 5'-OH (Scheme 8). B<sub>12</sub> was known to exert a quenching effect, completely<sup>75</sup> or partially.<sup>76,78</sup> Most clearly is the fact that the fluorescence of  $\alpha$ -ribazole (1- $\alpha$ -D-ribofuranosyl-5,6-DMB) was not observed in Cbl structure. Also, B<sub>12</sub> completely quenched several different fluorophores attached as  $\beta$ -nucleosides or  $\beta$ -alkyls.<sup>75</sup> Interaction between fluorophores and the corrin macrocycle accounted for the loss of fluorescence. Orienting the fluorophores away from the corrin was reported to prevent the quenching effect of B<sub>12</sub>.<sup>65</sup>

Several radionuclides were coupled to B<sub>12</sub> structure for TC-R imaging and biodistribution study. These included both  $\beta$ - and  $\gamma$ -emitters: [<sup>57</sup>Co], [<sup>125</sup>I], [<sup>131</sup>I], [<sup>111</sup>In], and [<sup>99m</sup>Tc]. Conjugation sites varied from corrin side chains (b, d, e)<sup>61-63</sup> to  $\beta$ -axial position.<sup>109</sup> Despite the commercial availability of [<sup>57</sup>Co]-B<sub>12</sub>, it is not suitable for clinical imaging. The long half-life (270.9 days) of <sup>57</sup>Co results in low specific activity (1  $\mu$ Ci/ $\mu$ g). Radioisotopes with short half-life and high specific activity are preferred.  $\gamma$ -rays are less harmful to tissues than  $\beta$ -particles. Therefore, [<sup>125</sup>I], [<sup>111</sup>In], and [<sup>99m</sup>Tc] are favored over [<sup>131</sup>I]. [<sup>99m</sup>Tc], with an optimal  $\gamma$ -energy (142 keV) and a short half-life (6 h), is the most important radioisotope in nuclear medicine.

## II Objectives

The aim of this thesis was to produce, in a coordination chemistry approach, therapeutic and diagnostic B<sub>12</sub> derivatives for cancer research. Antitumor metal complexes such as cisplatin and ruthenium (II) arene compounds were directly conjugated to B<sub>12</sub> via  $\beta$ -CN<sup>-</sup>. Organic chemotherapeutic drugs or fluorophores were coordinated to B<sub>12</sub> via  $\beta$ -[*trans*-Pt(NH<sub>3</sub>)<sub>2</sub>-CN]<sup>+</sup>-bridge (Scheme 14). Radioimaging agents [<sup>99m</sup>Tc] were introduced to the corrin side chain or the back loop (ribose). This allows the cellular behavior of these compounds to be studied. Besides, direct measurements of transition metals in these compounds also provided information of their cellular process. The release of native drugs was studied by reduction experiments, both electrochemically and chemically, in combination with HPLC and ESI-MS techniques. Cytotoxicity was compared among native drugs, prodrugs, and the released drugs.



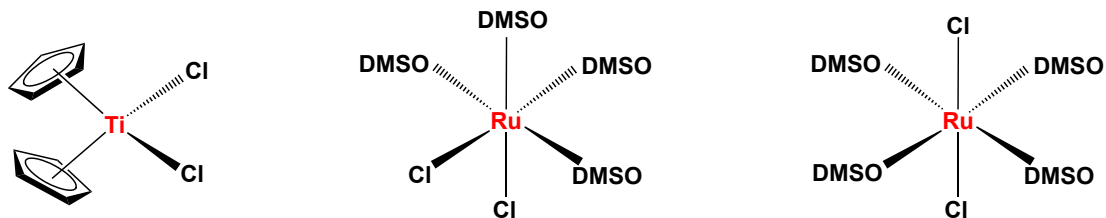
**Scheme 14:** B<sub>12</sub> conjugates to deliver active metal complexes (left and middle) or active organic compounds (Y) (right).

### III Results and discussion

#### III.1 {Metallodrug}-{B<sub>12</sub>} conjugates

The  $\beta$ -side modification of Cbl was mainly at the photo-instable organometallic Co-C(alkyl) bond. The handling of alkyl-Cbl is rather complicated.<sup>110</sup> The stronger Co-CN bond represents a better modification site.<sup>111</sup> Indeed stable complexes were previously synthesized by coordinating  $\beta$ -CN<sup>-</sup> to  $[M(OH_2)(L^2)(CO)_3]$  ( $M = Re, {}^{99m}Tc$ )<sup>112</sup> and  $[PtCl_x(NH_3)_{4-x}]$  ( $x=1-3$ ).<sup>113</sup> We therefore continue this strategy on recently rising anticancer metallodrugs. The presence of a labile ligand is required for substitution by the nucleophilic  $\beta$ -CN<sup>-</sup>. This feature is common in many metallodrugs (Scheme 10 and Scheme 15) as they were designed to mimic the action mechanism of cisplatin.

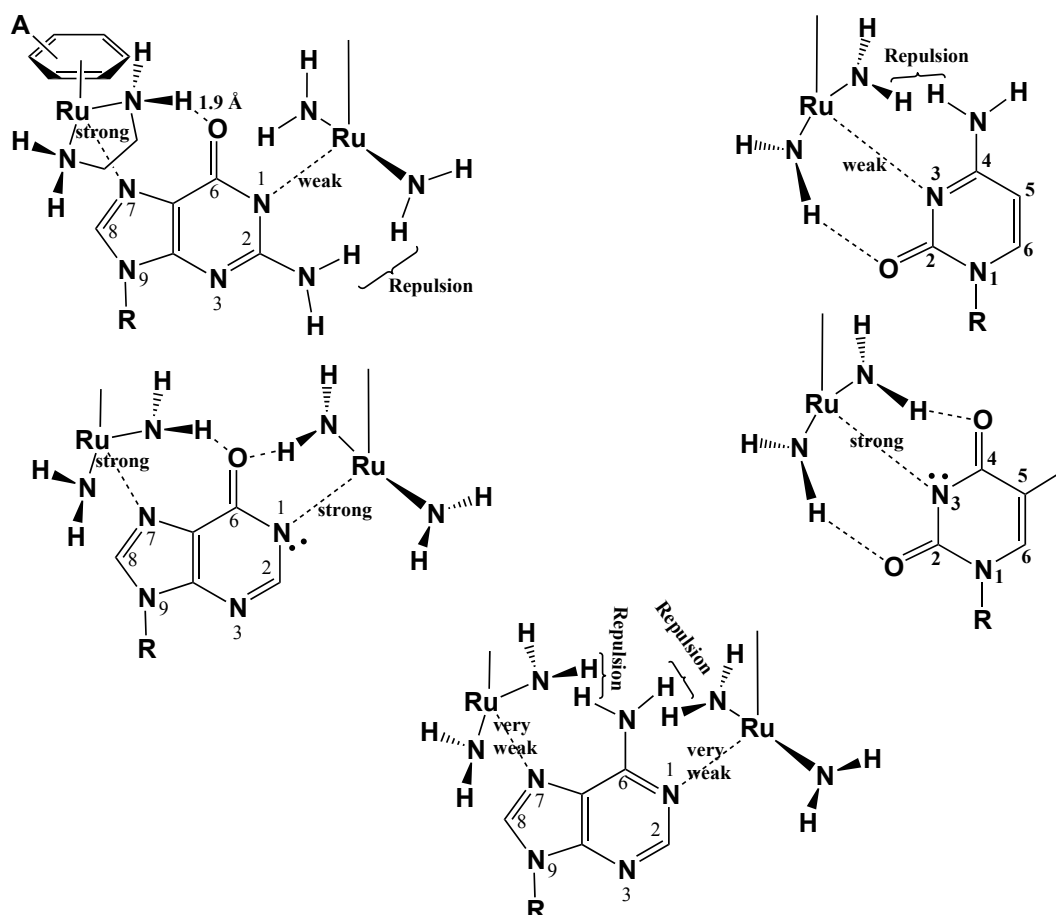
In this thesis, B<sub>12</sub> was coordinated to the increasingly important Ru- and Au- anticancer compounds. The products, if stable, would inherit the novel physical, chemical and biological properties of B<sub>12</sub> such as water solubility, steric feature, biocompatibility, and proliferation targeting.



**Scheme 15:** Structures of titanocene dichloride (left), *cis*- and *trans*-[RuCl<sub>2</sub>(DMSO)<sub>4</sub>] (middle and right, accordingly).

### III.1.1 {[Ru]-drug}-{B<sub>12</sub>} conjugate

$[(\eta^6\text{-arene})\text{Ru}(\text{en})\text{Cl}][\text{PF}_6]$  (Scheme 10) was selected as a candidate of Ru-arene-drugs for coordination of B<sub>12</sub>. Similar to cisplatin, it was activated by the intracellular hydrolysis of Ru-Cl bond, which allowed coordination of N7-guanine nucleophile to Ru. In addition, the en-NH<sub>2</sub> formed hydrogen bond to O6-guanine and the arene intercalates with DNA (Scheme 16).<sup>114, 115</sup> It could obviously be predicted that the substitution of Cl<sup>-</sup> by  $\beta\text{-CN}^-$  might influence the N7-guanine binding. However, this does not necessarily mean deterioration of DNA interaction, as en and the arene are still available. The rich collection of Ru-arene drugs from literature promises a wide range of {[Ru]-drugs}-{B<sub>12</sub>} compounds.



**Scheme 16:** Interaction of  $[\text{Ru}(\text{arene})(\text{en})]^{2+}$  with nucleobases.<sup>115</sup>



Formation of the sandwich coordinative compound  $[\{(\eta^6\text{-C}_6\text{H}_6)\text{Ru}(\text{en})\}\text{-}\{\text{B}_{12}\}][\text{PF}_6]_2$  **3** was, on the structural perspective, interesting. A shift of  $\nu_{\text{CN}}$  to higher energy in IR spectroscopy indicated the coordination of  $\{\text{Ru}\}$  to  $\text{CN}^-$ . Whereas the correct mass on ESI-MS showed the formation of **3**, the additional strong signal in  $^1\text{H-NMR}$ 's aromatic region besides the 5 signals of  $\text{B}_{12}$  (C10, R1, B7, B2, and B4) was a definite characteristic proof of **3** (Figure 1).

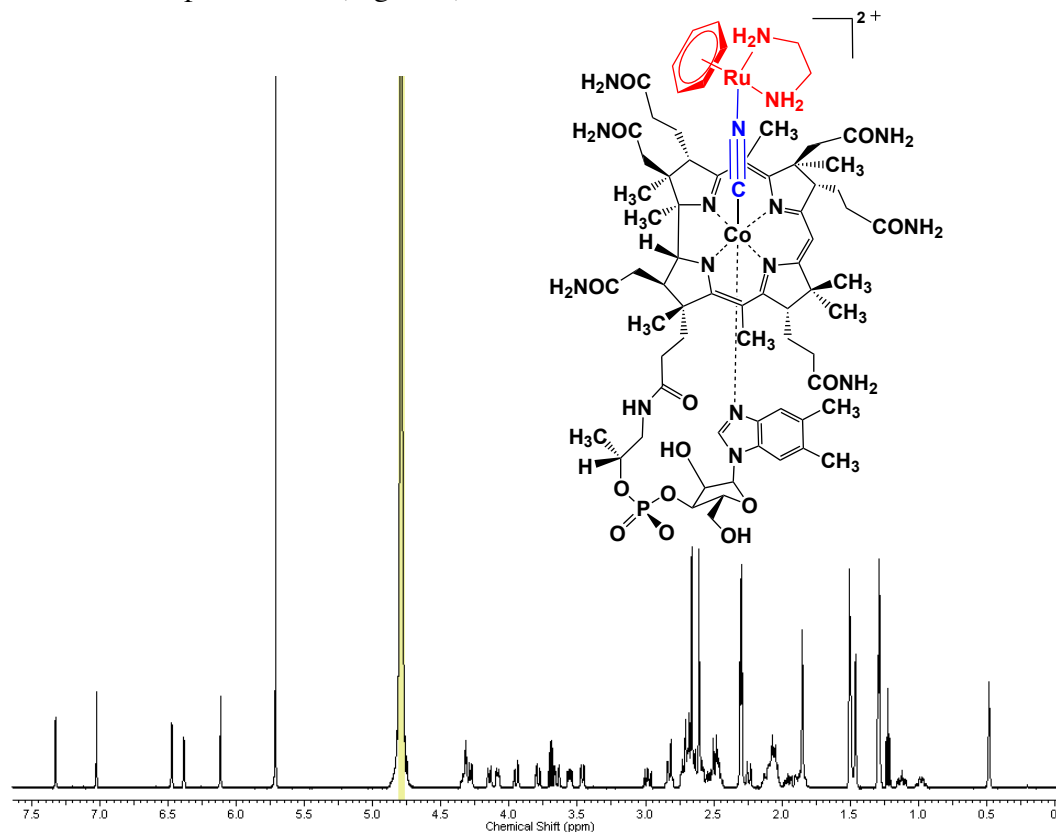
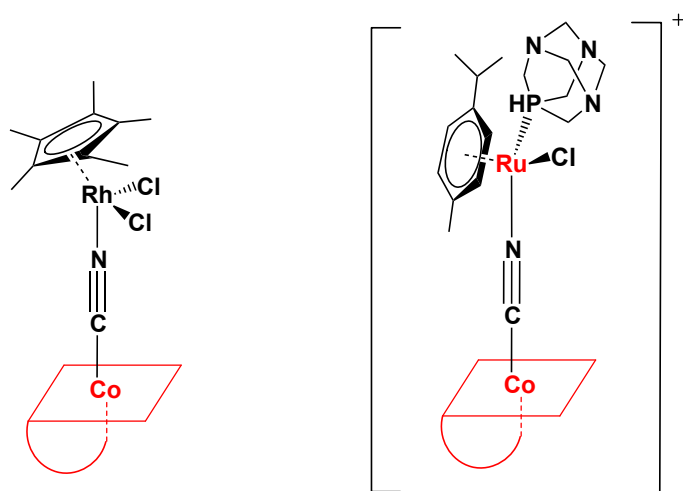


**Figure 1:**  $^1\text{H-NMR}$  spectrum of  $[\{(\eta^6\text{-C}_6\text{H}_6)\text{Ru}(\text{en})\}\text{-}\{\text{B}_{12}\}]^{2+}$ .

The most traditional technique for  $\text{B}_{12}$  separation and purification, chromatography, was not reliable as **3** decomposed through  $\text{C}_{18}$ -columns. Despite its distinguishable earlier retention time with respect to that of  $\text{B}_{12}$ , the collected HPLC fraction turned out to be  $\text{B}_{12}$  on ESI-MS and IR, indicating that the Ru-fragment was cleaved from  $\text{B}_{12}$  during the elution. It was likely bound to the silanol residues of the column. The decomposition of organometallic compounds during chromatographic separation has previously been described.<sup>116</sup> The reaction was monitored by HPLC but purification must be done by another method. Therefore **3** was precipitated from water solution with the counter ion  $[\text{PF}_6]^-$ . The product did not completely precipitate in water. It dissolved partially and appeared to be less stable than  $\{\text{cis/transplatin}\}\text{-}\{\text{B}_{12}\}$

conjugates, **1** and **2**. In details, 30%, 48%, and 63% of **3** (0.16  $\mu$ M) were decomposed to B<sub>12</sub>. Indeed  $[(\eta^6\text{-C}_6\text{H}_6)\text{Ru}(\text{en})]^{2+}$  is more sterically demanding than  $[\text{Pt}(\text{NH}_3)_2\text{Cl}]^+$ , which may account for its lower stability. Coordination of B<sub>12</sub> to the even more bulky  $[(\eta^6\text{-p-cymene})\text{Ru}(\text{en})]^{2+}$  or  $[(\eta^6\text{-THA})\text{Ru}(\text{en})]^{2+}$  (Scheme 10) was attempted but unsuccessful. As the cytotoxicity of Ru-arene drugs correlates to the arene lipophilicity/ bulkiness,<sup>117</sup> sufficiently stable {Ru-arene}-{B<sub>12</sub>} compounds are therefore unlikely.

B<sub>12</sub> was also coordinated to Ru-RAPTA-C (Scheme 10). The product formation was evident from IR and ESI-MS measurements. However, it could not be isolated. The increasing water solubility of Ru-RAPTA-C made it impossible to precipitate {Ru-RAPTA-C}-{B<sub>12</sub>} (Scheme 17). It was similar to  $\{(\text{Cp}^*)\text{Rh}(\text{Cl}_2)\}\text{-}\{\text{B}_{12}\}$ , the formation of which was observed (IR, ESI-MS) after mixing  $[\text{RhCl}_2\text{Cp}^*]_2$  with B<sub>12</sub> in MeOH. Purification was not possible due to decomposition on HPLC column. Purification by precipitation with a counter-ion did not apply as  $\{(\text{Cp}^*)\text{Rh}(\text{Cl}_2)\}\text{-}\{\text{B}_{12}\}$  is a neutral compound (Scheme 17).



**Scheme 17:** Unpurified [B<sub>12</sub>]-[(Cp<sup>\*</sup>)Rh(Cl<sub>2</sub>)] (left) and [B<sub>12</sub>]-[Ru-RAPTA-C] (right).

### III.1.2 {[Au]-drug}-{B<sub>12</sub>} conjugate

The [Au(phen)Cl<sub>2</sub>]Cl complex<sup>118</sup> (Scheme 9) represents a physiologically stable class of Au(III) complexes owing to the presence of the multidentate ligand phen. It was reported active against cisplatin-resistant cancer cell line<sup>88</sup> owing to its different cytotoxic mode, which was ascribed to the released phen under reducing condition in mammals.<sup>88</sup> However, it was ca. 3 times less cytotoxic than cisplatin in cisplatin-sensitive cell line.

β-CN<sup>-</sup> did not substitute the Cl<sup>-</sup> ligand in [Au(phen)Cl<sub>2</sub>]<sup>+</sup>. Efforts included performing reactions directly between B<sub>12</sub> and [Au(phen)Cl<sub>2</sub>]Cl in MeOH, H<sub>2</sub>O, DMF: H<sub>2</sub>O (1:1), or H<sub>2</sub>O at physiological pH (phosphate buffer), prolonged reaction time, and vigorous heating (up to 75°C). Alternatively, Cl<sup>-</sup> was removed by AgNO<sub>3</sub> before B<sub>12</sub> was added. However, no coordination was observed. [Au(phen)Cl<sub>2</sub>]Cl was poorly soluble. Longer reaction time and higher temperature resulted in decomposition of B<sub>12</sub> to Cbl-OH<sub>2</sub>. It was shown previously that the Cl<sup>-</sup> ligand is rather easily released.<sup>88</sup> Therefore, the sterically demanding ligand B<sub>12</sub> was likely to be the obstacle. As [Au]-drugs are generally bulky, the formation of stable {[Au]-drugs}-{B<sub>12</sub>} complexes is thus unlikely.<sup>85</sup>

In summary, B<sub>12</sub> is a bulky ligand. The corrin upward folding and its sentinel groups place certain dimensional confinement on the β-axial ligands.<sup>47</sup> Commonly-found spacious structures of metallodrugs fit hardly in the allowed pocket of the β-face.<sup>113</sup> Bulky complexes were not able to accommodate the sterically demanding B<sub>12</sub> ligand. Pt(COD)Cl<sub>2</sub>, [Au(phen)Cl<sub>2</sub>]Cl, [(η<sup>6</sup>-p-cymene)Ru(en)Cl][PF<sub>6</sub>], and [(η<sup>6</sup>-THA)Ru(en)Cl][PF<sub>6</sub>] were such examples. Stable {Metallodrug}-{B<sub>12</sub>} complexes can be achieved with reasonably-sized {Metallodrug}. Computer modeling can certainly support the screening of a suitable {Metallodrug}.

---

## III.2 {Organic-drug}-{B<sub>12</sub>} double prodrugs

### III.2.1 Synthesis of B<sub>12</sub> double prodrugs

Traditional drugs are mainly organic compounds. It is therefore interesting to conjugate these compounds to B<sub>12</sub>. A coordination chemistry approach to this goal was using transplatin as a mediator for conjugating of B<sub>12</sub> and organic drugs. Transplatin was selected to reduce {drug}-{B<sub>12</sub>} steric interaction. The strong *trans*-effect of CN<sup>-</sup> labilizes the *trans*-Cl<sup>-</sup>, which can then be substituted by a strong incoming ligand. On the other hand, CN<sup>-</sup> also labilizes the new group, which can be released under suitable conditions. However, substitution reactions with **2** are competed by decomposition of **2** at elevated temperature. At temperatures > 50°C or reaction times > 1 day, **2** decomposes. The β-axial ligand was replaced by water yielding Cbl-OH<sub>2</sub> as evident from HPLC detection. The syntheses of **4-6** were, therefore, performed at high concentration (10-30 mg/ml of **2**) and at T < 40°C. In case of **5**, HPLC and ESI-MS evidenced cleavage of methyl groups in Dac at T ~ 50°C.

The chemical shifts of the five aromatic protons in B<sub>12</sub> were preserved whereas those of the additional aromatic protons from Cyt, Dac and Ana were detected in the correct respective ratios (Figure 2 and Appendices). Resulting from the shielding effect of the new ligands Cyt, Dac and Ana in **4-6**, the platinum signal (<sup>195</sup>Pt-NMR) is shifted upfield.<sup>79, 113, 119, 120</sup> Cyt, Dac, and Ana rendered **4-6** more lipophilic as compared to **2**. This resulted in good HPLC separation from the starting material **2**, B<sub>12</sub>, and Cbl-OH<sub>2</sub> (Figure 3).

Whereas Dac and Ana dissolve slightly in water, **4-6** exhibit very good water solubility. Thus, water insoluble organic drugs can become water soluble when bound to B<sub>12</sub> as carrier. These compounds are prodrugs since the platinum complex as well as the organic drugs can be released from B<sub>12</sub> (vide infra). Newly-designed prodrugs must generally meet at least three requirements to be biologically applicable; i) sufficient plasma stability to ensure prodrug integrity until targeted organs are reached, ii) chemical modification must not influence the intended targeting properties, and iii) drugs must be released inside targeted organs to exhibit therapeutic activities. These criteria apply also for double prodrugs with two-step release mechanisms. Since targeted delivery of Cyt has attracted great attention, **4** was selected to further study the compliance with these three requirements.

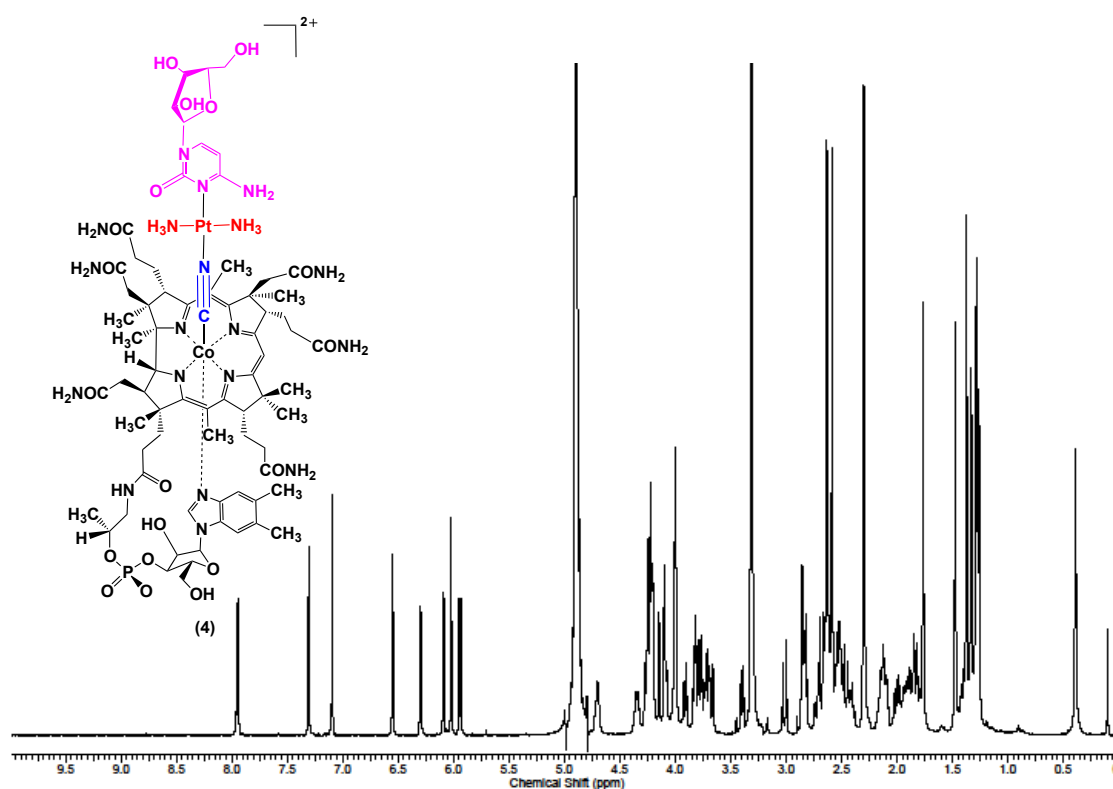


**Figure 2:** <sup>1</sup>H-NMR spectrum of cytarabine conjugated to B<sub>12</sub> via transplatin linker **4**.

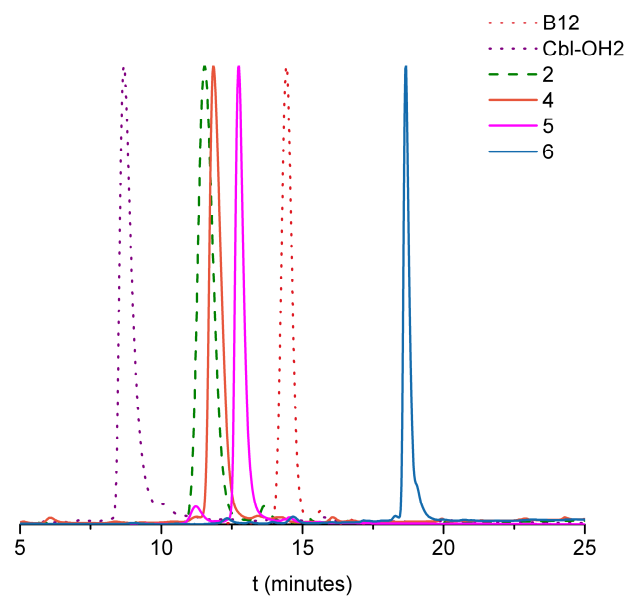


**Figure 3:** HPLC separation of compounds **4-6** from the starting material **2**, B<sub>12</sub>, and Cbl-OH<sub>2</sub>.

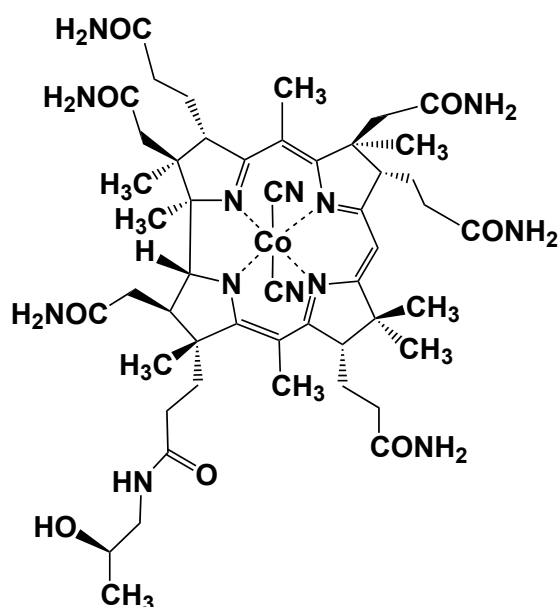
### III.2.2 Stability of B<sub>12</sub> double prodrugs

Following previous B<sub>12</sub>-prodrugs,<sup>79, 113</sup> the plasma stability of **4** was examined through binding to HSA in physiological conditions. The stability was monitored daily on HPLC columns 1 and 2 throughout a three-day period. Decomposition of compound **4** resulted in B<sub>12</sub> and platinated cytarabine species, which were detectable on RP-HPLC. In parallel, SEC-HPLC monitored variation of the ratio between the high and low molecular weight signals. After 3 days, ca. 3% of **4** or its decomposition products were bound to HSA, ca. 2.7% was present as free B<sub>12</sub>. It is known that B<sub>12</sub> does not bind significantly to HSA.<sup>113</sup> A blank experiment with B<sub>12</sub> showed ca. 1-2% associated to HSA under the same experimental condition. The observed HSA affinity is therefore not related to B<sub>12</sub>. In fact, Cbl-OH<sub>2</sub> as released after cleavage of [*trans*-CN-Pt(NH<sub>3</sub>)<sub>2</sub>]-{Cyt}]<sup>+</sup> exposed an available coordination site which is prone to be substituted by S- and N-donor sites from HSA.<sup>121</sup> Besides, the compound **4** can form lipophilic interaction with HSA similarly to B<sub>12</sub>.<sup>113</sup> The 3% HSA binding capacity of **4** underlines its higher stability with respect to **2**, which holds 11% HSA binding capacity only after 1 day. The Cl<sup>-</sup> ligand in **2** is obviously faster replaced by HSA than the aromatic amines in **4-6**.<sup>79, 113</sup>

---

### III.2.3 Affinity of B<sub>12</sub> double prodrugs to B<sub>12</sub> transport proteins

To assess requirement ii) for prodrugs, the binding properties of **4** to B<sub>12</sub> transport proteins were studied by DSF technique. TC binding is crucial for targeting tumors with over-expression of TC-Rs. The Cbl-affinities and specificities are high towards IF<sup>122</sup> and TC<sup>45</sup> whereas HC is known to tolerate even substantial variations of Cbl structures.<sup>41</sup> For example, cobinamide (Cbi) still binds firmly to HC albeit the absence of the nucleotide loop (Scheme 18).<sup>42</sup> In contrast, IF and TC do not binding to Cbi since the structure alterations are too substantial.



**Scheme 18:** Structure of Cbi.

In DSF technique, a fluorescent dye interacts with the hydrophobic sites of proteins upon thermal unfolding. The melting temperature ( $T_m$ ) of proteins can be inferred from the recorded fluorescence curves.<sup>123</sup> Differences in  $T_m$  between the ligand-bound and free forms of proteins ( $\Delta T_m$ ) indicate ligand-protein affinity. By comparing the measured  $\Delta T_m$  values for **4-6** to the obtained values with B<sub>12</sub> and Cbi, the affinity could be concluded. Despite the presence of rather bulky  $\beta$ -axial groups, **4-6** maintained good affinity to the B<sub>12</sub> transport proteins, indicated by similar  $\Delta T_m$  values as measured for B<sub>12</sub> (Figure 4). The  $\Delta T_m$  values for HC binding were  $\sim 16^\circ\text{C}$  for **4**,  $\sim 19^\circ\text{C}$  for **5**,  $\sim 15^\circ\text{C}$  for **6**, and  $\sim 22^\circ\text{C}$  for B<sub>12</sub>. In case of TC,  $\Delta T_m$  for B<sub>12</sub> is  $\sim 12^\circ\text{C}$ , which compares well with  $\sim 10^\circ\text{C}$  for **4-6**. The same situation was also found with IF. B<sub>12</sub> and **4-6** hold similar  $\Delta T_m \sim 7\text{-}8^\circ\text{C}$ . None of the compounds **4-6** showed similar

$\Delta T_m$  to those of Cbi in case of TC and IF ( $\sim 1$ -2°C). These results strongly indicated potential binding of **4-6** to all B<sub>12</sub> transport proteins.

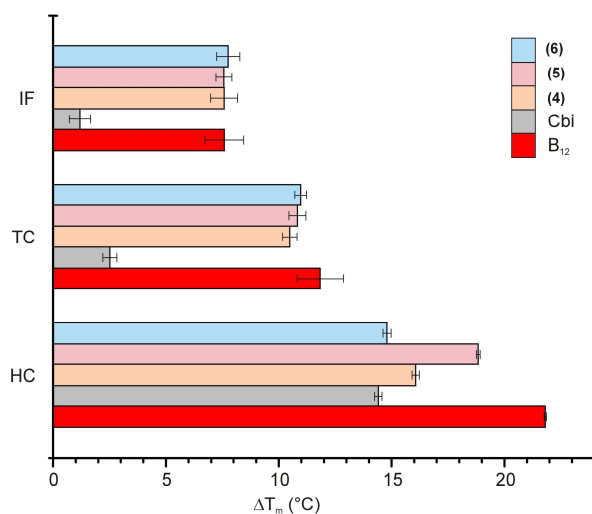
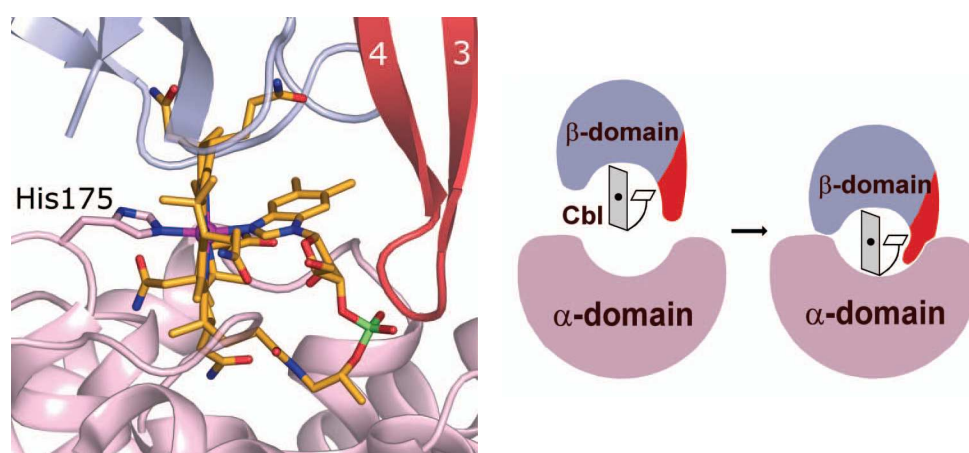


**Figure 4:** Thermal shift of **4-6**, B<sub>12</sub>, and Cbi to Cbl transport proteins.

All three transport proteins are known to have two-domain structures.<sup>124</sup> The crystal structure of holo-TC revealed that Cbl is captured in a cleft between these two domains. The Cbl binding sites of the protein interact with all side chains of the corrin ring and two oxygen atoms of the phosphate group. The  $\beta$ -axial group and the 5'-OH group on the nucleotide ribose are not involved in Cbl-TC interaction (Scheme 19). These positions are, as in this study, attractive for derivatizations without affecting affinities.<sup>64</sup> The  $\Delta T_m$  values found with **4-6** confirm this concept and are coincident with a number of other B<sub>12</sub> derivatives for diagnostic and therapeutic purposes.<sup>66, 67, 72, 73, 76, 112, 122</sup>



**Scheme 19:** Cbl bound to two domains of bovine TC: the corrin plane lied perpendicular to the domain interface. Histidine displaced water at  $\beta$ -position.<sup>125</sup>



### III.2.4 Reductive release of drugs from B<sub>12</sub> double prodrugs

In the cellular environment, Co<sup>III</sup> in B<sub>12</sub> is reduced to Co<sup>II</sup>, resulting in the cleavage of the  $\beta$ -axial ligand.<sup>126</sup> As we have shown in different assays, pure [Pt<sup>II</sup>]-complexes are cleanly freed through this process. The release of Cyt together with the Pt<sup>II</sup> complex from **4** was achieved by electrochemical and chemical reduction. At -700 mV, UV/Vis spectroscopy revealed a gradual increase of the absorbance at 476 nm and a decrease at 361 nm, an indicative feature for reduction of Co<sup>III</sup>  $\rightarrow$  Co<sup>II</sup> (Figure 5).

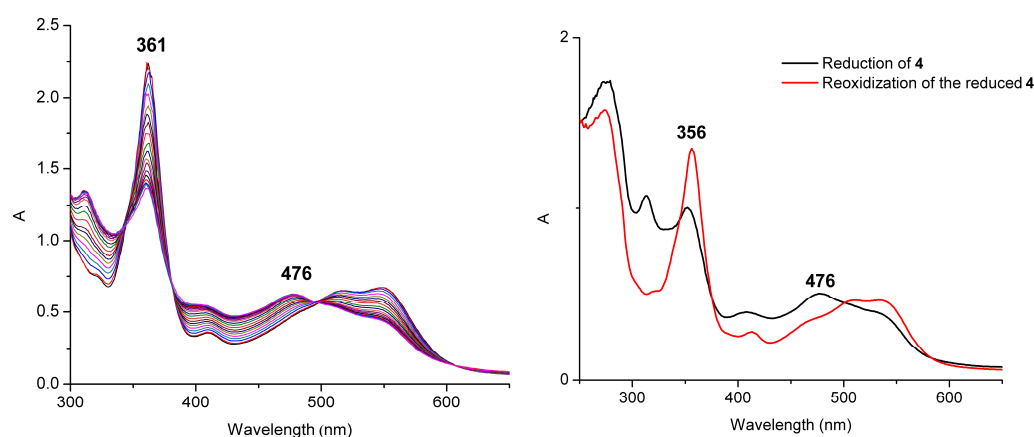


**Figure 5:** UV spectra changes in the reduction of **4** at -700mV (left) and after reduction with Zn/NH<sub>4</sub>Cl (red, right) followed by reoxidization (black, right)

Chemically, **4** was reduced with Zn<sup>0</sup> and subsequently reoxidized in air. The formation of Cbl-OH<sub>2</sub> was confirmed by absorbance maximum at 356 nm (Figure 5) and the detection of a Cbl-OH<sub>2</sub> peak in HPLC chromatogram. Besides the peak for Cbl-OH<sub>2</sub>, a species was eluted at a retention time similar to Cyt (Figure 6).

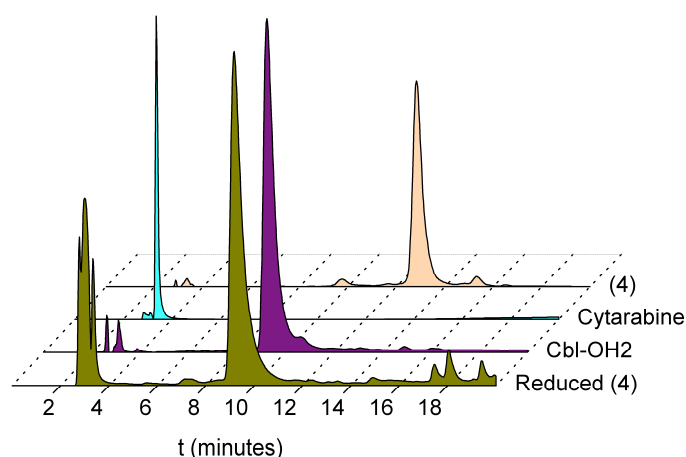
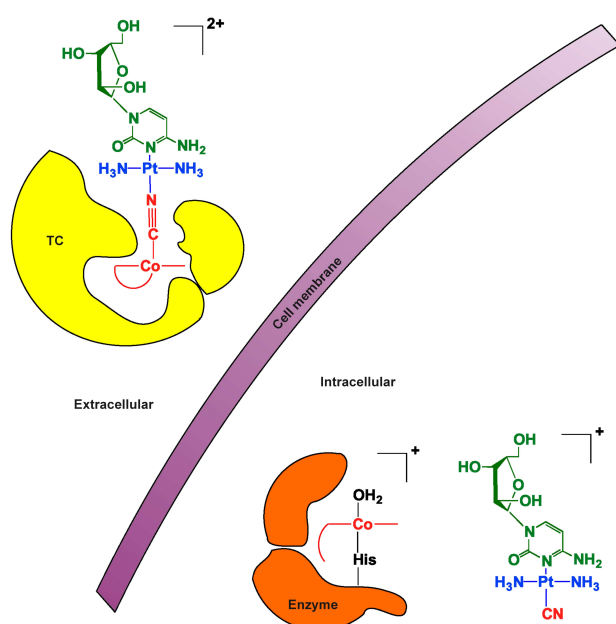


**Figure 6:** HPLC chromatograms of the product mix from reduction of **4** with Zn/NH<sub>4</sub>Cl.

An ESI-MS spectrum of the complete raw reaction mixture after chemical reduction evidenced  $[M+1]^+$  of Cyt (244.7),  $[M-H_2O+1]^{2+}$  of Cbl- $OH_2$  (665.1), and  $[M]^+$  of  $[trans\text{-Cyt-CN-Pt}(\text{NH}_3)_2]^+$  (498.2) (Figure 7). Over extended time period, ESI-MS evidenced disappearance of the  $[trans\text{-CN-Pt}(\text{NH}_3)_2]\text{-}\{\text{Cyt}\}^+$  signal whereas the signals of Cbl- $OH_2$  and Cyt persisted. A signal of Cyt dimer (487.2) also appeared (Figure 7), which could either be an artifact obtained during ionization process in the MS or a by-product of prolonged stirring the reaction mixture. In summary, the reduction of  $\text{Co}^{\text{III}} \rightarrow \text{Co}^{\text{II}}$  leads to cleavage of the entire  $\beta$ -axial ligand  $[trans\text{-CN-Pt}(\text{NH}_3)_2]\text{-}\{\text{Cyt}\}^+$  and over extended time periods, Cyt is cleaved from the  $\text{Pt}^{\text{II}}$  complex as well, nicely confirming the double prodrug concept (Scheme 20).



**Scheme 20:** Drug release mechanism of prodrug B<sub>12</sub> with a transplatin linker.

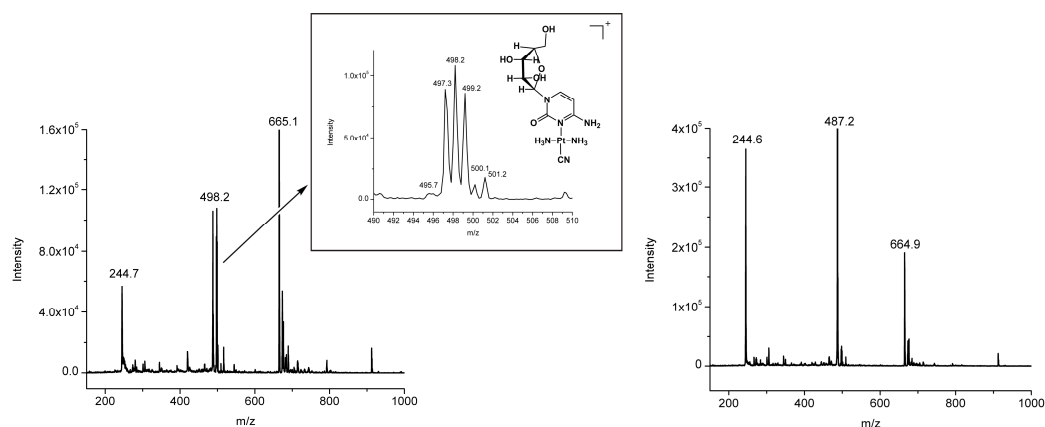


**Figure 7:** ESI-MS spectra of product mix from reduction of **4** with  $\text{Zn}/\text{NH}_4\text{Cl}$ : immediately after the reduction (left) and of the same mix after one day (right).

### III.2.5 In vitro cytotoxicity of B<sub>12</sub> double prodrug

Prodrugs or double prodrugs must not necessarily release their cargo before reaching their targets and therefore, the cytotoxicity of these compounds is a central concern. To assess if **4** was essentially non-toxic (no release of Cyt) or as toxic as the native drug, we investigated the in vitro cytotoxicity on the human chronic myelogenous leukemia cell line K562. For comparison, the double prodrug **4**, pure Cyt and chemically reduced **4** were studied. The double prodrug **4** showed an IC<sub>50</sub> in the nanomolar range ( $230 \pm 62$  nM) which is much lower than or comparable to the IC<sub>50</sub> for published B<sub>12</sub>-prodrugs; for instance, the cisplatin conjugate of B<sub>12</sub> **1** displayed an IC<sub>50</sub> value of about 8  $\mu$ M on a A2780 cell line<sup>126</sup> and a cobalt bound colchicine derivative of B<sub>12</sub> an LC<sub>50</sub> value of about 40-300 nM on different cell lines.<sup>72</sup> This IC<sub>50</sub> value mirrors the high cytotoxicity of Cyt (IC<sub>50</sub> =  $30 \pm 5$  nM), released from **4** via a slow, double cleavage process. Reduction of **4** with Zn/NH<sub>4</sub>Cl provided a convenient approach to examine cytotoxicity of the cleaved drug. Accordingly, the released complex [*trans*-Cyt-CN-Pt(NH<sub>3</sub>)<sub>2</sub>]<sup>+</sup>, being the active compound, exerted a similar cytotoxicity (IC<sub>50</sub> =  $30 \pm 11$  nM) as Cyt itself. In this approach, Cyt bound to Pt<sup>II</sup>, represents a single prodrug. After cell uptake, Cyt is cleaved from Pt<sup>II</sup> and exerts its cytotoxicity, comparable to pure Cyt. In the two-step release mechanism above, **4** is first taken up by the cell, the complex [*trans*-Cyt-CN-Pt(NH<sub>3</sub>)<sub>2</sub>]<sup>+</sup> is enzymatically cleaved from B<sub>12</sub> and then the Cyt is set free by substitution. The obtained approximately eight times lower IC<sub>50</sub> value is reasonable, taking the different chemical and biological processes related to the double-prodrug approach into account. A similar trend was also observed for other B<sub>12</sub> based single prodrugs.<sup>126</sup> The IC<sub>50</sub> of **4** reflects therefore a realistic effect of the double prodrug **4**.

---

### III.3 {Imaging agent}-{B<sub>12</sub>} conjugates

#### III.3.1 Fluorescent B<sub>12</sub> derivatives

Fluorescence microscopy has high spatial resolution, which makes it a robust visualization technique for subcellular accumulation of compounds. With a millimetre-ranged resolution,  $\gamma$ -radioimaging is widely applied in in-vivo visualization.<sup>127</sup> We initially aimed to produce a [<sup>99m</sup>Tc]-analogue of **22** from the precursor **21**. A complementary pair of radioactive and fluorescent B<sub>12</sub> derivatives would allow direct correlation of in-vivo and subcellular in-vitro imaging.

The fluorescence of **20** was based on the coordination of [bis(quinoline)] to [Re<sup>I</sup>(CO)<sub>3</sub>]<sup>+</sup>. This type of complexes was found to have long emission lifetime, good quantum yield, and large Stokes' shift suiting for biological application.<sup>128</sup> Doyle et. al reported the conjugation of such [Re-bis(quinoline)] fluorophore to B<sub>12</sub> **22**.<sup>66</sup> We, however, did not observe fluorescence of **22**. The quenching effect of B<sub>12</sub> on **20** was tested by adding equivalent amount of B<sub>12</sub> to a solution of 50  $\mu$ M **20**. The fluorescence of **20** was severely quenched (Figure 8). The fragile fluorescent property of **22** was confirmed later<sup>78</sup> by Doyle et. al.. Therefore, **22** was not studied further.

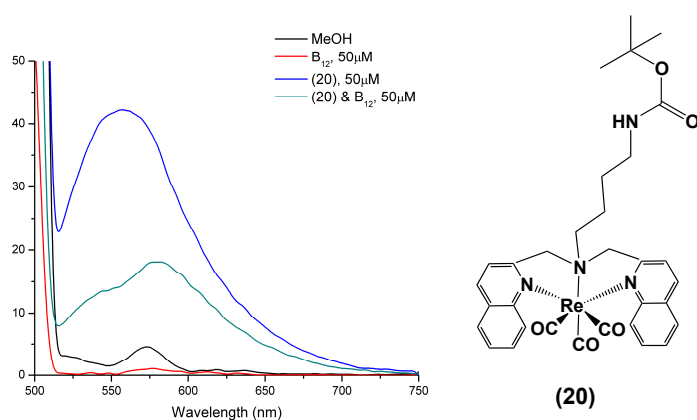


**Figure 8:** Quenching effect of B<sub>12</sub> on **20**.

The formation of {B<sub>12</sub>}-{dansylimidazole} conjugate **7** was characterized by the fourteen aromatic signals on <sup>1</sup>H-NMR (five signals from B<sub>12</sub> and nine signals from Dansylimidazole) (Figure 9). Similarly, compound **9** has seven aromatic <sup>1</sup>H-NMR signals (five from B<sub>12</sub> and two from NBD-CO-Hz) (Appendices).

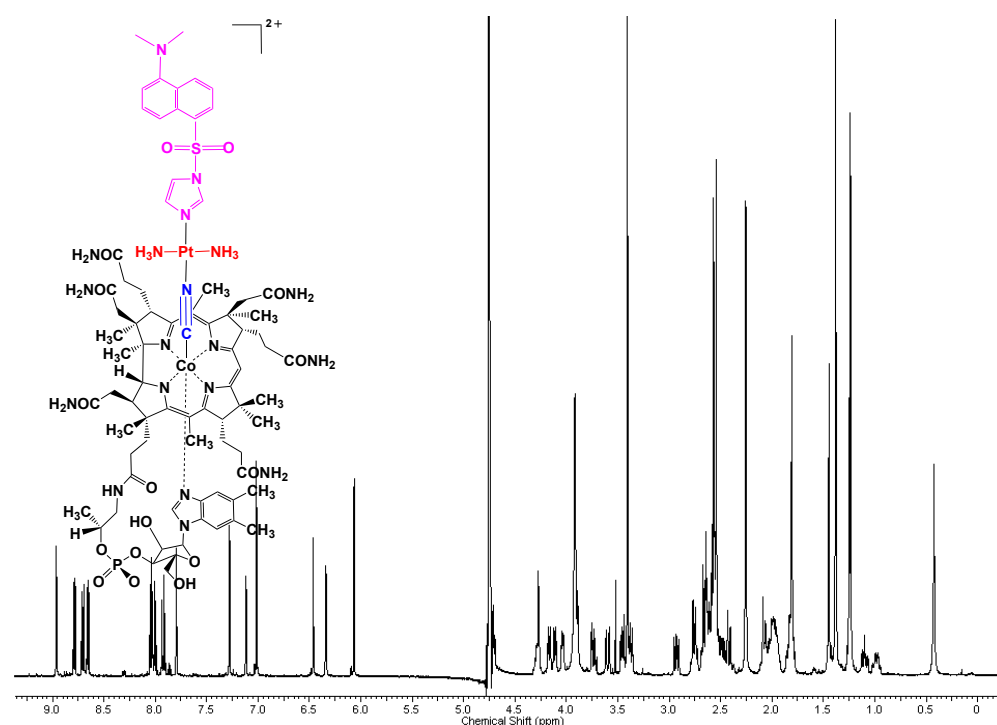


**Figure 9:**  $^1\text{H}$ -NMR spectrum of compound **7**, {B<sub>12</sub>}-{dansylimidazole} with a transplatin linker

Dansylimidazole<sup>129</sup> and NBD-CO-Hz<sup>130</sup> (Scheme 21) were not severely quenched by B<sub>12</sub> (Figure 10). This is similar to the conjugation of Dansyl to B<sub>12</sub> via [*cis*-Pt(NH<sub>3</sub>)<sub>2</sub>-CN-imidazole]<sup>+</sup> bridge.<sup>131</sup> Dansyl fluorophore was previously conjugated to the Co-center of Cbl via a propylamine linker (Scheme 8,b); however, fluorescence was completely quenched by Cbl.<sup>75</sup> As fluorophore-corrin interaction was accounted for the quenching effect of Cbl, the retained fluorescence of **7** hinted that the linker [*cis*/*trans*-Pt(NH<sub>3</sub>)<sub>2</sub>-CN-imidazole]<sup>+</sup> oriented the dansyl fluorophore further away from the corrin ring compared to propylamine linker.

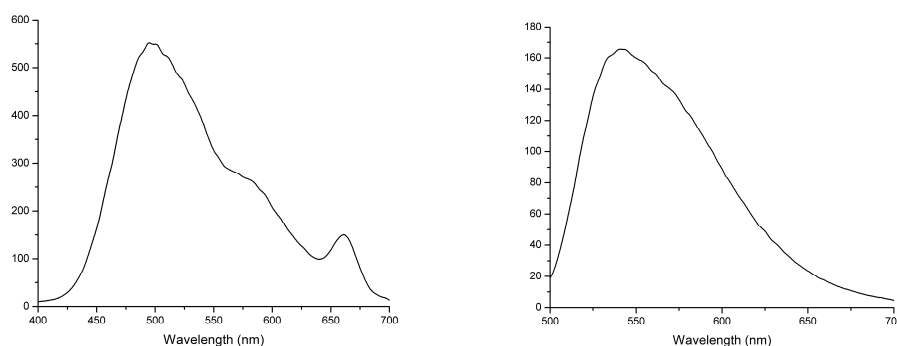
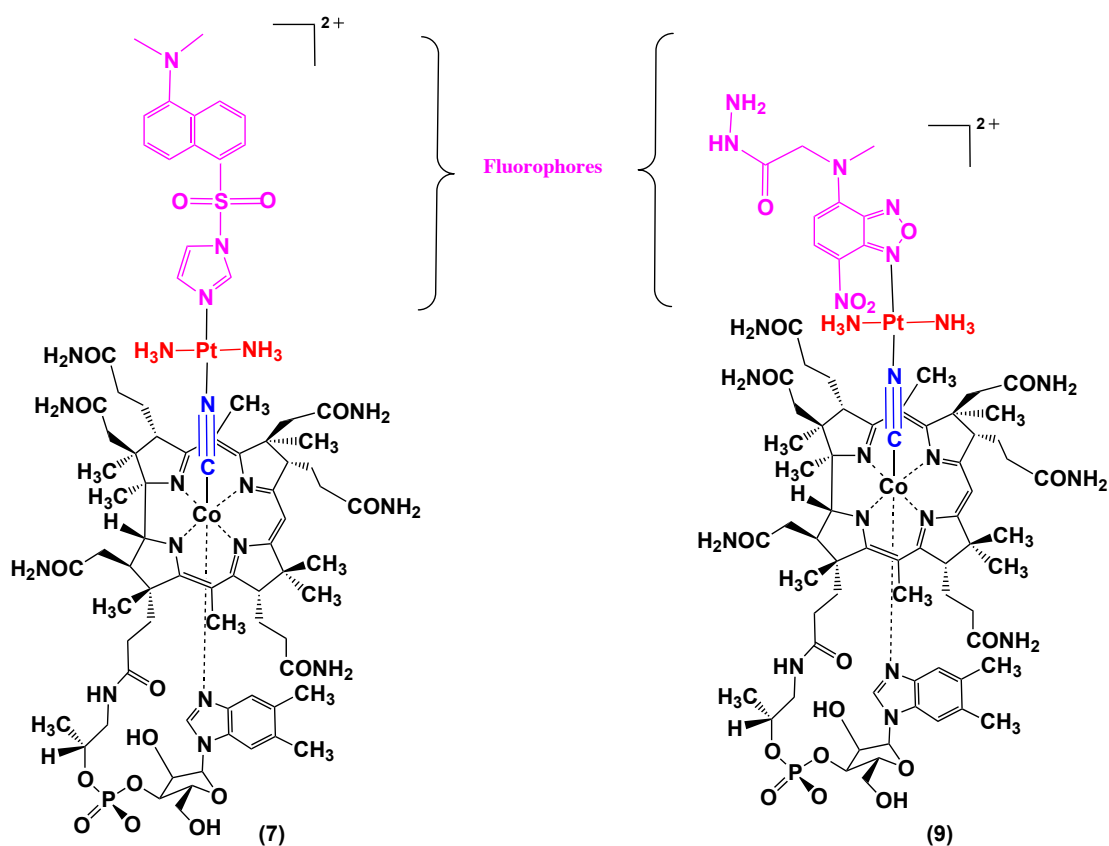


**Figure 10:** Emission spectrum of **7** (left) and **9** (right) at a concentration of 50  $\mu\text{M}$ . Excitation wavelengths were 330nm and 483nm, correspondingly.

Compounds **7** and **9** were stable in water and light. The fluorophores were, however, cleaved off in the presence of HSA.

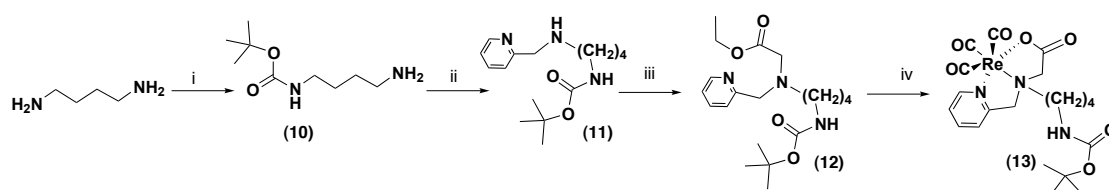


**Scheme 21:** Structures of B<sub>12</sub> conjugates with fluorophores dansylimidazole (left) and NBD-CO-Hz (right) via the transplatin linker.

### III.3.2 [ $^{99m}\text{Tc}$ ]-labeled- $\text{B}_{12}$ prodrugs

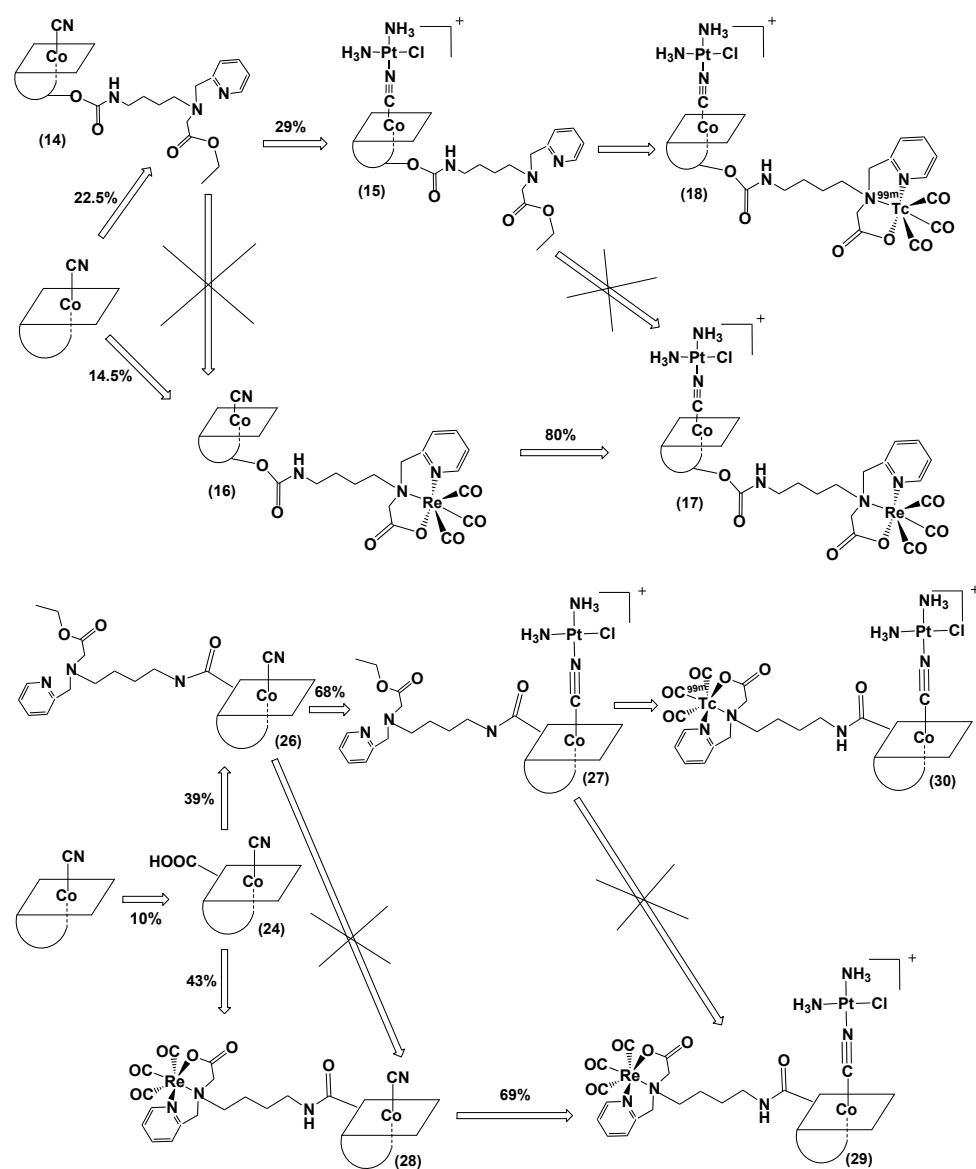
#### III.3.2.1 Synthesis of $\text{B}_{12}$ prodrugs

The tridentate [N,N,O] ligand **12** was chelated to  $[\text{Re}^{\text{I}}(\text{CO})_3]^+$  to form **13** (Scheme 22) before coupling to  $\text{B}_{12}$ . In this manner, competitive coordinations of  $[\beta\text{-CN}^-]\text{-}[\text{Re}^{\text{I}}]$  and  $[\text{N,N,O}]\text{-}[\text{Pt}^{\text{II}}]$  were avoided.<sup>112</sup> Both  $\{\text{Re}^{\text{I}}(\text{CO})_3\}\text{-}\{\text{B}_{12}\}$  conjugates, **16** and **28**, posed  $\beta\text{-CN}^-$  as the only coordination site to  $\text{Pt}^{\text{II}}$  in the last step (Scheme 23). Conjugation of the tridentate ligand to  $\{\text{B}_{12}\}$  resulted in additional four aromatic  $^1\text{H}$ -NMR signals for compounds **14-17** and **26-29** (Appendices).



**Scheme 22:** Reaction pathway to produce chelate ligand **12** and its Re-complex **13**.

$[\text{Re}^{99m}\text{Tc}]$ -labeled-products are of low concentration as  $[\text{Re}^{99m}\text{TcO}_4]^-$  is commercially available only at  $10^{-8}$ - $10^{-7}\text{M}$ . As the coordination of  $[\beta\text{-CN}^-]\text{-}[\text{Pt}^{\text{II}}]$  requires mM-concentration,<sup>79</sup> the synthesis order to produce  $\{\text{Re}^{99m}\text{Tc}\}\text{-}\{\text{B}_{12}\}\text{-}\{\text{cisplatin}\}$  conjugates, **18** and **30**, was different from their cold Re-analogues. The [N,N,O] tridentate ligand remained open during the formation coordinative  $[\beta\text{-CN}^-]\text{-}[\text{Pt}^{\text{II}}]$  bond. Only thereafter it was chelated with  $[\text{Re}^{99m}\text{Tc}(\text{CO})_3]^+$  (Scheme 23). The final, labeled products were characterized by comparing HPLC retention times with their cold Re-analogues, **17** and **29**. The ca. 5 minute-difference of elution time between the labeled products and their cold starting materials, **15** and **27**, allowed convenient purification by HPLC (Figure 11).



**Scheme 23:** Reaction pathways for producing TC-binder **17** (above), non-binder **29** (below) and their  $^{99m}\text{Tc}$ -labeled analogues **18**, **30**.

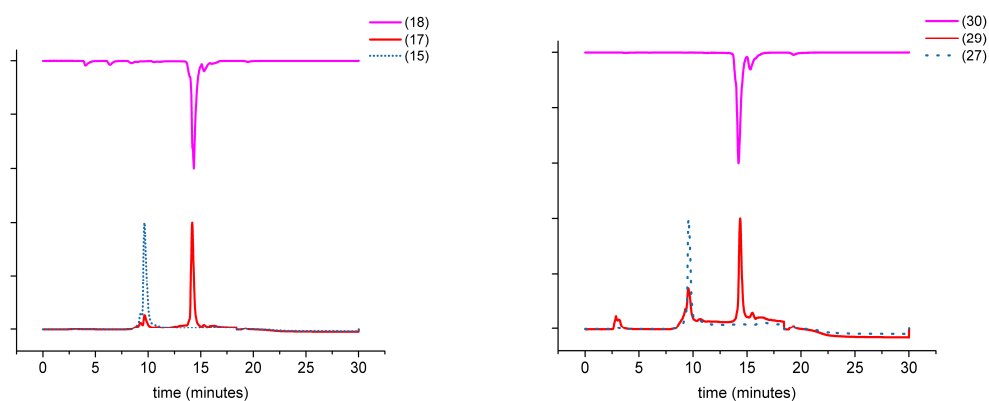


**Figure 11:** HPLC traces of radioactive **18**, **30** with respect to the cold analogues **17**, **29** and the starting materials **15**, **27**.



### III.3.2.2 Affinity of B<sub>12</sub> prodrugs to transcobalamin

Crystal structure of holo-TC pointed out that the ribose 5'-OH did not involve in TC binding (Scheme 19).<sup>64</sup> The ribose-derivative **17** indeed showed  $\Delta T_m$  similar to those of B<sub>12</sub>. This confirmed that it maintained interaction with all Cbl transport proteins. As Tc and Re share analogous properties owing to “lanthanide contraction”, a biological system does not distinguish **17** from **18**. We, therefore, conclude that **18** also holds affinities to HC, TC, and IF.

In contrast, Scheme 19 showed H-bonds between the b-side of Cbl-OH<sub>2</sub> and the C-terminal  $\beta$ -domain of TC.<sup>64</sup> This indicated that modification at the b-side is critical to Cbl-TC affinity. In a previous publication, binding to TC was deteriorated by a b-side-derivative of B<sub>12</sub>.<sup>70</sup> This increased the tumor-selectivity of the compound's dissemination in mice. HC was appointed to mediate the tumor uptake. Following this strategy, compounds **29** and **30** were also derivatized at b-side to increase tumor-selectivity. Indeed,  $\Delta T_m$  values of **29** with TC and IF indicated it was not bound to both proteins (Figure 12) as the two values were in the same range with those of Cbi (Figure 4). Based on the “lanthanide contraction”, we conclude that **30** also lost affinity to both TC and IF.

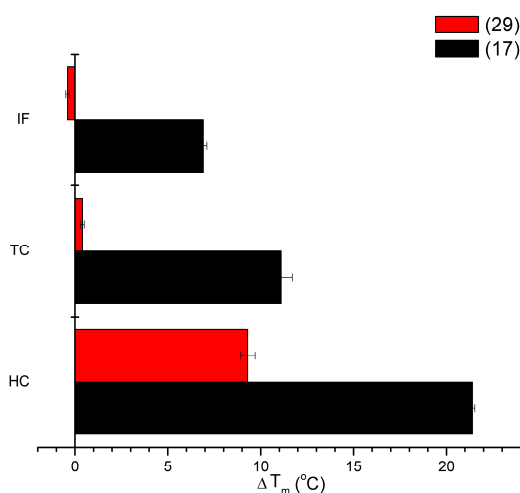


**Figure 12:** Thermal shift of **17** and **29** to transport proteins.

### III.3.2.3 Cell uptake of B<sub>12</sub> prodrugs

The importance of TC in mediating uptake of **18** and **30** was studied on leukemia K562 culture. The Cbl-and-folic-acid depleted medium was obtained commercially and FCS was treated with QUSO in order to exclude background TC/Cbl.<sup>83</sup> Internalization of TC-**18** was up to 10-20 times higher than free **18** whilst the presence of TC did not affect significantly cellular import of **30** (Figure 13). As K562 cells do not produce TC,<sup>132</sup> the added TC accounted for the total TC in culture. The results confirmed that a Cbl with affinity to TC benefits from increased cellular import of TC-mediated-endocytosis.

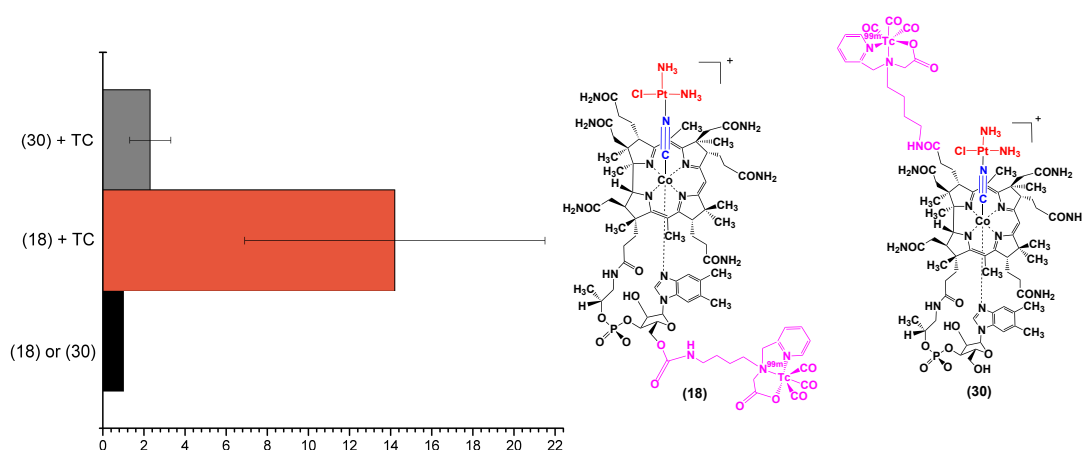


**Figure 13:** Relative uptake of **18** and **30** in the presence and absence of TC.

ICPMS is a reliable technique for trace element analysis, especially metals. It is woven from the robust sample atomization of argon plasma and the sensitive detection of mass spectrometry. A nebulizer turns liquid sample into aerosol of fine droplets, which will be introduced into a spray chamber. This step excludes larger droplets and allows only small-sized droplets to enter the 6000°C plasma of the ICP torch. The high temperature dries the droplets out and atomizes the samples. The atoms subsequently lose an electron and single-charged ions are formed. The ions pass through an interface before reaching the vacuum of mass spectrometer. A quadrupole filters out neutrons and photons. Its voltage can be set to allow only ions with certain preset mass-to-charge ratio to hit the mass detector (Figure 14).

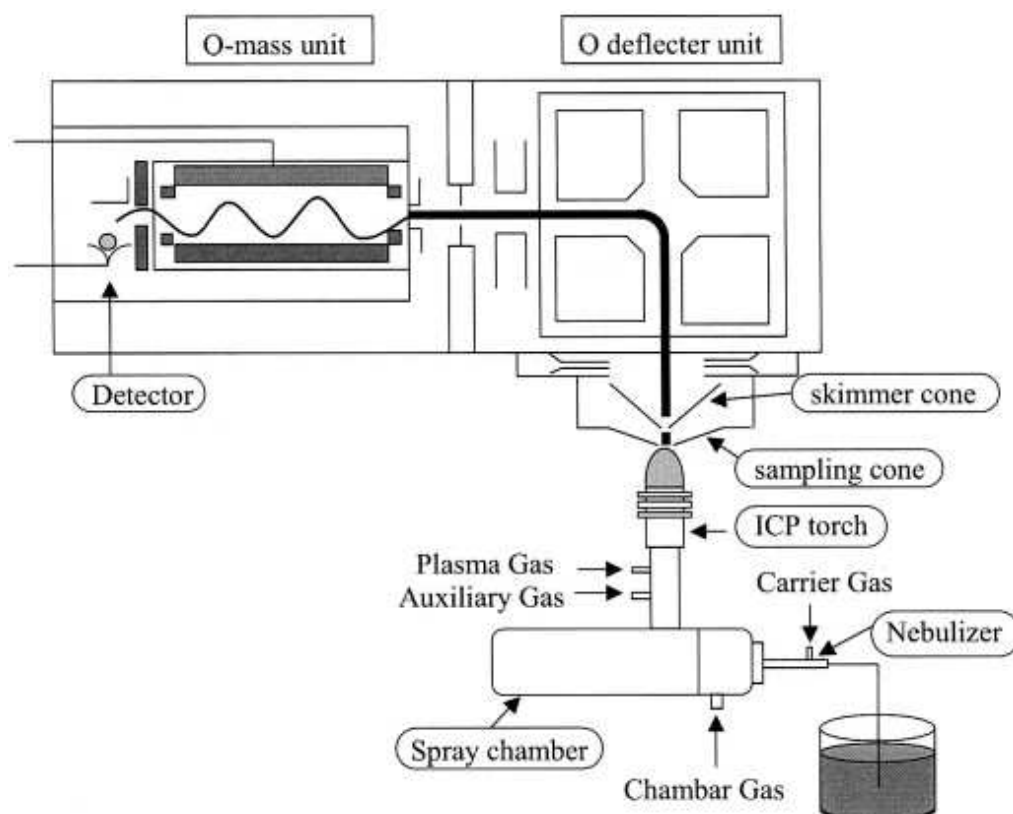


**Figure 14:** Sketch of an ICPMS instrument.<sup>133</sup>

ICPMS can measure quantitative correlation of the transition metals ( $^{59}\text{Co}$ ,  $^{195}\text{Pt}$ , and  $^{187}\text{Re}$ ) in  $\text{B}_{12}$  derivatives, which revealed their intracellular distribution (Figure 15). In this experiment, the leukemia culture was treated with a high dose of Cbl (ca.  $200\mu\text{g}$ ) compared to a healthy person's daily intake ( $4\mu\text{g/day}$ )<sup>45, 134</sup> and the TC-deficiency treatment dose (ca.  $0.5\text{-}2\text{ mg/ week}$ ).<sup>135</sup> The total uptake only accounted for less than 0.1% of the administered dose ( $\text{B}_{12}$  derivatives and  $\text{Cbl-OH}_2$ ), which is low compared to 4% and 1% uptake for  $50\mu\text{g}$  and  $1\text{-}2\text{mg}$  dose in human.<sup>136</sup> This is in agreement with the observation that the absorbed Cbl decreased with increasing dose.<sup>134, 136</sup> 80% of the administered dose remained in culture medium. The rest was probably membrane-bound and thus lost in the washing steps. Except for  $\text{B}_{12}$ , the absolute uptake was indeed high (ca.  $30\text{-}40\text{ pmol/mg protein}$ ) (Figure 15). It was ca. 5 times higher than an earlier report of Cbl content in liver (ca.  $7\text{ pmol/ mg protein}$ ). Liver was reported to store the highest Cbl amount in the body.<sup>134, 137</sup>

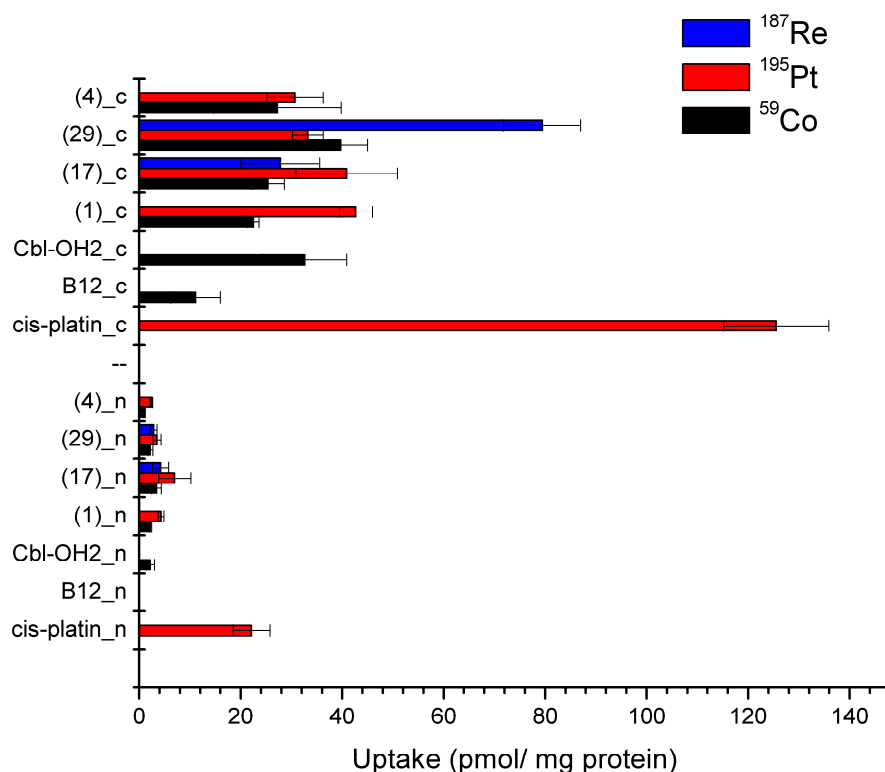


**Figure 15:** ICPMS uptake of platinated B<sub>12</sub> prodrugs. Cisplatin, B<sub>12</sub>, and Cbl-OH<sub>2</sub> were used as control samples.

Owing to different different cellular internalization pathways, the subcellular amounts of cisplatin are much higher than other platinated B<sub>12</sub> prodrugs **1**, **4**, **17**, and **29** (Figure 15). In case cisplatin were cleaved from B<sub>12</sub> structure before cellular internalization, the Pt-signals of **1**, **17**, and **29** would increase to the level of native cisplatin. However, the Pt-signals of these prodrugs remained rather similar to their Co-signals, which were close to the Co-signal of control Cbl-OH<sub>2</sub>. This confirmed that the B<sub>12</sub> derivatives protected properly cisplatin.

As apo-TC was not added in this assay, calf serum (10%) was the only source of TC in the culture. TC in calf serum can exist in both apo- and holo-forms. It was known that TC concentration in human serum is ca. 1nM, 10% of which is in the holo-form.<sup>13</sup> Though the exact quantity of apo-TC in culture was not determined, it was unlikely to be sufficient to transport the high-dose of administered Cbl (120 nmol). The background Cbl, which was found to be ca. 0.1 nmol, would certainly occupy available apo-TC, if any. Figure 15 showed an unexpected lower uptake of B<sub>12</sub> compared to that of the prodrugs. Even more surprisingly, it was also lower than

uptake of Cbl-OH<sub>2</sub>. As all administered Cbls, except for **29**, bind well to TC, these findings confirmed that the observed internalization was not based on the regular TC-mediated endocytosis.

Cbl-OH<sub>2</sub>, similar to other platinated B<sub>12</sub>-prodrugs, is a charged molecule whilst B<sub>12</sub> is a neutral compound. This indicated the existence of a charge-dependent uptake mechanism that neutral molecule like B<sub>12</sub> was not included. Whether charged Cbl compounds were distinctly recognized by a Cbl-specific receptor or they actually passed ionic channels on cell membrane requires further study. Behavioral differences between charged and neutral B<sub>12</sub> prodrugs were indeed previously observed.<sup>126</sup> Besides, uptake difference between B<sub>12</sub> and Cbl-OH<sub>2</sub> was earlier reported in human skin fibroblasts culture. In the presence of 10% serum, Cbl-OH<sub>2</sub> was better internalized and retained than B<sub>12</sub>.<sup>138</sup> The observation was, nevertheless, not rationalized.

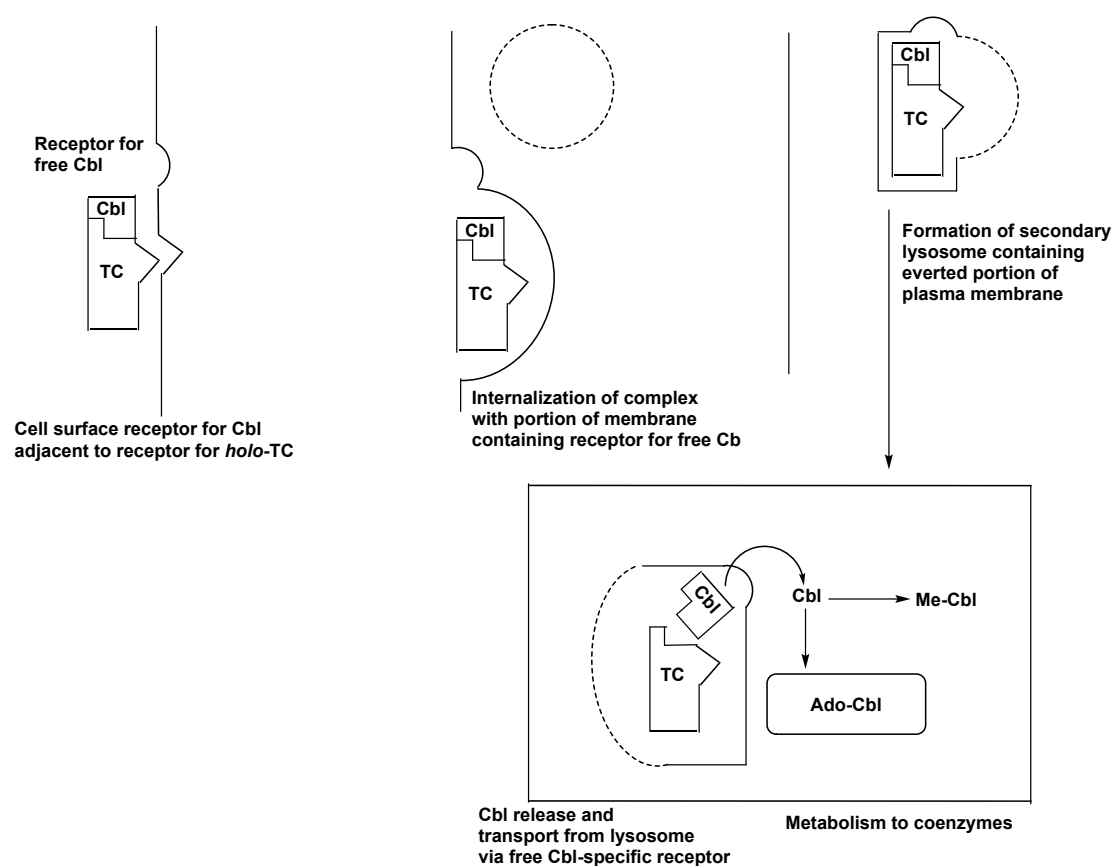
TC-independent uptake of Cbl was previously reported.<sup>139-142</sup> HeLa cells internalized only 1-2% of free B<sub>12</sub> with respect to holo-TC.<sup>139</sup> This agreed with a later finding that free Cbl supported cell growth ca. 100 to 1000-fold less efficiently than holo-TC.<sup>83</sup> These data indicated the existence of an uptake mechanism which is less efficient than the commonly-known TC-dependent pathway. However, the uptake of free-Cbl appeared to be dependent on the cell type. It was found to exceed 20% of holo-TC uptake in human skin fibroblasts.<sup>140</sup> It was proposed that free-Cbl could be internalized by either a cell membrane receptor or a serum protein. Berliner proposed a free B<sub>12</sub>-specific receptor on the cell membrane (Scheme 24). Hitzig suggested an  $\alpha$ 2-globulin-like protein in serum. In the latter experiment, a surplus dose of free B<sub>12</sub> (3 mg or 2.2  $\mu$ mol/week) sufficed to correct TC congenital deficiency.<sup>143</sup> The appearance of an  $\alpha$ 2-globulin-like protein was detected. It was found to increase the B<sub>12</sub> binding capacity. These findings, together with our suggestion of the charged-dependent Cbl uptake reflected once again the complexity of Cbl dissemination. Many pathways were uncovered; however, the complete understanding was still not achieved.

The different uptake patterns between **17** and **29** are puzzling. The [Re]-chelate was attached to the B<sub>12</sub> structure through a carbamate bond in **17**. Equivalent amounts of [<sup>59</sup>Co] and [<sup>187</sup>Re] in **17** indicated that the carbamate bond remained intact after cell internalization. [<sup>59</sup>Co]/[<sup>187</sup>Re] signals are lower than that of [<sup>195</sup>Pt] in **1**, **4**, and **17**. It

---

was possibly because the coordination CN-Pt bond is not as stable as the carbamate bond. If [ $^{195}\text{Pt}$ ]-fraction fell off, it would be internalized via the more efficient cisplatin import pathway.

The abnormal increase of [ $^{187}\text{Re}$ ] in **29**, on the other hand, hinted that the amide bond was possibly hydrolyzed before cellular entrance. This implied the lower bond strength of amide relative to carbamate. On the other hand, there may be protein involvement in weakening the amide bond as it was located at a critical site for protein interaction (b-side) whilst the ribose side was known to not influence affinity of Cbl to proteins.



**Scheme 24:** Cellular uptake pathway for free B<sub>12</sub>, proposed by Berliner et al.<sup>140</sup>

### III.3.3 [ $^{57}\text{Co}$ ]-labeled $\text{B}_{12}$ prodrug

The [ $^{57}\text{Co}$ ] analogue of [ $\{cis\text{-Pt}(\text{NH}_3)_2\}\text{-}\{\text{B}_{12}\}\}^+$  conjugate **1** was previously prepared.<sup>144</sup> However, significant activity loss to the reaction flask's wall was observed. It affected further in-vitro assays on the compound. In this project, **33** was successfully synthesized in a straightforward procedure. The  $\gamma$ -counter reading indicated ca. 88% of the radioactivity was recovered. Identity of the purified product was confirmed by cross-comparison of HPLC retention time with that of **1** (Figure 16). The product **33** has good stability. After four days (r.t., 0.9% NaCl), ca. 21% of **33** was decomposed to [ $^{57}\text{Co}$ ]- $\text{B}_{12}$ . Though **18** behaved similarly to **1**, **33** represented the closest structure similarity. It can serve as a good model to gain knowledge about behaviour of **1**.

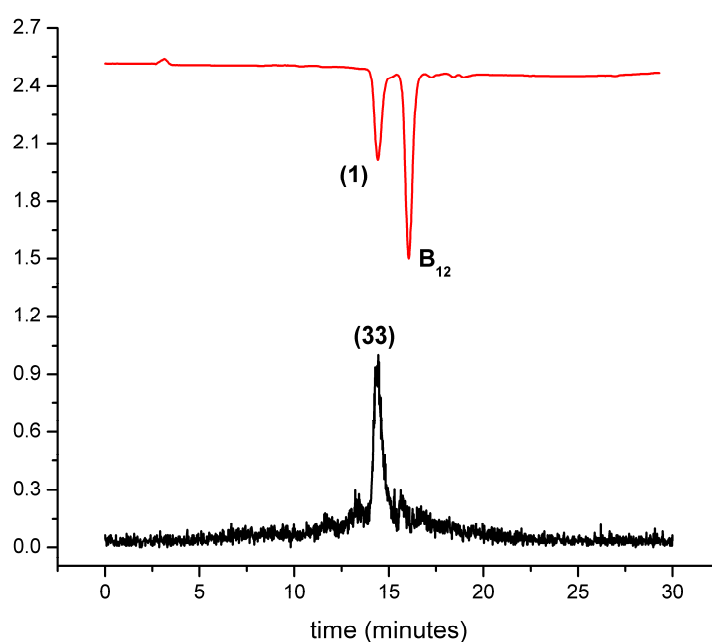


**Figure 16:** HPLC traces of  $\text{B}_{12}$ , **1** and **33** confirm successful coordination of [ $^{57}\text{Co}$ ]- $\text{B}_{12}$  to [ $cis\text{-Pt}(\text{NH}_3)_2\text{Cl}$ ] $^+$ .

## IV Conclusions

The primary aim of the project was to study the coordination of metallodrugs to vitamin B<sub>12</sub> via the CN<sup>-</sup>-bridge. In contrast with cisplatin, other metallodrugs did not form stable coordinative compounds with B<sub>12</sub> owing to steric restriction of both B<sub>12</sub> and the drugs. Most metallodrugs were designed with spacious geometries to achieve specific interaction with biomolecules. Polyaryl or cyclic ligands were commonly found. This sumptuous asset of metallodrugs hindered formation of stable conjugates with B<sub>12</sub>. Sufficient stability was only achieved with most small molecules like *cis*- and *trans*platin. Besides, expansion of [M] out of the [Pt<sup>II</sup>] border requires, in many cases, non-chromatographic purification. The availability of [M] and the convenience of separation techniques determine the success of this approach.

Extra space between drugs and bulky B<sub>12</sub> was achieved by extending the CN-bridge into the [*trans*-Pt(NH<sub>3</sub>)<sub>2</sub>-CN]<sup>+</sup>-bridge. This reduced the risk of structural restrictions in the conjugate. The double prodrug **4** is a good example of this strategy. It was stable at physiological condition. The delivery pathway of B<sub>12</sub> was preserved. More importantly, **4** was cytotoxic owing to a two-step release of the native drug. In addition, fluorophores were conjugated to B<sub>12</sub> via [*trans*-Pt(NH<sub>3</sub>)<sub>2</sub>-CN]<sup>+</sup>-bridge. Severe quenching effect of B<sub>12</sub> was not observed.

B<sub>12</sub> derivatives were labeled with either [<sup>57</sup>Co] or [<sup>99m</sup>Tc] as cellular distribution of these products can be measured. Derivatization was at both the corrin side chains and the back loop. The presence of TC enhanced uptake. This once more highlighted the importance of TC in studying biological behaviors of B<sub>12</sub> derivatives. B<sub>12</sub> prodrugs were, however, still internalized independent of TC. This uptake was measured by following signals of transition metals (<sup>59</sup>Co, <sup>195</sup>Pt, and <sup>187</sup>Re) in prodrug structures. This strategy allowed comparison between the prodrug and the native metallodrug. A lower uptake was observed for the prodrug, which was in agreement with lower cytotoxicity. Unexpectedly, this study showed that charged Cbls were preferably internalized into cells. This is noteworthy for future design of B<sub>12</sub> biological conjugates.

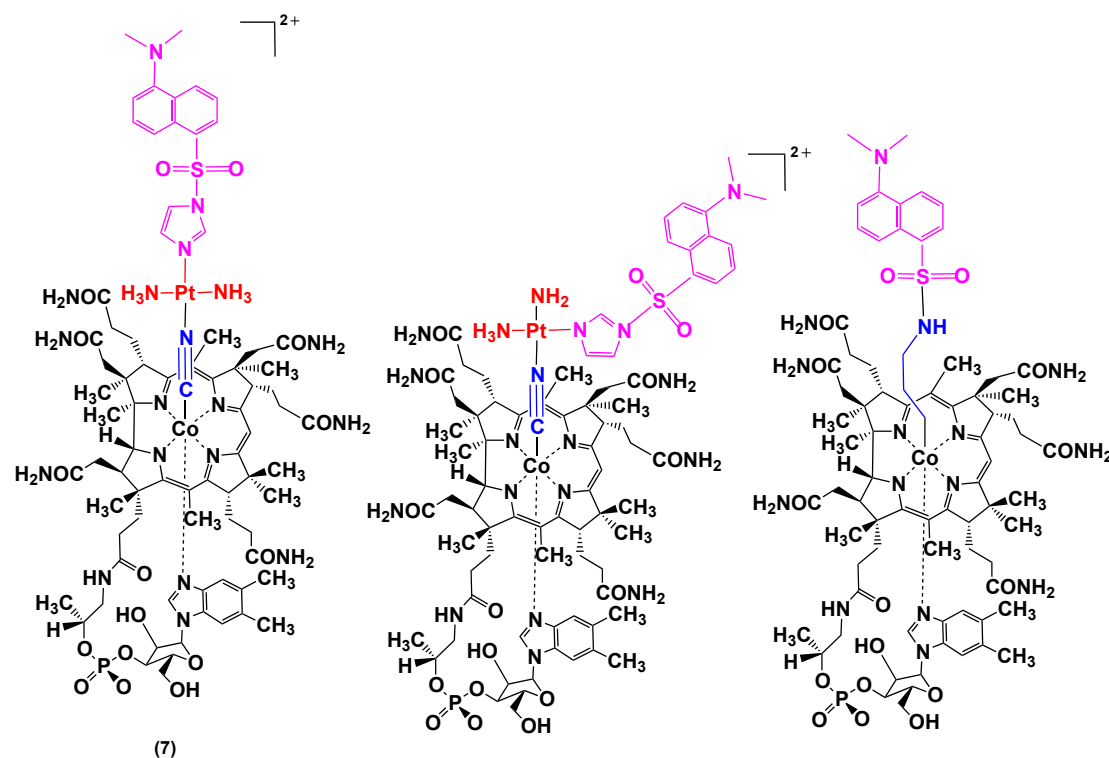


In conclusion, drugs (organic and metallo-compounds) and fluorophores can be conveniently conjugated to B<sub>12</sub> via the β-CN<sup>-</sup> bridge, whether or not extended by a [*trans*-Pt(NH<sub>3</sub>)<sub>2</sub>]<sup>2+</sup>-link. Coordination at the β-CN<sup>-</sup> was indicated by IR. Conjugation of aromatic drugs, fluorophores, or tridentate ligands resulted in the appearance of corresponding aromatic <sup>1</sup>H-NMR signals in addition to the ones from B<sub>12</sub>. This is a reliable fingerprint to characterize such complex B<sub>12</sub> derivatives. Inside the cells, the axial moieties are reductively released together with [*trans*-Pt(NH<sub>3</sub>)<sub>2</sub>-CN]<sup>+</sup>. The original drug or probe will subsequently be cleaved to exhibit their activities. Cellular internalization can be increased by bringing charges to structure of the conjugates. Biological behaviors of these conjugates can be measured by attaching a radioactive entity into their structures or by simply measuring the metal correlation.

---

## V Outlook

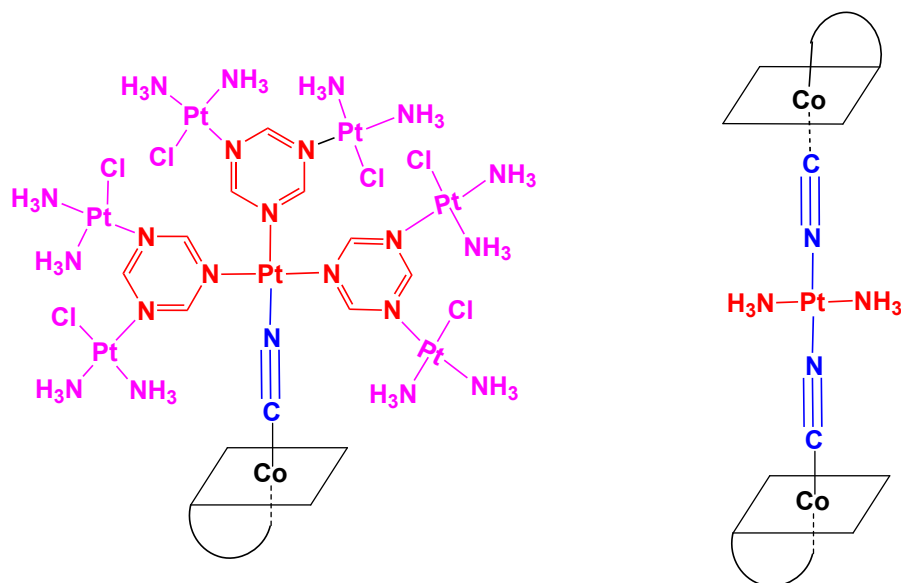
Whilst uptake of the B<sub>12</sub> prodrugs was reported for K562 cancer cell line in this thesis, the measurement of these compounds in a control healthy cell line shall be included. This would allow comparison about the targeting efficiency of B<sub>12</sub> prodrugs. The fact that B<sub>12</sub> did not quench dansyl and NBD-CO-Hz introduced at the *cis*- and *trans*-[Pt(NH<sub>3</sub>)<sub>2</sub>-CN-imidazole]<sup>+</sup>-bridge deserves further investigation (Scheme 25).<sup>131</sup> It was previously reported that propylamine-bridge did not prevent dansyl from being quenched by B<sub>12</sub>. The question then lies on what made a key difference between the metal-complex and organic bridges: whether the geometry of Pt-complexes or the addition of an imidazole played a more essential role in orienting the fluorophore away from the coring ring. In addition, the actual stability of such fluorescent B<sub>12</sub> derivatives shall be assessed in complex with TC before cell visualization experiments.



**Scheme 25:** Structures of three different {B<sub>12</sub>}-{dansyl} conjugates via [*cis*-/ *trans*-Pt(NH<sub>3</sub>)<sub>2</sub>-CN-imidazole]<sup>+</sup> (7 and middle) and propylamine bridges (right).<sup>75, 131</sup>

The drug loading capacity of B<sub>12</sub> is generally considered to be a limiting factor for its use as a delivery agent. This problem can be overcome if the [CN-Pt]-bridge complex has aromatic N-heterocycle ligands instead of NH<sub>3</sub>. Such ligands can coordinate to additional cisplatin molecules. An example is [Pt(triazine)<sub>3</sub>-CN]<sup>2+</sup>-bridge, which can allow total coordination of six cisplatin molecules (Scheme 26).

As transplatin allowed the coordination of other moieties into B<sub>12</sub>, it is interesting to know if it can allow the coordination of a second vitamin B<sub>12</sub>. The resulting sandwich dimer has a complex structure which may be interesting for catalysis purpose (Scheme 26).



**Scheme 26:** Structures of a multi-cisplatin-B<sub>12</sub> conjugate (left) and a sandwich dimer B<sub>12</sub> (right).

## VI Bibliography

1. M. T. Q. Tran, E. Furger and R. Alberto, *Org. Biomol. Chem.*, 2013, **11**, 3247-3254.
  2. A. Piro, G. Tagarelli, P. Lagonia, A. Tagarelli and A. Quattrone, *Ann. Nutr. Metab.*, 2010, **57**, 85-88.
  3. R. Banerjee, *Chemistry and biochemistry of B12*, John Wiley & Sons, New York, 1999.
  4. K. Okuda, *Journal of Gastroenterology and Hepatology*, 1999, **14**, 301-308.
  5. E. L. Smith, *Nature*, 1948, **161**, 638.
  6. E. L. Rickes, N. G. Brink, F. R. Koniuszy, T. R. Wood and K. Folkers, *Science*, 1948, **107**, 396-397.
  7. D. C. Hodgkin, J. Pickworth, J. H. Robertson, K. N. Trueblood, R. J. Prosen and J. G. White, *Nature*, 1955, **176**, 325-328.
  8. P. G. Lenhert and D. C. Hodgkin, *Nature*, 1961, **192**, 937-938.
  9. H. P. C. Hogenkamp, in *Chemistry and biochemistry of B12*, ed. R. Banerjee, John Wiley & Sons, New York, Editon edn., 1999, pp. 3-8.
  10. B. Kräutler, D. Arigoni and B. T. Golding, *Vitamin B12 and B12-proteins*, WILEY-VCH, Weinheim, 1998.
  11. M. J. Nielsen, M. R. Rasmussen, C. B. Andersen, E. Nexø and S. K. Moestrup, *Nat. Rev. Gastroenterol. Hepatol.*, 2012, **9**, 345-354.
  12. S. T. Callender and L. G. Lajtha, *Blood*, 1951, **6**, 1234-1239.
  13. S. N. Fedosov, *Subcell. Biochem.*, 2012, **56**, 347-367.
  14. L. Randaccio, S. Geremia, N. Demitri and J. Wuerges, *Molecules*, 2010, **15**, 3228-3259.
  15. C. L. Drennan, M. M. Dixon, D. M. Hoover, J. T. Jarrett, C. W. Goulding, R. G. Matthews and M. L. Ludwig, in *Vitamin B12 and B12-proteins*, eds. B. Kräutler, D. Arigoni and B. T. Golding, WILEY-VCH, Weinheim, Editon edn., 1998, pp. 133-155.
  16. J. T. Jarrett, M. Amaratunga, C. L. Drennan, J. D. Scholten, R. H. Sands, M. L. Ludwig and R. G. Matthews, *Biochemistry*, 1996, **35**, 2464-2475.
  17. D. Lexa and J. M. Saveant, *Acc. Chem. Res.*, 1983, **16**, 235-243.
  18. R. G. Matthews, in *Chemistry and biochemistry of B12*, ed. R. Banerjee, John Wiley & Sons, New York, Editon edn., 1999, pp. 681-706.
  19. R. Banerjee and S. W. Ragsdale, *Annu. Rev. Biochem.*, 2003, **72**, 209-247.
  20. R. Banerjee and S. Chowdhury, in *Chemistry and biochemistry of B12*, ed. R. Banerjee, John Wiley & Sons, New York, Editon edn., 1999, pp. 707-729.
  21. P. R. Evans and F. Mancía, in *Vitamin B12 and B12-proteins*, eds. B. Kräutler, D. Arigoni and B. T. Golding, WILEY-VCH, Weinheim, Editon edn., 1998, pp. 217-226.
  22. C. L. Drennan, S. Huang, J. T. Drummond, R. G. Matthews and M. L. Lidwig, *Science*, 1994, **266**, 1669-1674.
  23. F. Mancía, N. H. Keep, A. Nakagawa, P. F. Leadlay, S. McSweeney, B. Rasmussen, P. B. Secke, O. Diat and P. R. Evans, *Structure* 1996, **4**, 339-350.
  24. R. Banerjee, *Chem. Biol.*, 1997, **4**, 175-186.
  25. D. H. Alpers and G. J. Russell-Jones, in *Chemistry and biochemistry of B12*, ed. R. Banerjee, John Wiley & Sons, New York, Editon edn., 1999, pp. 411-440.
  26. Y. Kohgo, J. Kato, R. Nakaya, Y. Mogi, H. Yago, Y. Sakai, H. Matsushita and Y. Niitsu, *Hybridoma*, 1993, **12**, 591-598.
  27. Q. He, M. Madsen, A. Kilkenney, B. Gregory, E. I. Christensen, H. Vorum, P. Hojrup, A. A. Schaffer, E. F. Kirkness, S. M. Tanner, A. de la Chapelle, U. Giger, S. K. Moestrup and J. C. Fyfe, *Blood*, 2005, **106**, 1447-1453.
  28. S. K. Moestrup and P. J. Verroust, *Annu. Rev. Nutr.*, 2001, **21**, 407-428.
  29. E. V. Quadros, Y. Nakayama and J. M. Sequeira, *Biochem. Biophys. Res. Commun.*, 2005, **327**, 1006-1010.
  30. P. A. Seligman and R. H. Allen, *J. Biol. Chem.*, 1978, **253**, 1766-1772.
  31. S. Bose, S. Seetharam and B. Seetharam, *J. Biol. Chem.*, 1995, **270**, 8152-8157.
  32. C. A. Hall, P. D. Colligan and J. A. Begley, *J. Cell. Physiol.*, 1987, **133**, 187-191.
-

33. J. Lindemans, A. C. M. Kroes, J. v. Geel, J. van Kapel, M. Schoester and J. Abels, *Exp. Cell. Res.*, 1989, **184**, 449-460.
  34. G. R. McLean, M. J. Williams, C. S. Woodhouse and H. J. Ziltener, *Leukemia Lymphoma*, 1998, **30**, 101-109.
  35. H. Birn, *Am. J. Physiol. Renal Physiol.*, 2006, **291**, F22-36.
  36. A. Del Corral and R. Carmel, *Gastroenterology*, 1990, **98**, 1460-1466.
  37. E. Kittang and H. Schjonsby, *Scand. J. Gastroentero.*, 1987, **22**, 1031-1037.
  38. R. H. Allen, B. Seetharam, N. C. Allen, E. R. Podell and D. H. Alpers, *J. Clin. Invest.*, 1978, **61**, 1628-1634.
  39. J. F. Kolhouse and R. H. Allen, *J. Clin. Invest.*, 1977, **60**, 1381-1392.
  40. E. Stupperich and E. Nexø, *Eur. J. Biochem.*, 1991, **199**, 299-303.
  41. S. N. Fedosov, N. U. Fedosova, B. Kräutler, E. Nexø and T. E. Petersen, *Biochemistry*, 2007, **46**, 6446-6458.
  42. J. Wuerges, S. Geremia and L. Randaccio, *Biochem. J.*, 2007, **403**, 431-440.
  43. C. A. Hall, *Clin. Sci. Mol. Med.*, 1977, **53**, 453-457.
  44. L. M. Meyer, I. F. Miller and E. Gizis, *P. Soc. Exp. Biol. Med.*, 1974, **146**, 747-750.
  45. E. Nexø, in *Vitamin B12 and B12-proteins*, eds. B. Kräutler, D. Arigoni and B. T. Golding, WILEY-VCH, Weinheim, Editon edn., 1998, pp. 461-471.
  46. R. Banerjee, C. Gherasim and D. Padovani, *Curr. Opin. Chem. Biol.*, 2009, **13**, 484-491.
  47. L. Randaccio, S. Geremia, G. Nardin and J. Wuerges, *Coordin. Chem. Rev.*, 2006, **250**, 1332-1350.
  48. J. M. Pratt, in *Chemistry and biochemistry of B12*, ed. R. Banerjee, John Wiley & Sons, New York, Editon edn., 1999, pp. 73-112
  49. M. D. Wirt, I. Sagi, E. Chen, S. M. Frisbie, R. Lee and M. R. Chance, *J. Am. Chem. Soc.*, 1991, **113**, 5299-5304.
  50. M. D. Wirt, I. Sagi and M. R. Chance, *Biophys. J.*, 1992, **63**, 412-417.
  51. G. A. Walker, S. Murphy and F. M. Huennekens, *Arch. Biochem. Biophys.*, 1969, **134**, 95-102.
  52. M. V. Fonseca and J. C. Escalante-Semerena, *J. Biol. Chem.*, 2001, **276**, 32101-32108.
  53. R. Deacon, M. Lumb, J. Perry, I. Chanarin, B. Minty, M. Halsey and J. Nunn, *Eur. J. Biochem.*, 1980, **104**, 419-423.
  54. Y. Kano, S. Sakamoto, K. Sakuraya, T. Kubota, T. Kasahara, K. Hida, K. Suda and F. Takaku, *Cancer Res.*, 1983, **43**, 1493-1496.
  55. B. Christensen, A. B. Guttormsen, J. Schneede, B. Riedel, H. Refsum, A. Svardal and P. M. Ueland, *Anesthesiology*, 1994, **80**, 1046-1056.
  56. P. R. Walker, B. Smith, C. Carson, J. LeBlanc, M. Sikorska, C. S. Woodhouse and A. C. Morgan, *Cell Death Differ.*, 1997, **4**, 233-241.
  57. J. H. Matthews, *Blood*, 1997, **89**, 4600-4607.
  58. K. Zhou and F. Zelder, *Angew. Chem. Int. Ed.*, 2010, **49**, 5178-5180.
  59. K. Zhou, R. M. Oetterli, H. Brandl, F. E. Lyatuu, W. Buckel and F. Zelder, *ChemBioChem*, 2012, **13**, 2052-2055.
  60. P. M. Pathare, D. S. Wilbur, S. Heusser, E. V. Quadros, P. McLoughlin and A. C. Morgan, *Bioconjug Chem*, 1996, **7**, 217-232.
  61. D. A. Collins and H. P. Hogenkamp, *J. Nucl. Med.*, 1997, **38**, 717-723.
  62. J. Q. Yang, Y. Li, J. Lu and X. B. Wang, *J. Radioanal. Nucl. Ch.*, 2005 **265**, 467-472.
  63. B. Spingler, S. Mundwiler, P. Ruiz-Sánchez, D. R. van Staveren and R. Alberto, *Eur. J. Inorg. Chem.*, 2007, **2007**, 2641-2647.
  64. J. Wuerges, G. Garau, S. Geremia, S. N. Fedosov, T. E. Petersen and L. Randaccio, *Proc. Natl. Acad. Sci. USA*, 2006, **103**, 4386-4391.
  65. M. Lee and C. B. Grissom, *Org. Lett.*, 2009, **11**, 2499-2502.
  66. N. Viola-Villegas, A. E. Rabideau, M. Bartholoma, J. Zubieta and R. P. Doyle, *J. Med. Chem.*, 2009, **52**, 5253-5261.
-

67. P. Siega, J. Wuerges, F. Arena, E. Gianolio, S. N. Fedosov, R. Dreos, S. Geremia, S. Aime and L. Randaccio, *Chem-Eur. J.*, 2009, **15**, 7980-7989.
  68. A. K. Petrus, A. R. Vortherms, T. J. Fairchild and R. P. Doyle, *ChemMedChem*, 2007, **2**, 1717-1721.
  69. C. H. Fazen, D. Valentin, T. J. Fairchild and R. P. Doyle, *J. Med. Chem.*, 2011, **54**, 8707-8711.
  70. R. Waibel, H. Treichler, N. G. Schaefer, D. R. van Staveren, S. Mundwiler, S. Kunze, M. Kuenzi, R. Alberto, J. Nuesch, A. Knuth, H. Moch, R. Schibli and P. A. Schubiger, *Cancer Res.*, 2008, **68**, 2904-2911.
  71. W. A. Howard, A. Bayomi, E. Natarajan, M. A. Aziza, O. El-Ahmady, C. B. Grissom and F. G. West, *Bioconjug Chem*, 1997, **8**, 498-502.
  72. J. D. Bagnato, A. L. Eilers, R. A. Horton and C. B. Grissom, *J. Org. Chem.*, 2004, **69**, 8987-8996.
  73. R. Mukherjee, E. G. Donnay, M. A. Radomski, C. Miller, D. A. Redfern, A. Gericke, D. S. Damron and N. E. Brasch, *Chem. Commun.*, 2008, **32**, 3783-3785.
  74. J. A. Bauer, B. H. Morrison, R. W. Grane, B. S. Jacobs, S. Dabney, A. M. Gamero, K. A. Carnevale, D. J. Smith, J. Drazba, B. Seetharam and D. J. Lindner, *J. Natl. Cancer Inst.*, 2002, **94**, 1010-1019.
  75. D. W. Jacobsen, R. J. Holland, Y. Montejano and F. M. Huennekens, *J. Inorg. Biochem.*, 1979, **10**, 53-65.
  76. C. C. Smeltzer, M. J. Cannon, P. R. Pinson, J. D. Munger, F. G. West and C. B. Grissom, *Org. Lett.*, 2001, **3**, 799-801.
  77. J. M. McGreevy, M. J. Cannon and C. B. Grissom, *J. Surg. Res.*, 2003, **111**, 38-44.
  78. A. R. Vortherms, A. R. Kahkoska, A. E. Rabideau, J. Zubieta, L. L. Andersen, M. Madsen and R. P. Doyle, *Chem. Commun.*, 2011, **47**, 9792-9794.
  79. S. Mundwiler, B. Spingler, P. Kurz, S. Kunze and R. Alberto, *Chem-Eur. J.*, 2005, **11**, 4089-4095.
  80. A. K. Petrus, D. G. Allis, R. P. Smith, T. J. Fairchild and R. P. Doyle, *ChemMedChem*, 2009, **4**, 421-426.
  81. A. K. Petrus, T. J. Fairchild and R. P. Doyle, *Angew. Chem. Int. Edit.*, 2009, **48**, 1022-1028.
  82. S. M. Clardy, D. G. Allis, T. J. Fairchild and R. P. Doyle, *Expert Opin. Drug Del.*, 2010, **8**, 127-140.
  83. G. R. McLean, E. V. Quadros, S. P. Rothenberg, A. C. Morgan, J. W. Schrader and H. J. Ziltener, *Blood*, 1997, **89**, 235-242.
  84. D. L. Lildballe, E. Mutti, H. Birn and E. Nexø, *PLoS ONE*, 2012, **7**, e46657.
  85. E. R. T. Tieckink, *Crit. Rev. Oncol. Hemat.*, 2002, **42**, 225-248.
  86. A. Bindoli, M. P. Rigobello, G. Scutari, C. Gabbiani, A. Casini and L. Messori, *Coordin. Chem. Rev.*, 2009, **253**, 1692-1707.
  87. A. Casini, C. Hartinger, C. Gabbiani, E. Mini, P. J. Dyson, B. K. Keppler and L. Messori, *J. Inorg. Biochem.*, 2008, **102**, 564-575.
  88. L. Messori, F. Abbate, G. Marcon, P. Orioli, M. Fontani, E. Mini, T. Mazzei, S. Carotti, T. O'Connell and P. Zanello, *J. Med. Chem.*, 2000, **43**, 3541-3548.
  89. M. J. McKeage, L. Maharaj and S. J. Berners-Price, *Coordin. Chem. Rev.*, 2002, **232**, 127-135.
  90. W. H. Ang, E. Daldini, C. Scolaro, R. Scopelliti, L. Juillerat-Jeannerat and P. J. Dyson, *Inorg. Chem.*, 2006, **45**, 9006-9013.
  91. S. Kapitzka, M. Pongratz, M. A. Jakupec, P. Heffeter, W. Berger, L. Lackinger, B. K. Keppler and B. Marian, *J. Cancer Res. Clin.*, 2005, **131**, 101-110.
  92. E. S. Antonarakis and A. Emadi, *Cancer Chemother. Pharmacol.*, 2010, **66**, 1-9.
  93. R. E. Morris, R. E. Aird, P. del Socorro Murdoch, H. Chen, J. Cummings, N. D. Hughes, S. Parsons, A. Parkin, G. Boyd, D. I. Jodrell and P. J. Sadler, *J. Med. Chem.*, 2001, **44**, 3616-3621.
  94. C. S. Allardyce, P. J. Dyson, D. J. Ellis and S. L. Heath, *Chem. Commun.*, 2001, 1396-1397.
-

95. R. Aird, J. Cummings, A. Ritchie, M. Muir, R. E. Morris, E. Chen, P. Sadler and D. I. Jodrell, *Brit. J. Cancer*, 2002, **86**, 1652-1657.
96. C. Scolaro, A. Bergamo, L. Brescacin, R. Delfino, M. Cocchietto, G. Laurenczy, T. J. Geldbach, G. Sava and P. J. Dyson, *J. Med. Chem.*, 2005, **48**, 4161-4171.
97. M. Groessl, E. Reisner, C. G. Hartinger, R. Eichinger, O. Semenova, A. R. Timerbaev, M. A. Jakupec, V. B. Arion and B. K. Keppler, *J. Med. Chem.*, 2007, **50**, 2185-2193.
98. M. Shah and B. Agarwal, *Indian J. Pediatr.*, 2008, **75**, 831-837.
99. M. L. Slevin, E. M. Piali, G. W. Aherne, A. Johnston and T. A. Lister, *Cancer Chemoth. Pharm.*, 1983, **10**, 112-114.
100. S. S. Cohen, *Med. Biol.*, 1976, **54**, 299-326.
101. B. S. Chhikara and K. Parang, *Expert Opin. Drug Del.*, 2010, **7**, 1399-1414.
102. P. P. Saunders and G. A. Schultz, *Biochem. Pharmacol.*, 1970, **19**, 911-919.
103. J. Pourahmad, M. Amirmostofian, F. Kobarfard and J. Shahraki, *Cancer Chemother. Pharmacol.*, 2009, **65**, 89-96.
104. N. S. Mizuno, R. W. Decker and B. Zakis, *Biochem. Pharmacol.*, 1975, **24**, 615-619.
105. S. M. Lee, N. Thatcher, M. Dougal and G. P. Margison, *Br. J. Cancer*, 1993, **67**, 216-221.
106. L. Meer, R. C. Janzer, P. Kleihues and G. F. Kolar, *Biochem. Pharmacol.*, 1986, **35**, 3243-3247.
107. A. U. Buzdar, *Clin. Cancer Res.*, 2003, **9**, 468s-472s.
108. M. Milani, G. Jha and D. A. Potter, *Clin. Med. Ther.*, 2009, **2009**, 141.
109. P. Ruiz-Sanchez, S. Mundwiler, A. Medina-Molner, B. Spingler and R. Alberto, *J. Organomet. Chem.*, 2007, **692**, 1358-1362.
110. F. Watanabe, K. Abe, S. Takenaka, T. Fujita and Y. Nakano, *J. Agr. Food Chem.*, 1997, **45**, 4661-4663.
111. L. Randaccio, S. Geremia and J. Wuerger, *J. Organomet. Chem.*, 2007, **692**, 1198-1215.
112. S. Kunze, F. Zobi, P. Kurz, B. Spingler and R. Alberto, *Angew. Chem. Int. Edit.*, 2004, **43**, 5025-5029.
113. P. Ruiz-Sanchez, S. Mundwiler, B. Spingler, N. R. Buan, J. C. Escalante-Semerena and R. Alberto, *J. Biol. Inorg. Chem.*, 2008, **13**, 335-347.
114. H. Chen, J. A. Parkinson, S. Parsons, R. A. Coxall, R. O. Gould and P. J. Sadler, *J. Am. Chem. Soc.*, 2002, **124**, 3064-3082.
115. H. Chen, J. A. Parkinson, R. E. Morris and P. J. Sadler, *J. Am. Chem. Soc.*, 2003, **125**, 173-186.
116. R. B. King, in *Organometallic syntheses*, eds. J. J. Eisch and R. B. King, Academic press, Editon edn., 1965, vol. 1, pp. 31-35.
117. A. Habtemariam, M. Melchart, R. Fernández, S. Parsons, I. D. H. Oswald, A. Parkin, F. P. A. Fabbiani, J. E. Davidson, A. Dawson, R. E. Aird, D. I. Jodrell and P. J. Sadler, *J. Med. Chem.*, 2006, **49**, 6858-6868.
118. B. P. Block and J. J. C. Bailar, *J. Am. Chem. Soc.*, 1951, **73**, 4722-4725.
119. D. P. Bancroft, C. A. Lepre and S. J. Lippard, *J. Am. Chem. Soc.*, 1990, **112**, 6860-6871.
120. A. I. Ivanov, J. Christodoulou, J. A. Parkinson, K. J. Barnham, A. Tucker, J. Woodrow and P. J. Sadler, *J. Biol. Chem.*, 1998, **273**, 14721-14730.
121. E. L. Lien and J. M. Wood, *Biochimica et Biophysica Acta (BBA) - General Subjects*, 1972, **264**, 530-537.
122. S. N. Fedosov, C. B. Grissom, N. U. Fedosova, S. K. Moestrup, E. Nexø and T. E. Petersen, *FEBS J.*, 2006, **273**, 4742-4753.
123. F. H. Niesen, H. Berglund and M. Vedadi, *Nat. Protoc.*, 2007, **2**, 2212-2221.
124. S. N. Fedosov, N. U. Fedosova, L. Berglund, S. K. Moestrup, E. Nexø and T. E. Petersen, *Biochemistry*, 2004, **43**, 15095-15102.
125. J. Wuerger, S. Geremia, S. N. Fedosov and L. Randaccio, *IUBMB Life*, 2007, **59**, 722-729.
126. P. Ruiz-Sanchez, C. König, S. Ferrari and R. Alberto, *J. Biol. Inorg. Chem.*, 2011, **16**, 33-44.
-

127. K. A. Stephenson, S. R. Banerjee, T. Besanger, O. O. Sogbein, M. K. Levadala, N. McFarlane, J. A. Lemon, D. R. Boreham, K. P. Maresca, J. D. Brennan, J. W. Babich, J. Zubieta and J. F. Valliant, *J. Am. Chem. Soc.*, 2004, **126**, 8598-8599.
  128. L. Wei, J. W. Babich, W. Ouellette and J. Zubieta, *Inorg. Chem.*, 2006, **45**, 3057-3066.
  129. S. A. Hilderbrand, M. H. Lim and S. J. Lippard, *J. Am. Chem. Soc.*, 2004, **126**, 4972-4978.
  130. T. Santa, A. Takeda, S. Uchiyama, T. Fukushima, H. Homma, S. Suzuki, H. Yokosu, C. K. Lim and K. Imai, *J. Pharm. Biomed. Anal.*, 1998, **17**, 1065-1070.
  131. P. Ruiz-Sanchez, S. Mundwiler and R. Alberto, *Chimia*, 2007, **61**, 190-193.
  132. R. Carmel, *Brit. J. Haematol.*, 1972, **22**, 43-51.
  133. M. B. Shabani, Y. Shiina, F. G. Kirscht and Y. Shimanuki, *Mater. Sci. Eng. B*, 2003, **102**, 238-246.
  134. E. V. Quadros, *Brit. J. Haematol.*, 2010, **148**, 195-204.
  135. D. S. Froese and R. A. Gravel, *Expert Rev Mol Med*, 2010, **12**, e37.
  136. R. Carmel, *Blood*, 2008, **112**, 2214-2221.
  137. M. E. Rappazzo, H. A. Salmi and C. A. Hall, *Brit. J. Haematol.*, 1970, **18**, 425-434.
  138. I. Mellman, H. F. Willard, P. Youngdahl-Turner and L. E. Rosenberg, *J. Biol. Chem.*, 1979, **254**, 11847-11853.
  139. C. A. Hall, W. H. Hitzig, P. D. Green and J. A. Begley, *Blood*, 1979, **53**, 251-263.
  140. N. Berliner and L. E. Rosenberg, *Metabolism*, 1981, **30**, 230-236.
  141. M. Ramasamy, D. H. Alpers, C. Tiruppathi and B. Seetharam, *Am. J. Physiol.*, 1989, **257**, G791-797.
  142. K. S. Ramanujam, S. Seetharam, M. Ramasamy and B. Seetharam, *Am. J. Physiol.*, 1991, **260**, G416-422.
  143. W. H. Hitzig, U. Dohmann, H. J. Pluss and D. Vischer, *J. Pediatr.*, 1974, **85**, 622-628.
  144. P. Ruiz-Sanchez, Ph.D. Thesis, University of Zurich, 2009.
  145. J. F. Pons, J. L. Fauchère, F. Lamaty, A. Molla and R. Lazaro, *Eur. J. Org. Chem.*, 1998, **1998**, 853-859.
  146. R. Alberto, R. Schibli, A. Egli, P. August Schubiger, W. A. Herrmann, G. Artus, U. Abram and T. A. Kaden, *J. Organomet. Chem.*, 1995, **493**, 119-127.
  147. R. Alberto, R. Schibli, A. Egli, A. P. Schubiger, U. Abram and T. A. Kaden, *J. Am. Chem. Soc.*, 1998, **120**, 7987-7988.
  148. A. Stichelberger, *Nucl. Med. Biol.*, 2003, **30**, 465-470.
  149. J. Park and J. Kim, *Protein J.*, 2012, **31**, 158-165.
  150. S. N. Fedosov, N. B. Laursen, E. Nexø, S. K. Moestrup, T. E. Petersen, E. O. Jensen and L. Berglund, *Eur. J. Biochem.*, 2003, **270**, 3362-3367.
  151. E. Furger, S. N. Fedosov, D. Launholt Lildballe, R. Waibel, R. Schibli, E. Nexø and E. Fischer, *PLoS ONE*, 2012, **7**, e37421.
  152. J. Grunberg, K. Knogler, R. Waibel and I. Novak-Hofer, *Biotechniques*, 2003, **34**, 968-972.
  153. H. S. Tastesen, J. B. Holm, J. Møller, K. A. Poulsen, C. Møller, S. Sturup, E. K. Hoffmann and I. H. Lambert, *Cell. Physiol. Biochem.*, 2010, **26**, 809-820.
-



## VII Experimental section

### VII.1 Materials and methods

Chemicals were purchased from Sigma, Fluka, and Strem. HPLC analyses were performed using a Merck-Hitachi L-7000 system equipped with a diode-array UV/Vis spectrometer. The following HPLC columns were used: column 1, Macherey Nagel Nucleosil C<sub>18</sub> (5  $\mu$ m, 100 Å, 250 mm x 3 mm); column 2, Agilent Zorbax GF-250 (4  $\mu$ m, 250 mm x 9.4 mm); column 3, Macherey-Nagel Nucleodur C<sub>18</sub> Gravity (5  $\mu$ m, 250 mm x 3 mm). The following solvent systems were used: solvent system 1, 0.1% TFA (solvent A), MeOH (solvent B); solvent system 2, 130 mM NaCl, 20 mM Na<sub>2</sub>HPO<sub>4</sub>, pH 7 (solvent A); solvent system 3, 50 mM TEAP, pH 2.5 (solvent A), CAN (solvent B), solvent system 4, 0.1% TFA in 10% MeOH (solvent A), MeOH (solvent B). The following solvent gradients were used: gradient 1, 0-5 minutes: 75% A, 5-30 minutes: 0% A; gradient 2, 0-5 minutes: 50% A, 5-15 minutes: 40% A, 15-40 minutes: 40% A; gradient 3, 0-20 minutes: 100% A; gradient 4, 0-3 minutes: 100% A, 3-6 minutes: 75% A, 6-12 minutes: 66% A, 12-23 minutes: 0%A; gradient 5: 0-5 minutes: 100%A, 5-15 minutes: 0%A, 15-25 minutes: 0%A. Preparative HPLC purification was performed on a Varian Prostar system with two Prostar 215 pumps and a Prostar 320 UV/Vis detector, using Macherey Nagel Nucleosil C<sub>18</sub> (7  $\mu$ m, 100 Å, 250 mm x 40 mm) and at a flow rate of 35 ml/ minute. MeOH was removed from the product fractions under vacuum, the products were then lyophilized. Product purity was analyzed by analytical HPLC, IR, and NMR. IR spectra were recorded by a Bio-Rad FTS-45 spectrometer with samples in compressed KBr pills. NMR spectra were recorded by a Bruker DRX 500 MHz spectrometer. Chemical shifts were reported relative to residual solvent protons and carbons. The chemical shifts of <sup>195</sup>Pt NMR spectra were relative to Na<sub>2</sub>PtCl<sub>6</sub> in D<sub>2</sub>O.

Lysis buffer was prepared from 150 mM NaCl, 20mM HEPES buffer, 1 mM EDTA, 0.5% Triton X-100 (Pharmacia Biotech AB), 1% protease inhibitor cocktail (freshly added), 1 mM NaVO<sub>3</sub> (freshly added), NaCl/ KCl (30mM/ 120mM).

All aqueous solutions for ICPMS measurement were prepared in purified water (>18.2M $\Omega$ ) from Milli-Q deionization unit. Standards and samples were prepared in a mixture of HNO<sub>3</sub> 0.65% : HCl 1%.

---

## VII.2 Synthesis

b-carboxylic acid of vitamin B<sub>12</sub> **23**,<sup>60</sup> N-tert-butyloxycarbonyldiamines **10** (Scheme 22),<sup>145</sup> [NEt<sub>4</sub>]<sub>2</sub>[ReBr<sub>3</sub>(CO)<sub>3</sub>],<sup>146</sup> and [<sup>99m</sup>Tc(OH<sub>2</sub>)<sub>3</sub>(CO)<sub>3</sub>]<sup>+147</sup> were prepared according to literature. Compounds [*cis*-Pt(NH<sub>3</sub>)<sub>2</sub>Cl{B<sub>12</sub>}][CF<sub>3</sub>CO<sub>2</sub>] **1** and [*trans*-Pt(NH<sub>3</sub>)<sub>2</sub>Cl{B<sub>12</sub>}][CF<sub>3</sub>CO<sub>2</sub>] **2** were synthesized according to previous publications.<sup>79, 113</sup>

### [Ru(C<sub>6</sub>H<sub>6</sub>)(en){B<sub>12</sub>}][PF<sub>6</sub>]<sub>2</sub> (**3**)

25.3 mg [Ru(C<sub>6</sub>H<sub>6</sub>)(en)Cl][PF<sub>6</sub>]<sup>93</sup> (60.24 μmol) was mixed with 15.2 mg AgPF<sub>6</sub> (60 μmol) in 2 ml H<sub>2</sub>O at 40°C overnight. The precipitate was filtered away and the yellow liquid was mixed with 47.9 mg B<sub>12</sub> (35.3 μmol). The reaction was left at 50°C for one day. The purple precipitate was washed with cold water and dried (28 mg, 42%).

<sup>1</sup>H NMR (500 MHz, D<sub>2</sub>O, 300K) δ: 0.48 (s, 3H, C20), 0.98 (m, 1H, C60), 1.12 (m, 1H, C41), 1.29 (m, 6H, C46, Pr3), 1.46 (s, C47, 3H), 1.50 (s, C36, 3H), 1.51 (s, C54, 3H), 1.85 (s, C25, 3H), 1.94 (m, 2H, C55, C60'), 2.1 (m, 7H, C41', C42, C48, C30), 2.24 (d, 1H, J=12.5Hz, C37), 2.30-2.31 (d, 6H, B10, B11), 2.48 (m, 4H, C26, C31), 2.61-2.75 (m, 14H, C35, C53, C49, C55, Ruen(CH<sub>2</sub>)<sub>2</sub>), 2.83 (m, 2H, C18, C56), 2.99 (m, 1H, Pr'1), 3.46 (m, 1H, C13), 3.56 (m, 1H, C8), 3.65 (m, 1H, Pr1), 3.79 (m, 1H, R'5), 4.08 (m, 1H, R4), 4.15 (d, 1H, J=10Hz, C19), 4.28 (m, 1H, C3), 4.32 (m, 2H, R2, Pr2), 5.71 (s, 6H, Ruar), 6.12 (s, 1H, C10), 6.38 (d, 1H, J=4.5Hz, R1), 6.47 (s, 1H, B7), 7.03 (s, 1H, B2), 7.33 (s, 1H, B4). IR (KBr, cm<sup>-1</sup>): 2162 (CN). ESI-MS m/z: 797.3[M]<sup>2+</sup>.

**[*trans*-Pt(NH<sub>3</sub>)<sub>2</sub>(Cyt){B<sub>12</sub>}] [CF<sub>3</sub>CO<sub>2</sub>]<sub>2</sub> (**4**)**

To a solution of 25.4 mg (15.7 μmol) **2** in 1.5 ml water, 15.4 mg (63.3 μmol) Cyt was added. The mixture was stirred at 40°C for one day. Compound **4** was collected after purification with preparative HPLC, solvent system 1, and gradient 1 (11.1mg, 39%).

<sup>1</sup>H NMR (500MHz, MeOD, 300K) δ: 0.39 (s, 3H, C20), 1.26-1.38 [m, 14H, C41 (1H), C46 (3H), Pr3 (3H), C54 (3H), C36 (3H), C60 (1H)], 1.47 (s, 3H, C47), 1.76 (s, 3H, C25), 1.80-2.15 [m, 9H, C55 (1H), C42 (1H), C60 (1H), C48 (2H), C41 (1H), C30 (1H), C42 (1H), C37 (1H)], 2.3 (m, 6H, B10&B11), 2.39-2.54 [m, 6H, C26 (2H), C55 (1H), C56 (1H), C31 (2H)], 2.59-2.63 (m, 6H, C35&C53), 2.70-3.03 [m, 6H, C49 (2H), C56 (1H), C37 (1H), C18 (1H), Pr1 (1H)], 3.66-4.27 [m, 14H, C13 (1H), C8 (1H), Pr1 (1H), R'5 (1H), R5 (1H), C19 (1H), R4 (1H), C3 (1H), Pr2 (1H), Cyt (5H)], 4.35 (m, 1H, R2), 4.71 (m, 1H, R3), 5.94(d, J=7.5, 1H, Cyt), 6.02 (s, 1H, C10), 6.09 (d, J=4Hz, 1H, Cyt), 6.30 (d, J=3.5Hz, 1H, R1), 6.55 (s, 1H, B7), 7.09 (s, 1H, B2), 7.30 (s, 1H, B4), 7.95 (d, J=7.5Hz, 1H, Cyt). <sup>195</sup>Pt NMR (107MHz, MeOD, 20°C) δ: -2589. <sup>31</sup>P NMR (200MHz, MeOD, 20°C) δ: 1.14. IR (KBr, cm<sup>-1</sup>): 2195 (CN). ESI-MS m/z: 913.9 [M+1]<sup>2+</sup>, 1826.7 [M]<sup>+</sup>.

**[*trans*-Pt(NH<sub>3</sub>)<sub>2</sub>(Dac){B<sub>12</sub>}] [CF<sub>3</sub>CO<sub>2</sub>]<sub>2</sub> (**5**)**

To a solution of 56.8 mg (35 μmol) **2** in 2 ml H<sub>2</sub>O, 24.3 mg (133 μmol) Dac was added. The mixture was stirred at 38°C for one day. Compound **5** was collected after purification with preparative HPLC, solvent system 1, and gradient 1 (31 mg, 50%).

<sup>1</sup>H NMR (500MHz, MeOD, 300K) δ: 0.38 (s, 3H, C20), 1.26-1.29 [m, 7H, C41 (1H), C46 (3H), Pr3 (3H)], 1.32-1.39 [m, 7H, C60 (1H), C54 & C36 (6H)], 1.47 (s, 3H, C47), 1.71 (m, 1H, C42), 1.79 (s, 3H, C25), 1.84-2.16 [m, 8H, C55 (1H), C48 (2H), C60 (1H), C41' (1H), C30 (1H), C42' (1H), C37 (1H)], 2.29 (m, 6H, B10 & B11), 2.39-2.75 [m, 16H, C26 (2H), C56 (1H), C55' (1H), C37' (1H), C56' (1H), C49 (2H), C31 (2H)], 2.82-2.86 [m, 2H, Pr1(1H), C18 (1H)], 3.40 (m, 1H, C13), 3.65-4.01 [m, 10H, C8 (1H), Pr1 (1H), R'5 (1H), R5 (1H), Dac (6H)], 4.07-4.21 [m, 4H, R4 (1H), C19 (1H), C3(1H), R2 (1H)], 4.35 (m, 1H, Pr2), 4.71 (m, 1H, R3), 6.04 (s, 1H, C10), 6.30 (d, J=3Hz, 1H, R1), 6.56 (s, 1H, B7), 7.08 (s, 1H, B2), 7.29 (s, 1H, B4), 7.96 (s, 1H, Dac). <sup>195</sup>Pt NMR (107MHz, MeOD): -2449. <sup>31</sup>P NMR (200MHz, MeOD, 20°C) δ: 1.05. IR (KBr, cm<sup>-1</sup>): 2192 (CN). ESI-MS m/z: 1766.0 [M]<sup>+</sup>.

**[*trans*-Pt(NH<sub>3</sub>)<sub>2</sub>(Ana){B<sub>12</sub>}][CF<sub>3</sub>CO<sub>2</sub>]<sub>2</sub> (6)**

To a solution of 16 mg (9.9 μmol) **2** in 1.2 ml water was added 10 mg (34 μmol) Ana. The reaction was stirred at 40°C through one day. **6** was collected after purification with preparative HPLC, solvent system 1, gradient 1 (10.7 mg, 58%).

<sup>1</sup>H NMR (500MHz, MeOD, 298K) δ: 0.41 (s, 3H, C20), 1.25-1.28 [m, 7H, C41 (1H), Pr3 (3H), C46 (3H)], 1.31-1.36 (m, 7H, C60 (1H), C54 (3H), C36 (3H)], 1.48 (s, 3H, C47), 1.71-1.80 [m, 20H, C55 (1H), C42 (1H), Ana (12H), C25 (3H), C60' (1H), C48 (2H)], 1.84-2.16 [m, 4H, C41' (1H), C30 (1H), C42' (1H), C37 (1H)], 2.29 [m, 6H, B10 (3H), B11 (3H)], 2.38-2.56 [m, 4H, C26 (2H), C56' (1H), C55' (1H)], 2.60 [m, 6H, C55 (3H), C35 (3H)], 2.62-2.71 [m, 6H, C37' (1H), C56 (1H), C49 (2H), C31 (2H)], 2.81-2.85 [m, 2H, C18 (1H), Pr'1 (1H)], 3.61 (m, 1H, C8), 3.65 (m, 1H, Pr1), 3.75 (m, 1H, R'5), 3.91 (m, 1H, R5), 4.08 (m, 1H, R4), 4.20 [m, 2H, C19 (1H), C3 (1H)], 4.34 (m, 1H, R2), 4.39 (m, 1H, Pr2), 4.69 (m, 1H, R3), 5.58 (s, 2H, Ana), 6.04 (s, 1H, C10), 6.29 (d, J=3Hz, 1H, R1), 6.55 (s, 1H, B7), 7.10 (s, 1H, B2), 7.30 (s, 1H, B4), 7.58 (d, J=2Hz, 2H, Ana), 7.65 (t, J=2Hz, 1H, Ana), 8.25 (s, 1H, Ana), 9.23 (s, 1H, Ana). <sup>195</sup>Pt NMR (107MHz, MeOD, 20°C): -2560. <sup>31</sup>P NMR (200MHz, MeOD, 20°C) δ: 1.15. IR (KBr, cm<sup>-1</sup>): 2239 (CN, Ana), 2193 (CN, B<sub>12</sub>). ESI-MS m/z: 938.9 [M+H]<sup>2+</sup>, 1876.7 [M]<sup>+</sup>.

**[*trans*-Pt(NH<sub>3</sub>)<sub>2</sub>(dansylimidazole){B<sub>12</sub>}][CF<sub>3</sub>CO<sub>2</sub>]<sub>2</sub> (7)**

21.2 mg (70.4 μmol) dansylimidazole<sup>129</sup> was added to a solution of 26 mg (16 μmol) **2** in H<sub>2</sub>O/ MeOH (3/2) (1.2 ml/ 0.8 ml). The reaction was stirred overnight at 45°C. **7** was collected after purification with preparative HPLC, solvent system 1, gradient 1 (3.5 mg, 12%).

<sup>1</sup>H NMR (500MHz, D<sub>2</sub>O, 300K) δ: 0.46 (s, 3H, C20), 1.14 (m, 1H, C41), 1.28 (m, 7H, Pr3, C46, C60), 1.42 (s, 6H, C54, C36), 1.49 (s, C47, 3H), 1.86 (s, 3H, C25), 2.29 (d, 6H, B10, B11), 2.58 (s, 3H, C35), 2.61 (s, 3H, C55), 3.41 (m, 1H, Pr1), 3.45 (s, 6H, N(CH<sub>3</sub>)<sub>2</sub>, dansyl), 3.49 (m, 1H, C18), 3.64 (m, 1H, R5), 3.78 (m, 1H, R'5), 3.93 (m, 1H, B4), 4.08 (m, 1H, R4), 4.15 (m, 1H, C19), 4.21 (m, 1H, Pr2), 4.31 (m, 2H, C3, R3), 6.11 (s, 1H, C10), 6.38 (d, J= 3Hz, 1H, R1), 6.50 (s, 1H, B7), 7.05 (s, 1H, B2), 7.16 (m, 1H, imidazole), 7.32 (s, 1H, B4), 7.84 (m, 1H, imidazole), 7.96 (t, J=8.5Hz, 1H, dansyl), 8.05 (t, J=7.5Hz, 1H, dansyl), 8.08 (d, J=8Hz, 1H, dansyl), 8.70 (d, J=8.5Hz, 1H, dansyl), 8.74 (d, J=8.5Hz, 1H, dansyl), 8.83 (d, J=7Hz, 1H, dansyl), 9.00 (m, 1H, imidazole). ESI-MS m/z: 942.6 [M]<sup>2+</sup>.

**[*trans*-Pt(NH<sub>3</sub>)<sub>2</sub>(imidazole){B<sub>12</sub>}][CF<sub>3</sub>CO<sub>2</sub>]<sub>2</sub> (8)**

Only the byproduct **8** was formed when the reaction solvent mixture was 300 µl H<sub>2</sub>O/400 µl MeOH.

<sup>1</sup>H NMR (500MHz, MeOD, 298K) δ: 0.42 (s, 3H, C20), 1.26 (d, J=6.5Hz, 3H, Pr3), 1.30 (s, 3H, C46), 1.37 (m, 6H, C54, C36), 1.48 (s, 3H, C25), 2.30 (m, 6H, B10, B11), 2.61 (s, 6H, C55, C35), 3.42 (m, 1H, C18), 3.65 (m, 2H, Pr1, R5), 3.76 (m, 1H, R'5), 3.91 (m, 1H, C19), 4.09 (m, 1H, B4), 4.38 (m, 2H, R2, Pr2), 6.05 (s, 1H, C10), 6.29 (d, J=3Hz, 1H, R1), 6.56 (s, 1H, B7), 7.07 (m, 1H, imidazole), 7.11 (s, 1H, B2), 7.30 (m, 2H, B4, imidazole), 8.04 (s, 1H, imidazole). ESI-MS m/z: 826 [M]<sup>2+</sup>.

**[*trans*-Pt(NH<sub>3</sub>)<sub>2</sub>(NBD-CO-Hz){B<sub>12</sub>}][CF<sub>3</sub>CO<sub>2</sub>]<sub>2</sub> (9)**

5.7 mg (21.4 µmol) NBD-CO-Hz was added to a solution of 9.8 mg (6 µmol) **2** in 1 ml water. The reaction was stirred overnight at 40°C. **9** was collected after purification with preparative HPLC, solvent system 1, gradient 1 (3.7 mg, 33%).

<sup>1</sup>H NMR (500MHz, MeOD, 300K) δ: 6.03 (s, 1H, C10), 6.28 (d, J=2.5Hz, 1H, R1), 6.50 (d, J=12Hz, 1H, NBD-CO-Hz), 6.52 (s, 1H, B7), 7.09 (s, 1H, B2), 7.29 (s, 1H, B4), 8.59 (d, J=12.5Hz, 1H, NBD-CO-Hz). ESI-MS m/z: 925 [M]<sup>2+</sup>

**[4-(pyridine-2-ylmethyl)amino]-buthylcarbamic acid tert-buthyl ester (11) and [4-(ethylacetate)-(pyridine-2-ylmethyl)amino]-buthylcarbamic acid tert-buthyl ester (12)**

**11** and **12** were prepared as described in an earlier publication<sup>148</sup> with following modifications.

2 g **10**<sup>145</sup> (11 mmol) was dissolved in 100 ml MeOH. 1.3 g Pyridine-2-carbaldehyde (12 mmol) was added dropwise. The mixture was stirred at r.t. for 3h. The solvent was removed. The imine product was dissolved in 50 ml EtOH. 1.5g NaBH<sub>4</sub> was added in five portions during 2h. The solvent was removed. The residue was dissolved in diluted NaHCO<sub>3</sub>. The product was extracted with CH<sub>2</sub>Cl<sub>2</sub>. The organic phase was washed with water and dried with MgSO<sub>4</sub>. It was then filtered and the solvent was removed. The purification of **11** was performed on silicagel column (EtOAc, MeOH) (2.8 g, 91%).

<sup>1</sup>H-NMR (200 MHz, MeOD, 300K): δ: 1.94-1.42 (m, 13H), 3.29 (m, 2H), 3.32 (m, 2H), 4.37 (s, 2H), 7.41 (m, 1H), 7.49(m, 1H), 7.87(m, 1H), 8.63(m, 1H). R<sub>f</sub>=0.28 (NH<sub>4</sub>OH/ MeOH/ EtOAc, 1:10:89). ESI-MS: m/z=302.3 [M+H+Na]<sup>2+</sup>.

1.5 g **11** was mixed with 1ml TEA in 50 ml EtOH. The mixture was cooled to 0°C. 600 µl bromoacetic acid ethylester was added dropwise within 5 minutes. After stirring at r.t. for 30 minutes at 0°C and 16h, the solvent was removed. The residue was dissolved in CH<sub>2</sub>Cl<sub>2</sub>. Extraction was performed with CH<sub>2</sub>Cl<sub>2</sub>/H<sub>2</sub>O. The organic phase was dried with MgSO<sub>4</sub>, filtered and the solvent was removed. The product **12** (1.2 g, 60%) was collected as brownish oil.

<sup>1</sup>H-NMR (200 MHz, MeOD, 300K): δ: 1.20-2.61 (m, 15H), 2.65 (t, J=6.6, 6.8 Hz, 2H), 3.06 (d, J= 6 Hz, 2H), 3.36 (s, 2H), 3.89 (s, 2H), 4.13 (q, J= 7.2, 7, 7.2 Hz, 2H), 4.73 (m, 1H), 7.13 (m, 1H), 7.47 (d, J=7.8 Hz, 1H), 7.63 (m, 1H), 8.51 (m, 1H). ESI-MS: m/z=366.3 [M+H]<sup>+</sup>.

**4-{tricarbonylrhenium(I)-[(N,N,O)-(aceticacid)-(pyridin-2-ylmethyl)amino]}-buthylcarbamic acid tert-buthyl ester (**13**)**

60mg (1.5mmol) NaOH in 1ml H<sub>2</sub>O was added to a solution of 176.2mg (0.48mmol) of **12** in 2.5ml MeOH. The reaction was stirred overnight. The pH was adjusted to 7 with HCl 2M and saturated NaHCO<sub>3</sub> was added to have a buffer medium. 374mg (0.48mmol) [NEt<sub>4</sub>]<sub>2</sub>[ReBr<sub>3</sub>(CO)<sub>3</sub>]<sup>146</sup> in 7ml methanol was added. The mixture was refluxed at 60°C for 4 hours. The solvent was then removed. The product **13** was washed with H<sub>2</sub>O (235mg, 80%).

<sup>1</sup>H-NMR (500 MHz, CD<sub>3</sub>CN, 300K): δ:1.4 (s, 13H), 1.48 (m, 2H), 1.81 (m, 2H), 3.08 (m, 2H), 3.32 (d, J=17Hz, 1H), 3.56 (m, 2H), 3.70 (d, J=18Hz, 1H), 4.40 (d, J=15.5Hz, 1H), 4.57 (d, J=16Hz, 1H), 5.33 (s, 1H), 7.47 (t, J=6.5Hz, 1H), 7.59 (d, J=8Hz, 1H), 8.02 (t, J=8.5Hz, 1H), 8.77 (d, J=5.5Hz, 1H). IR (KBr, cm<sup>-1</sup>):2018, 1889, 1872 (CO). ESI-MS: m/z=630.3 [M+Na]<sup>+</sup>.

---

**5'-{[4-(ethylacetate)-(pyridine-2-ylmethyl)amino]-buthyl-carbamate}cyanocobalamin (14)**

41mg **12** (112μmol) was mixed with 1ml HCl 2M and 2ml H<sub>2</sub>O. The solution was stirred overnight to deprotect the Boc-group. The product was dried.

100mg B<sub>12</sub> (74μmol) was dissolved in 2ml anhydrous DMSO. 25mg CDI (154μmol) was added. The mixture was stirred at 60°C overnight. The above Boc-deprotected product was added together with 1ml TEA. The reaction was left for 2 hours until no further product was formed. The product **14** (27.5 mg, 22.5%) was separated by preparative HPLC, solvent system 1, gradient 1.

<sup>1</sup>H-NMR (500 MHz, MeOD, 300K): δ: 8.72 (d, J=5Hz, 1H), 8.10 (t, J=8.5, 1H), 7.70 (d, J=8Hz, 1H), 7.62 (t, J=7Hz, 1H), 7.25 (s, 1H, B7), 7.16 (s, 1H, B2), 6.6 (s, 1H, B4), 6.25 (d, J=3Hz, 1H, R1), 6.07 (s, 1H, C10), 4.62 (m, 1H, R3), 4.60 (s, 2H, CH<sub>2</sub>-pyr of PAMA4), 4.55 (m, 1H, Pr2), 4.42 (m, 1H, R2), 4.29 (m, 2H, CH<sub>2</sub>O of PAMA4), 4.23 (m, 3H, C3, C19, R4), 4.20 (m, 1H, R5), 4.17 (m, 1H, R'5), 4.15 (s, 2H, CH<sub>2</sub>CO of PAMA4), 3.66 (m, 2H, CH<sub>2</sub>N of PAMA4), 2.90 (m, 2H, CH<sub>2</sub>NH<sub>2</sub> of PAMA4), 2.61 (m, 6H C53, C35), 2.41 (d, J=10Hz, 2H, C26), 2.32 (s, 3H, B10), 2.30 (s, 3H, B11), 1.91 (s, 3H, C25), 1.78 (m, 4H, 2xCH<sub>2</sub> of PAMA4), 1.48 (s, 3H, C47), 1.41 (s, 3H, C54), 1.39 (s, 3H, C36), 1.31 (t, J=4Hz, CH<sub>3</sub> of PAMA4), 1.27 (d, J=6.5Hz, 3H, Pr3), 1.21 (s, 3H, C46), 0.49 (s, 3H, C20). IR (KBr, cm<sup>-1</sup>): 2137 (CN).

ESI-MS: m/z= 824.3 [M+2H]<sup>2+</sup>, 1646.8 [M+H]<sup>+</sup>.

**5'-{[4-(ethylacetate)-(pyridine-2-ylmethyl)amino]-buthylcarbamate}{cisplatinum diammine-chloride-cyano}cobalamin (15)**

12mg (40μmol) of cisplatin and 6.7mg (39μmol) of AgNO<sub>3</sub> was mixed together in 1ml H<sub>2</sub>O in the absence of light. The reaction was stirred at 40°C for 4h. The mixture was filtered twice before 45mg (27μmol) of **14** was added. The reaction was stirred at 45°C for one day. Separation of **15** was performed on preparative HPLC, solvent system 1, gradient 1 (15mg, 29%).

<sup>1</sup>H-NMR (500 MHz, MeOD, 300K): δ: 6.04 (s, 1H), 6.33 (d, J=5Hz, 1H), 6.47 (s, 1H), 7.05 (s, 1H), 7.27 (s, 1H), 7.60 (m, 1H), 7.70 (d, J=10Hz, 1H), 8.10 (m, 1H), 8.61 (m, 1H). <sup>195</sup>Pt-NMR (107MHz, MeOD, δ in ppm): δ=-2350.6. IR (KBr, cm<sup>-1</sup>): 2200 (CN). ESI-MS: m/z=955.9 [M+2H]<sup>2+</sup>.

**5'-[[4-tricarbonylrhenium(I)-[(N,N,O)-(aceticacid)-(pyridin-2-ylmethyl)amino]]-buthyl carbamate}-cyanocobalamin (16)**

1ml TFA was added to 50mg (82.5 $\mu$ mol) of (13) in 3ml CH<sub>2</sub>Cl<sub>2</sub>. After stirring for 1h at 0°C, the Boc group was fully deprotected from (13). The solvent was removed.

To a solution of 150mg (0.11mmol) B<sub>12</sub> in 3.5ml dry DMSO was added 24mg (0.15mmol) CDT. The mixture was stirred for 1 hour at 60°C. Then the above Boc-deprotected product was added together with 4ml dry DMSO and 0.8ml TEA. The reaction was stirred overnight. DEE was added to precipitate the product mixture. Separation of **16** was performed on preparative HPLC, solvent system 1, gradient 1 (31 mg, 14.5%)

<sup>1</sup>H-NMR (500 MHz, MeOD, 300K):  $\delta$ : 5.97 (s, 1H), 6.24 (s, 1H), 6.57 (s, 1H), 7.13 (d, J=4Hz, 1H), 7.25 (s, 1H), 7.52 (m, 1H), 7.71 (t, J=6.5Hz, 1H), 8.07 (m, 1H), 8.81 (d, J=5.5Hz, 1H). IR (KBr, cm<sup>-1</sup>): 2136 (CN); 2028, 1918, 1902 (CO). ESI-MS: m/z= 1888 [M+H]<sup>+</sup>, 945 [M+2H]<sup>2+</sup>.

**{5'-[4-tricarbonylrhenium(I)-[(N,N,O)-(aceticacid)-(pyridin-2-ylmethyl)amino]]-buthyl-carbamate}-{cisplatinumdiamminechloride cyano}cobalamin (17)**

12mg (40 $\mu$ mol) of cisplatin and 6.7mg (39 $\mu$ mol) of AgNO<sub>3</sub> was mixed together in 1ml H<sub>2</sub>O. The reaction was stirred in the absence of light at 40°C for 4h. The mixture was filtered twice. 1.9ml (19 $\mu$ mol) of the filtrate was added to 22mg (11.6 $\mu$ mol) of **16**. The reaction was stirred at 45°C for one day in the absence of light. The product was purified by preparative HPLC, solvent system 1, gradient 1 (20mg, 80%)

<sup>1</sup>H-NMR (500 MHz, MeOD, 300K):  $\delta$ : 5.99 (s, 1H), 6.26 (s, 1H), 6.58 (s, 1H), 7.14 (s, 1H), 7.25 (s, 1H), 7.54 (m, 1H), 7.72 (m, 1H), 8.08 (d, J=6Hz, 1H), 8.80 (d, J=5Hz, 1H). <sup>195</sup>Pt-NMR (107MHz, MeOD,  $\delta$  in ppm):  $\delta$ =-2354. IR (KBr, cm<sup>-1</sup>): 2200 (CN); 2026, 1916, 1904 (CO). ESI-MS: m/z= 1076.6 [M+2H]<sup>2+</sup>

**{5'-[4-tricarbonyl-<sup>99m</sup>Tc(I)-[(N,N,O)-(aceticacid)-(pyridin-2-ylmethyl)amino]]-buthyl-carbamate}-{cisplatinumdiamminechloride cyano}cobalamin (18)**

Labeling of **15** with [<sup>99m</sup>Tc(CO)<sub>3</sub>(OH)<sub>2</sub>]<sup>+</sup> resulted in the formation of **18**. Reactions were performed following a previously published labeling procedure for vitamin B<sub>12</sub> derivatives.<sup>63</sup> The authenticity of **18** was confirmed by comparing its HPLC retention time with that of **17**. HPLC was performed on column 1, solvent system 3, and gradient 3 with a flow rate of 0.5 ml/ minute.



**[4-(bis-quinolin-2-ylmethyl)-amino]-buthylcarbamic acid tert-buthyl ester (19),  
[4-tricarbonylrhenium(I)-[(N,N,N)-(bis-quinolin-2-ylmethyl)-amino]]-buthyl-  
carbamic acid tert-buthyl ester (20)**

Compound **19** and **20** were synthesized according to literature<sup>66</sup> with some modifications. In details, 197 mg **10** (1 mmol) (97%) were mixed together with 345 mg (2.1 mmol) of 2-quinolinecarboxaldehyde (97%) in 30 ml dichloroethane. The reaction was stirred under Ar. After 30 minutes, 667 mg (3 mmol) of sodium triacetoborohydride (97%) was added. The reaction continued overnight. The solvent was evaporated to collect **19** (250 mg, 53%).

<sup>1</sup>H-NMR (500 MHz, MeOD, 300K):  $\delta$ : 1.44 (s, 14H), 1.64 (m, 2H), 2.07 (m, 2H), 2.66 (m, 2H), 3.07 (m, 2H), 4.05 (s, 4H), 4.75 (s, 1H), 7.54 (t, J=7Hz, 2H), 7.73 (m, 4H), 7.81 (d, J=8Hz, 2H), 8.10 (d, J=8.5Hz, 2H), 8.16 (d, J=8.5Hz, 2H). ESI-MS: m/z=471.4 [M+H]<sup>+</sup>.

158mg (335  $\mu$ mol) **19** was in 7 ml MeOH was mixed with 262 mg (340  $\mu$ mol) of [NEt<sub>4</sub>]<sub>2</sub>[ReBr<sub>3</sub>(CO)<sub>3</sub>]<sup>146</sup> at 60°C for 4h. The solvent was evaporated. The product **20** was washed with cold water (219mg, 88%).

<sup>1</sup>H-NMR (500 MHz, MeOD, 300K):  $\delta$ : 1.28 (m, 2H), 1.41 (m, 12H), 1.65 (m, 2H), 2.03 (m, 2H), 3.16 (m, 2H), 3.88 (m, 2H), 5.05 (d, J=20Hz, 2H), 5.24 (d, J=20Hz, 1H), 7.61 (m, 2H), 7.71 (m, 2H), 7.88 (m, J=8.5Hz, 2H), 8.03 (m, 2H), 8.55 (m, 4H). ESI-MS: m/z=741.3 [M]<sup>+</sup>.

**5'-{[4-(bis-quinolin-2-ylmethyl)-amino]-buthyl-carbamate}- cyanocobalamin (21)  
and compound 5'-{[4-tricarbonylrhenium(I)-[(N,N,N)-(bis-quinolin-2-ylmethyl)-  
amino]]-buthylcarbamate}-cyanocobalamin (22)**

To a solution of 95 mg (70  $\mu$ mol) B<sub>12</sub> in 10 ml dry DMSO was added 17 mg (104  $\mu$ mol) CDT. The mixture was stirred at 60°C for 30 minutes.

35mg (74  $\mu$ mol) of (19) was dissolved in 1.5 ml CH<sub>2</sub>Cl<sub>2</sub>. 0.7ml TFA was added. The reaction was stirred at 0°C for one hour. The solvent was removed and 7 ml (49  $\mu$ mol B<sub>12</sub>) of the activated B<sub>12</sub> above together with 1.3 ml TEA was added. The reaction was stirred overnight. The reaction mixture was precipitated with diethylether. Purification of the product **21** (12 mg, 14%) was performed on preparative HPLC, solvent system 1, gradient 1.

<sup>1</sup>H-NMR (500 MHz, D<sub>2</sub>O, 300K):  $\delta$ : 5.98 (s, 1H), 6.21 (s, 1H), 6.48 (s, 1H), 7.04 (s, 1H), 7.13 (s, 1H), 7.40 (d, J=9Hz, 2H), 7.47 (t, J=7Hz, 2H), 7.68 (m, 4H), 7.85 (s, J=8.5Hz, 2H), 8.08 (d, J=8Hz, 2H). ESI-MS: m/z=1752.9 [M+H]<sup>+</sup>.

36 mg (48  $\mu$ mol) **20** was dissolved in 1.5 ml CH<sub>2</sub>Cl<sub>2</sub>. 0.7 ml TFA was added. The reaction was stirred at 0°C for one hour to remove the Boc-group. The solvent was subsequently removed. 3 ml (21  $\mu$ mol B<sub>12</sub>) of the activated B<sub>12</sub> above was added. 0.6ml TEA was added. The reaction continued overnight. The reaction mixture was precipitated with DEE. Purification of the product **22** (6mg, 14%) was performed on preparative HPLC, solvent system 1, gradient 2.

<sup>1</sup>H-NMR (500 MHz, D<sub>2</sub>O, 300K):  $\delta$ : 5.85 (s, 1H), 6.33 (m, 1H), 6.59 (s, 1H), 7.01 (s, 1H), 7.31 (m, 2H), 7.41 (d, J=8.5Hz, 1H), 7.64 (m, 3H), 7.72 (m, 1H), 7.86 (d, J=8.5Hz, 1H), 7.96 (m, 2H), 8.11 (d, J=9Hz, 1H), 8.40 (d, J=8.5Hz, 1H), 8.52 (d, J=8Hz, 1H). ESI-MS: m/z=1011.9 [M+2H]<sup>2+</sup>, 2021.8 [M+H]<sup>+</sup>.

Monocarboxylic acids b (**23**), d (**24**), and e (**25**) of vitamin B<sub>12</sub> were synthesized according to a previous publication.<sup>60</sup>

#### **{b-[4-(ethylacetate)-(pyridine-2-ylmethyl)amino]-buthyl}- cyanocobalamin (26)**

To avoid the lactam formation, 94 mg **12** (258 $\mu$ mol) was deprotected from the Boc-group with 1 ml HCl 2M just before the coupling reaction. The product was liophilized and then it was mixed with 1ml TEA.

50 mg (**23**) (37 $\mu$ mol) and 83 mg TBTU (259 $\mu$ mol) in a mixture of DMF/DMSO (5:1) were added. The reaction solution was stirred for ca. 2 hours to achieve full coupling. DEE was added to precipitate the product mixture. Separation of **26** was performed on preparative HPLC, solvent system 1, gradient 1 (23.4 mg, 39%).

<sup>1</sup>H-NMR (500 MHz, MeOD, 300K):  $\delta$ : 0.39 (s, 3H, C20), 1.14 (s, 3H, C46), 1.20 (m, 3H, Pr3), 1.22 (m, 3H, CH<sub>3</sub> of PAMA), 1.31 (m, 6H, C54, C36), 1.40 (s, C47, 3H), 1.49 (m, 2H, C55, C42), 1.67 (m, 4H, 2 x CH<sub>2</sub> of PAMA), 1.83 (s, 1H, C25), 2.21 (m, 6H, B10, B11), 2.31 (d, J=8Hz, 2H, C26), 2.50 (s, 3H, C53), 2.53 (s, 3H, C35), 2.80 (m, 2H, Pr'1, C8), 3.53 (m, 1H, C8), 3.63 (m, 1H, Pr1), 3.70 (m, 1H, R'5), 3.84 (m, 1H, R5), 3.96 (s, 2H, CH<sub>2</sub>CO of PAMA), 4.03 (m, 1H, R4), 4.07 (m, 1H, C19), 4.13 (m, 1H, C3), 4.19 (q, J=7Hz, 2H, CH<sub>2</sub>O of PAMA), 4.28 (m, 1H, R2), 4.42 (s, 2H, CH<sub>2</sub>-pyr of PAMA), 5.99 (s, 1H, C10), 6.22 (d, J=3Hz, 1H, R1), 6.51 (s, 1H, B4),

---

7.08 (s, 1H, B2), 7.20 (s, 1H, B7), 7.49 (m, 1H), 7.59 (d, J= 8Hz, 1H), 7.98 (t, J=8Hz, 1H), 8.59 (d, J=5Hz, 1H). IR (KBr, cm<sup>-1</sup>): 2137. ESI-MS: m/z=802.6 [M+2H]<sup>2+</sup>.

**{b-[4-(ethylacetate)-(pyridine-2-ylmethyl)amino]-buthyl}-{cisplatinumdiammine-chloride-cyano}cobalamin (27)**

4.8 mg cisplatin (16 μmol) was mixed with 2.7mg (16 μmol) of AgNO<sub>3</sub> in 1ml H<sub>2</sub>O. The reaction was stirred at 40°C for 4 hours in the absence of light. The solution was filtered twice before 15mg (9.4 μmol) of **26** was added. The reaction was stirred at 45°C for one day. Separation of **27** was performed on preparative HPLC, solvent system 1, gradient 1 (12mg, 68%).

<sup>1</sup>H-NMR (500 MHz, D<sub>2</sub>O, 300K): δ: 6.08 (s, 1H), 6.38 (d, 3Hz, 1H), 6.51 (s, 1H), 7.09 (s, 1H), 7.31 (s, 1H), 7.64 (m, 1H), 7.74 (d, J=8Hz, 1H), 8.14 (m, 1H), 8.65 (d, J=5Hz, 1H). <sup>195</sup>Pt-NMR (107MHz, MeOD, δ in ppm): δ=-2360. IR (KBr, cm<sup>-1</sup>): 2197. ESI-MS: m/z=934.4 [M+2H]<sup>2+</sup>.

**{b-[4-tricarbonylrhenium(I)-[(N,N,O)-(ethylacetate)-(pyridine-2-ylmethyl)amino]]-buthyl}-cyanocobalamin (28)**

55mg (40 μmol) **23** in 8ml DMF was mixed with 119 μmol Boc-protected **13**. 2ml TEA was added. 62mg (193 μmol) TBTU in 5ml DMF was added. The reaction mixture was stirred at r.t. for 1h. The product mixture was precipitated upon the addition of DEE. Preparative HPLC with solvent system 1, gradient 1 were employed to purify **28** (32mg, 43%).

<sup>1</sup>H-NMR (500 MHz, MeOD, 300K): δ: 6.07 (s, 1H), 6.28 (d, J=2.5Hz, 1H), 6.59 (s, 1H), 7.14 (s, 1H), 7.25 (s, 1H), 7.55 (t, J=6.5Hz, 1H), 7.71 (d, J=5Hz, 1H), 8.08 (t, J=8Hz, 1H), 8.82 (d, J=5Hz, 1H). IR (KBr, cm<sup>-1</sup>): 1893, 1912, 2024 (CO); 2137 (CN). ESI-MS: m/z= 923.4 [M+2H]<sup>2+</sup>, 1845.7 [M+H]<sup>+</sup>

**{b-[4-tricarbonylrhenium(I)-[(N,N,O)-(ethylacetate)-(pyridine-2-ylmethyl)amino]]-buthyl}-{cisplatinum-diammine-chloride-cyano}cobalamin (29)**

7 mg (23 μmol) cisplatin was added to a solution of 3.9 mg (23 μmol) AgNO<sub>3</sub> in 1ml water. The mixture was stirred at 0°C for 4h in the absence of light. It was subsequently filtered twice. 25mg (13.6 μmol) of **28** was added to the filtrate. The reaction was stirred for one day at 45°C. Purification of **29** was performed on preparative HPLC, solvent system 1, gradient 1 (20mg, 69%).

$^1\text{H}$ -NMR (500 MHz, MeOD, 300K):  $\delta$ : 5.99 (s, 1H), 6.28 (d,  $J=3\text{Hz}$ , 1H), 6.58 (s, 1H), 7.14 (s, 1H), 7.28 (s, 1H), 7.55 (t,  $J=6.5\text{Hz}$ , 1H), 7.72 (d,  $J=7.5\text{Hz}$ , 1H), 8.11 (m, 1H), 8.83 (d,  $J=5\text{Hz}$ , 1H).  $^{195}\text{Pt}$ -NMR (107MHz, MeOD,  $\delta$  in ppm):  $\delta=-2352$ . IR (KBr,  $\text{cm}^{-1}$ ): 1897, 1911, 2025 (CO), 2196 (CN). ESI-MS:  $m/z=1055.4$   $[\text{M}+2\text{H}]^{2+}$ .

**{b-[4-tricarbonyl- $^{99\text{m}}\text{Tc}(\text{I})$ -(N,N,O)-(ethylacetate)-(pyridine-2-ylmethyl)amino]]-buthyl}-{cisplatinum-diammine-chloride-cyano}cobalamin (30)**

Compound **30** was labelled as described above for **18**.

**{d-[4-(ethylacetate)-(pyridine-2-ylmethyl)amino]-buthyl}- cyanocobalamin (31)**

When **24** was used instead of **23**, the respective product was **31**.

$^1\text{H}$ -NMR (500 MHz, MeOD, 300K):  $\delta$ : 6.01 (s, 1H, C10), 6.28 (d,  $J=3\text{Hz}$ , 1H, R1), 6.58 (s, 1H, B7), 7.11 (s, 1H, B2), 7.23 (s, 1H, B4), 7.3 (m, 1H), 7.56 (m, 1H), 7.8 (m, 1H), 8.45 (m, 1H). ESI-MS:  $m/z=1604.5$   $[\text{M}+\text{H}]^+$ , 802.7  $[\text{M}+2\text{H}]^{2+}$ .

**{e-[4-(ethylacetate)-(pyridine-2-ylmethyl)amino]-buthyl}- cyanocobalamin (32)**

When **25** was used instead of **23**, the respective product was **32**.

$^1\text{H}$ -NMR (500 MHz,  $\text{D}_2\text{O}$ , 300K):  $\delta$ : 6.05 (s, 1H, C10), 6.30 (d,  $J=3\text{Hz}$ , 1H, R1), 6.60 (s, 1H, B7), 7.35 (s, 1H, B2), 7.26 (s, 1H, B4), 7.30 (m, 1H), 7.62 (m, 1H), 7.83 (m, 1H), 8.50 (m, 1H). ESI-MS:  $m/z=802.6$   $[\text{M}+2\text{H}]^{2+}$ .

**[{cis-Pt(NH<sub>3</sub>)<sub>2</sub>-Cl}-{B<sub>12</sub>}] [CF<sub>3</sub>CO<sub>2</sub>] (33)**

480  $\mu\text{l}$  [ $^{57}\text{Co}$ ]-B<sub>12</sub> (1,75 $\mu\text{Ci/ml}$  in sodium borate buffer pH 9.6 was adjusted to pH 5-6 with TFA 5%. To this solution was added 212  $\mu\text{l}$  of freshly prepared mono-aquocisplatin 100mM. The mixture was stirred for 9.5h at 50°C. Then it was loaded on C<sub>18</sub>-ec-sepak column. The Pt-residue was washed away with water. The product was eluted with MeOH. Eluted fractions of highest  $\gamma$ -radioactivity were pooled together. 1ml of saline 0.9% was added. MeOH was then dried under N<sub>2</sub>. Comparing HPLC retention time of the product with the cold analogue **1** confirms the identity of **33**.

### VII.3 Reductive release of drug from double prodrug

The reduction of **4** (100  $\mu$ M) was monitored at -700mV in tris(hydroxymethyl)aminomethane buffer (0.2 M, pH 8, 37°C). Pt net and Pt wires were working and counter electrodes. Reference electrode was Ag/AgCl. UV-Vis spectra were recorded every thirty minutes.

In addition, **4** (8 mM) was also reduced by Zn pellets (1 g) in NH<sub>4</sub>Cl (1%) at r.t. The final product mixture was identified by ESI-MS and HPLC. Zn was filtered. The filtrate was diluted substantially into a range of concentration (10 nM-100  $\mu$ M) for cell viability assay.

## VII.4 Biological study

### VII.4.1 Binding of double prodrug 4 to human serum albumin

A mixture of 200  $\mu$ M B<sub>12</sub>-derivatives and HSA in phosphate buffer (0.1 M, pH 7.4), 0.9% NaCl was stirred at r.t. for three days. The binding process was followed by size exclusion HPLC (column 2, solvent system 2, and gradient 3). Decomposition of 4 was followed by RP-HPLC column 1, solvent system 1, and gradient 1.

### VII.4.2 Affinity of double prodrug 4 to Cbl transport proteins

DSF was applied to measure the affinity of B<sub>12</sub>-derivatives to transport proteins. DSF is a fluorescence-based method to measure protein stability and ligand-induced changes in protein stability.<sup>149</sup> Transport proteins were incubated both alone and with different ligands. B<sub>12</sub> was used as a non-selective binder and Cbi as a selective binder. Cbi binds only to HC.

Preparation of recombinant Cbl transport proteins. Recombinant human (rh) HC (rhHC) and rhIF were expressed and purified as described elsewhere.<sup>150, 151</sup> rhTC was expressed according to rhHC.<sup>151</sup> In brief, the cDNA for human TC (pCMV6-TC RC200682), OriGene, Myc-DDK-tagged ORF clone of Homo sapiens TC, NCBI Reference Sequence: NM\_000355.2, transcript variant 1 as transfection-ready DNA purchased by Origene (Lab Force, Nunningen, Switzerland) was cloned into the EcoRII/XhoI site of pcDNA4/myc-His A vector (Invitrogen AG, Basel) by standard molecular biology techniques. The primers (Microsynth AG, Switzerland) were 5'-TAATACGACTCACTATAGGG-3' and 5'-CCGCTCGAGAGATCCACGCGGAACCAGCCAGCTAACCAGCCTCAGCTC-3'. All selected clones were verified by DNA sequencing (Microsynth AG, Balgach, Switzerland). HEK293 cells were transfected using Lipofectamine 2000 (Invitrogen AG, Switzerland) following the manufacturer's instructions. Stable transfected cells were isolated and grown as described elsewhere.<sup>152</sup> rhTC was purified using a Ni<sup>2+</sup> affinity column. Absorption was carried out at r.t. with gravity flow. The resin was washed with 6 volumes of PBS, 6 volumes of PBS and 1M NaCl, and 6 volumes of PBS and 0.5M NaCl, 20mM imidazole. Elution was carried out with PBS, 300mM imidazole. The peak fractions were polished using a Superdex<sup>TM</sup> 75 10/300 gel filtration column and Äkta<sup>TM</sup> prime

system (Amersham Biosciences). Gel filtration was conducted at r.t. with a flow rate of 24 ml/h using PBS. The fractions with rhTC were then pooled and frozen at -20°C. A Rotor-Gene cycler (Rotor-Gene 5plex HRM, QIAGEN) was chosen for protein stability measurement by DSF. Stability measurements were performed in PBS. SYPRO® Orange (Invitrogen, cat. no. S6651) was used at 50x concentration. Protein concentrations were between 300-450 nM. Ligand concentrations were about 20 µM. Excessive ligand was chosen to assure that total protein was ligand-bound. Thirty-six 100 µl samples were processed in 0.5 ml PCR tubes in the 36-Well Rotor of the Rotor-Gene cycler. HRM was programmed to ramp the temperature from 25°C to 95°C. Data were collected every 0.5°C, with an equilibration time of two seconds.

---

### VII.4.3 Cell viability assay

The human chronic myelogenous leukemia (CML) K562 cell line was seeded in 96-well plates (100µl/well, 500 cells/well) and incubated (37°C, 95% air / 5% CO<sub>2</sub>) one day before treatment. Cells were maintained in RPMI 1640-medium (PAA) supplemented with 10% fetal bovine serum (PAA), penicillin (100 U/mL), and streptomycin (100U/mL) (Gibco). 100 µl of drugs at different concentrations (10nM-100µM) were added to cells the next day. Cells were incubated for four days. 20µl 0.86mM resazurin was then added to each well. Incubation was continued for four hours. Fluorescence was measured at 590 nm emission (with an excitation wavelength of 540 nm) in the SpectraMax M5 microplate reader. Cells were treated with Cyt, **4**, reduced mixture of **4**. Vitamin B<sub>12</sub>, **2**, and NH<sub>4</sub>Cl were also given to cells as control. Three experiments were performed on separate cell batches during three months.

---



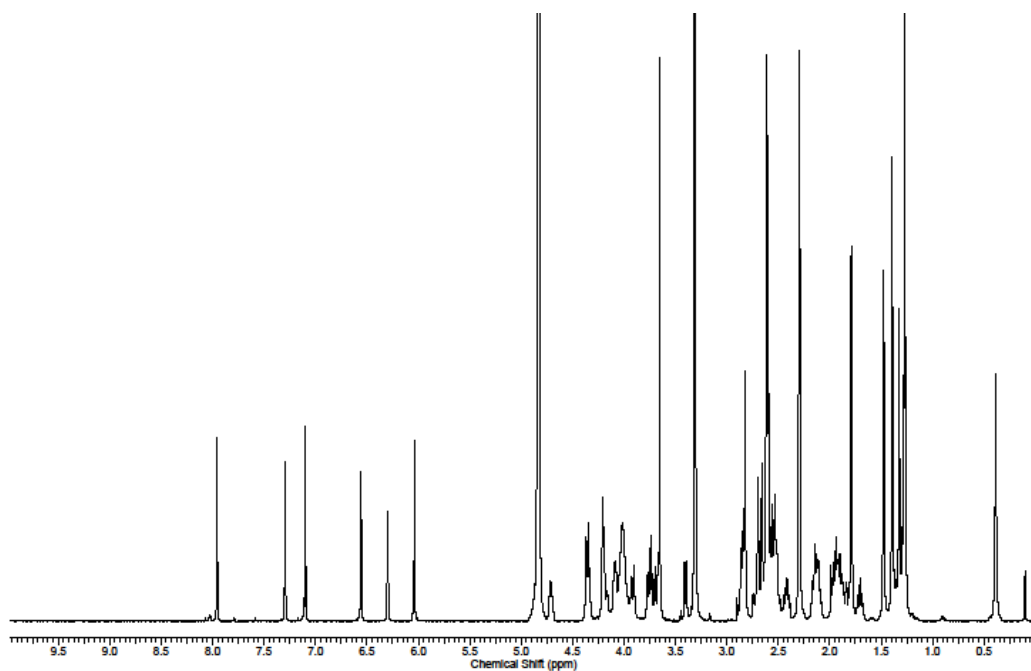
#### VII.4.4 Uptake measurement with [ $^{99m}\text{Tc}$ ]-radiolabeling

K562 cells were grown in complete media (RPMI-1640, 10% FCS). Before the assay, cells were transferred into RPMI-1640 medium depleted from B<sub>12</sub> and folic acid (Cell Culture Technologies). The medium was supplemented with 1  $\mu\text{M}$  Homocysteine and 1  $\mu\text{M}$  5-methyltetrahydrofolic acid whereas serum was not added. Two 6-well plates were required. Each well contained  $4 \times 10^5$  cells. In one plate, 3 wells were treated with (18) and the rest with (30). In the other plate, 3 wells were treated with TC-(18) and the rest with TC-(30) (2 equivalents of TC). Each well contained an amount of ca. 0.8 ng B<sub>12</sub> derivative. Subsequently, two plates were incubated for one day. Cell pellets were isolated by centrifugation (450xg, 4°C, 5 minutes). They were washed (x3) with PBS prior to measurement with a  $\gamma$ -counter.

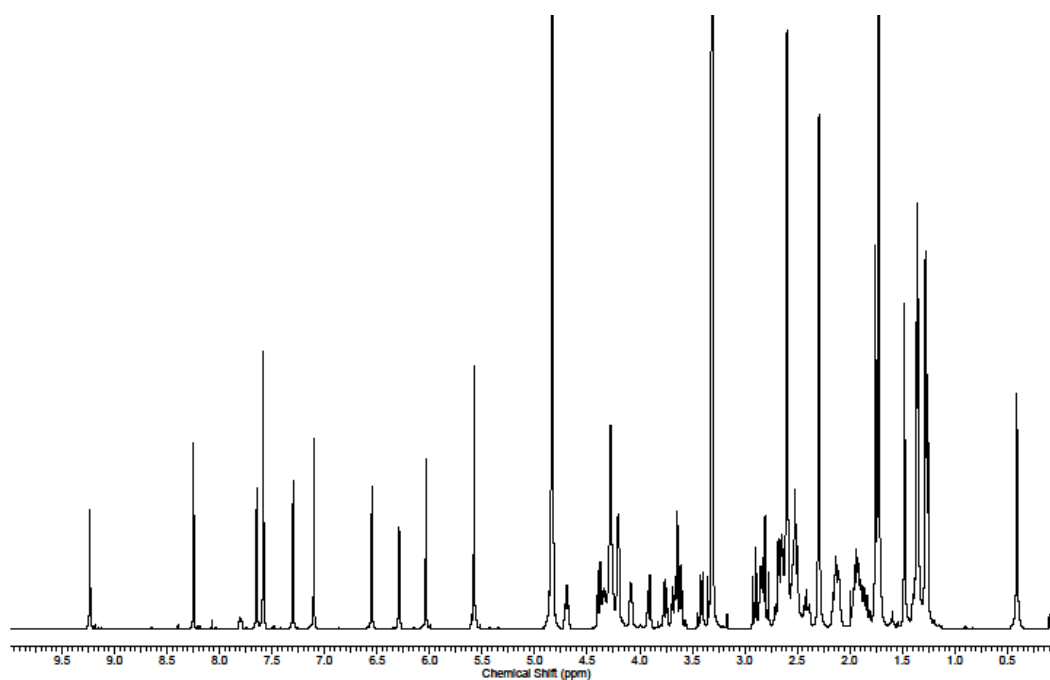
#### VII.4.5 Uptake measurement with ICPMS

K562 cells were seeded in seven T-75 flasks. The seeding density was  $3 \times 10^6$  cells/flask. The culture medium was 12 ml RPMI-1640 with 10% FCS and penicillin-streptomycin (100U/ml). After 1 day of incubation, each flask was treated with 10  $\mu\text{M}$  of a compound. These included cisplatin, B<sub>12</sub>, Cbl-OH<sub>2</sub>, **1**, **4**, and **17**. The remaining flask was not treated with any compound and served as the control sample. Cells were further maintained in culture for two days. Nucleic and cytosolic fractions were separated according to a previously published procedure with certain modifications.<sup>153</sup> In details, cells were centrifuged for 1 minute at 700xg and r.t.. The supernatant was discarded. Pellets were washed (x3) with 5ml PBS. Lysis was performed in 1 ml freshly- prepared ice-cold buffer of 150mM NaCl, 20mM HEPES buffer, 1mM EDTA, 0.5% Triton X-100, 1% protease inhibitor cocktail, 1 mM NaVO<sub>3</sub>, NaCl/ KCl (30mM/ 120mM). 20  $\mu\text{l}$  of the lysate was spared for protein determination (DC Protein Assay, Bio-Rad). The rest was centrifuged at 600xg, 4°C for 5 minutes. The pellet was washed (x3) with 1ml NaCl/ KCl (30mM/ 120mM) to isolate nuclei fraction. The supernatant was centrifuged at 5500xg, 4°C for 15 minutes. Cytosolic fraction was the supernatant part. The nuclei fractions were digested with 100  $\mu\text{l}$  concentrated HNO<sub>3</sub>. Both nucleic and cytosolic fractions were diluted 50 times for ICPMS measurement.

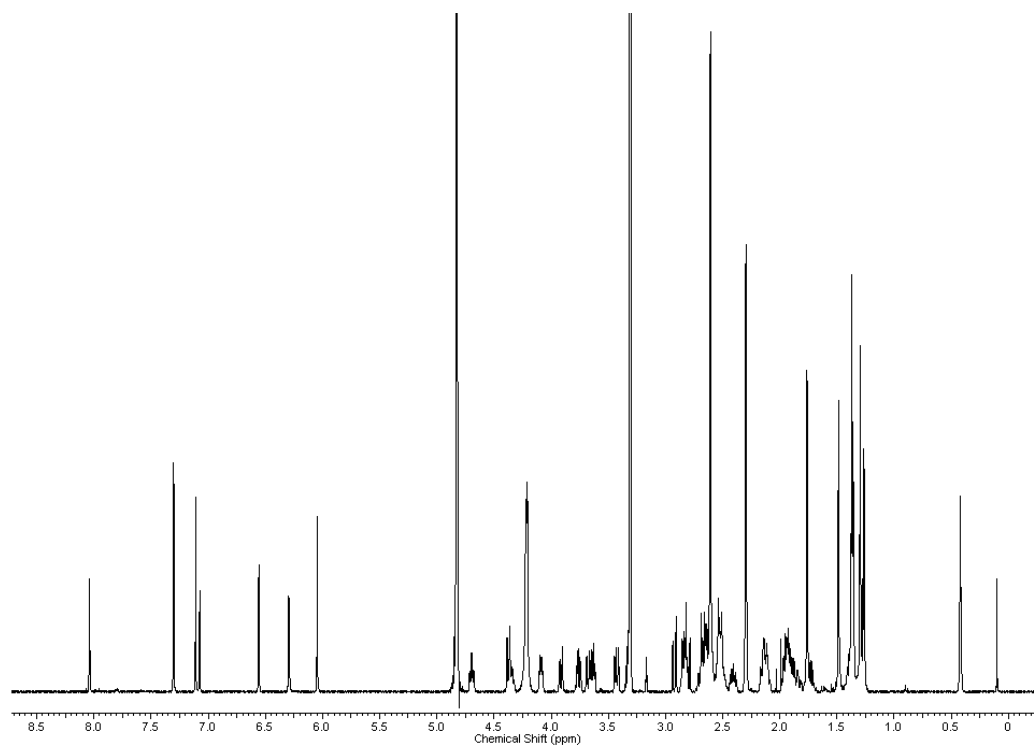
## VIII Appendices



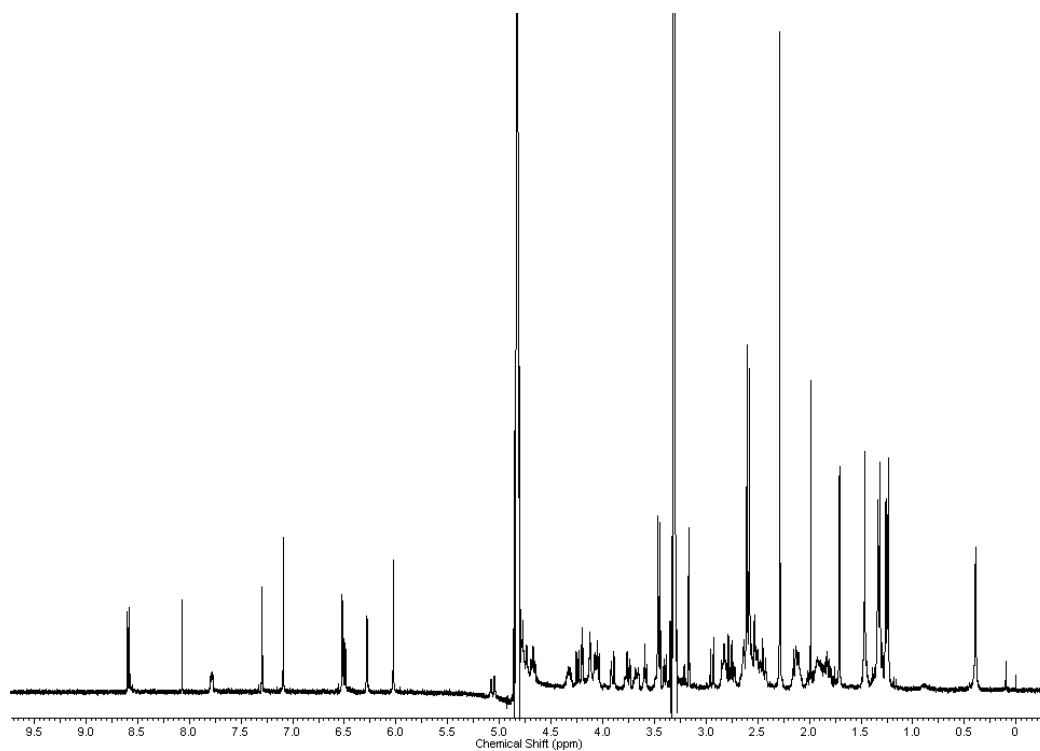
$^1\text{H}$  NMR from  $\beta$ -conjugate of  $\text{B}_{12}$  and dacarbazine **5**.



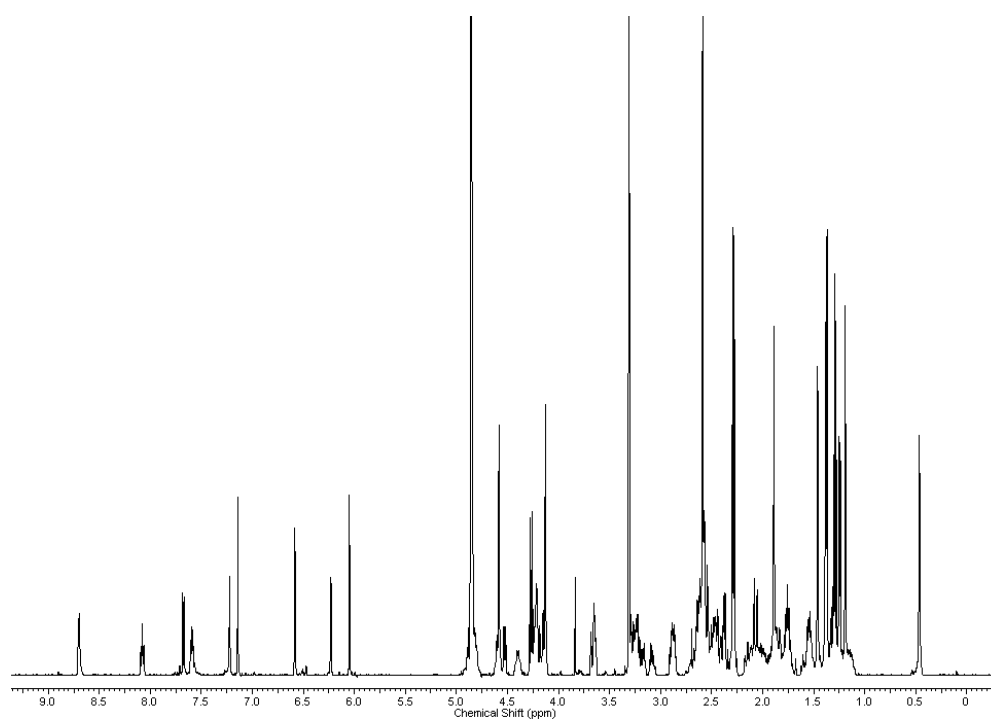
$^1\text{H}$  NMR from  $\beta$ -conjugate of  $\text{B}_{12}$  and anastrozole **6**.



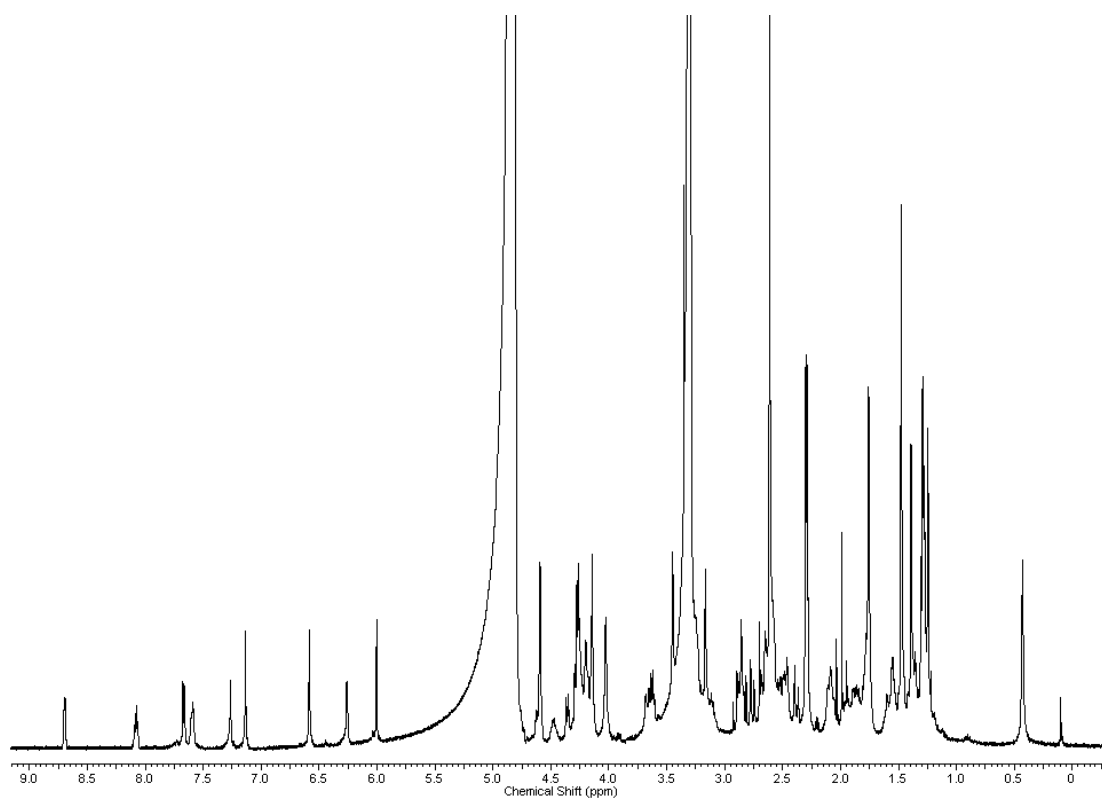
<sup>1</sup>H NMR from β-conjugate of B<sub>12</sub> and imidazole **8**.



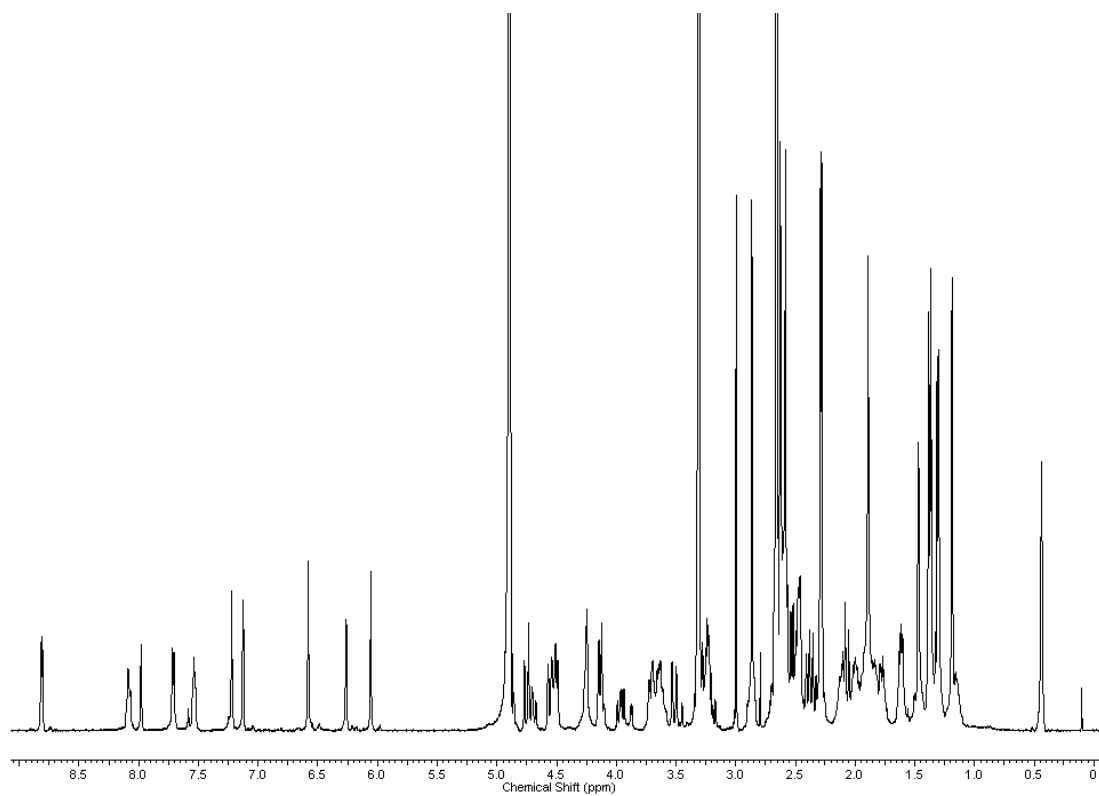
<sup>1</sup>H NMR from β-conjugate of B<sub>12</sub> and NBDCOHZ **9**.



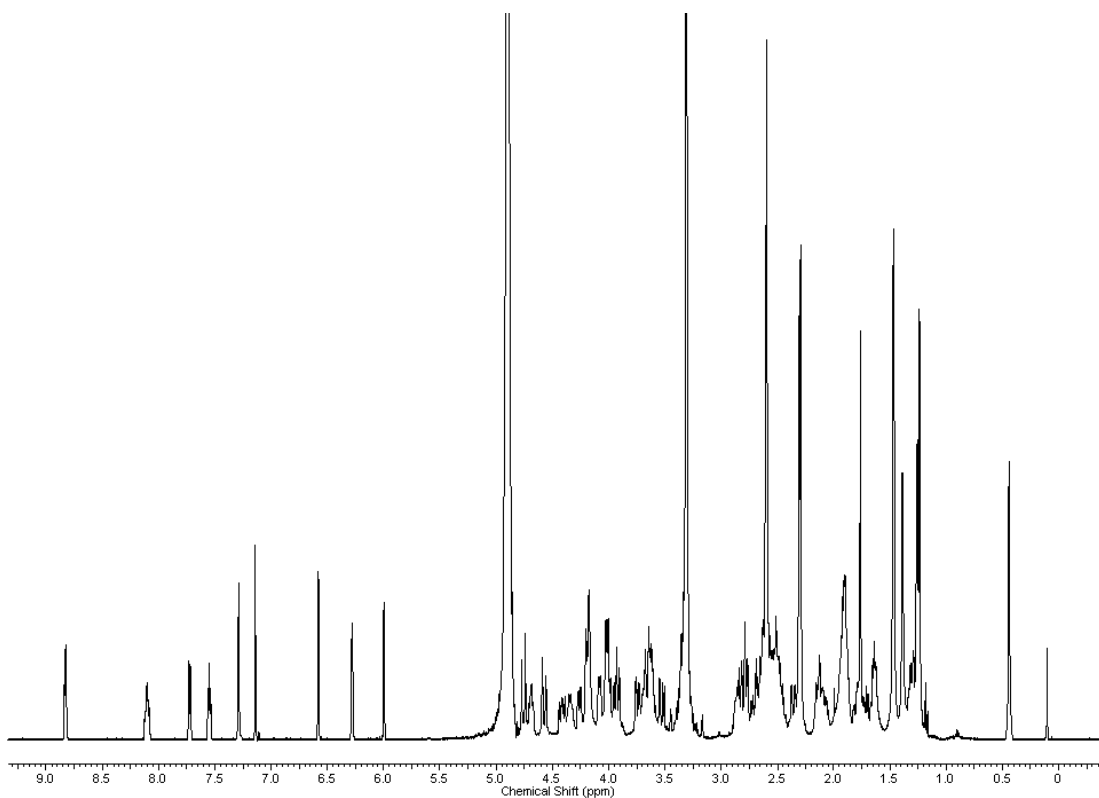
<sup>1</sup>H NMR from ribose-conjugate of B<sub>12</sub> and tridentate ligand **14**.



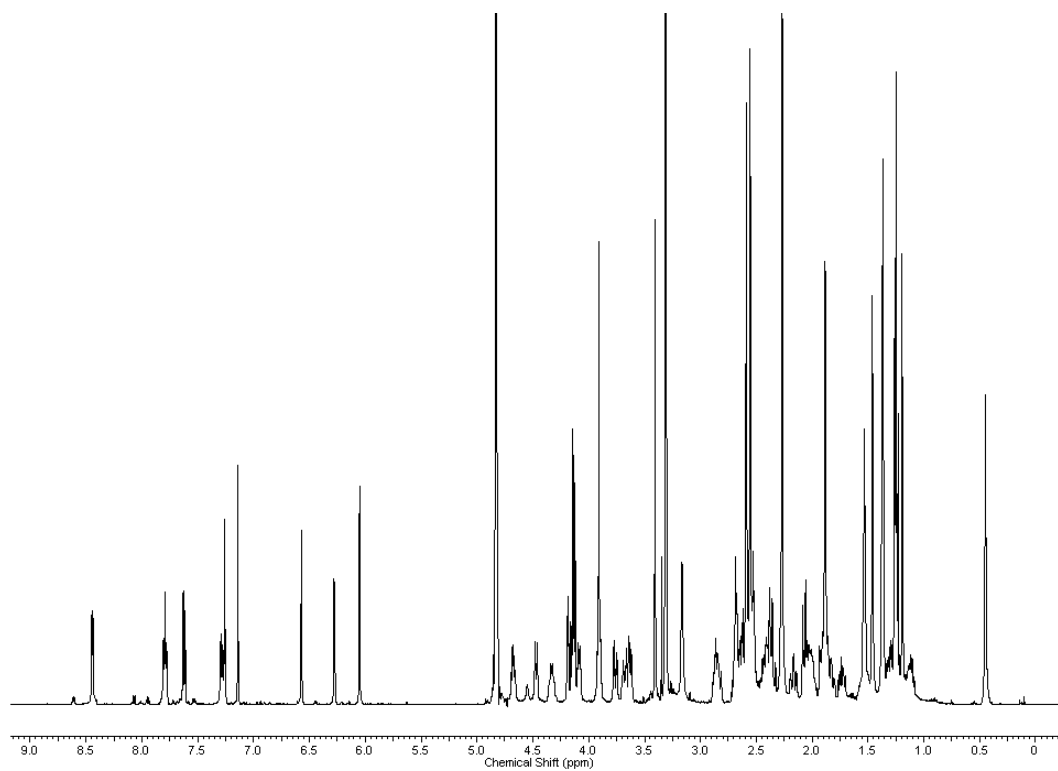
<sup>1</sup>H NMR from ribose,β-conjugate of B<sub>12</sub>, tridentate ligand, and cisplatin **15**.



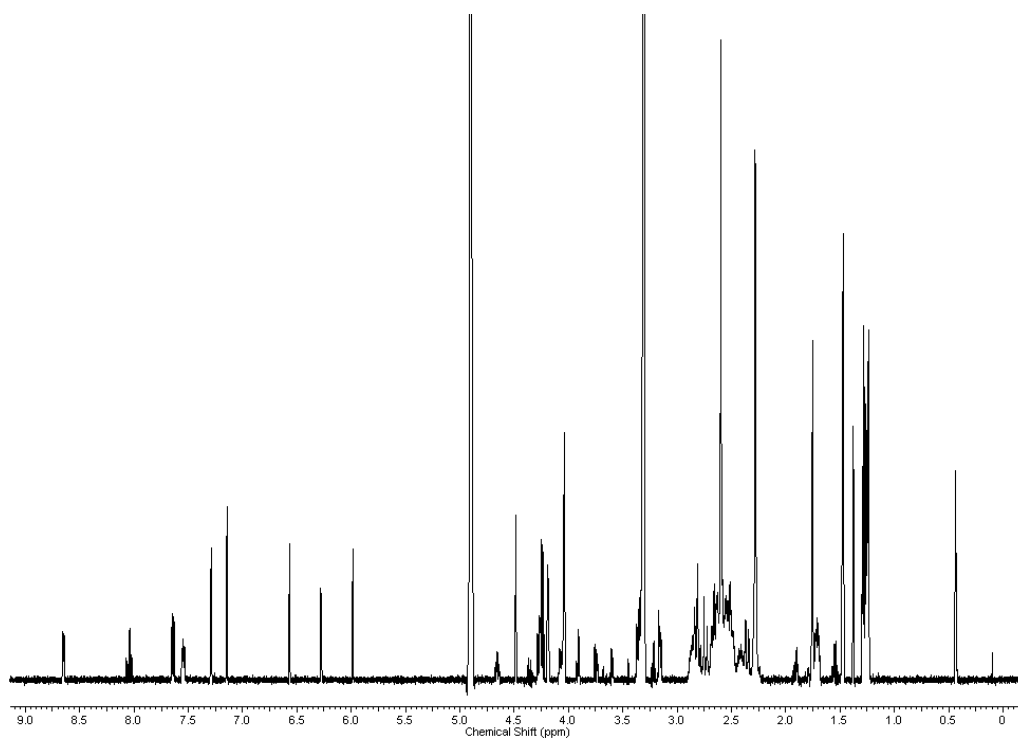
$^1\text{H}$  NMR from ribose-conjugate of  $\text{B}_{12}$  and Re-chelate **16**.



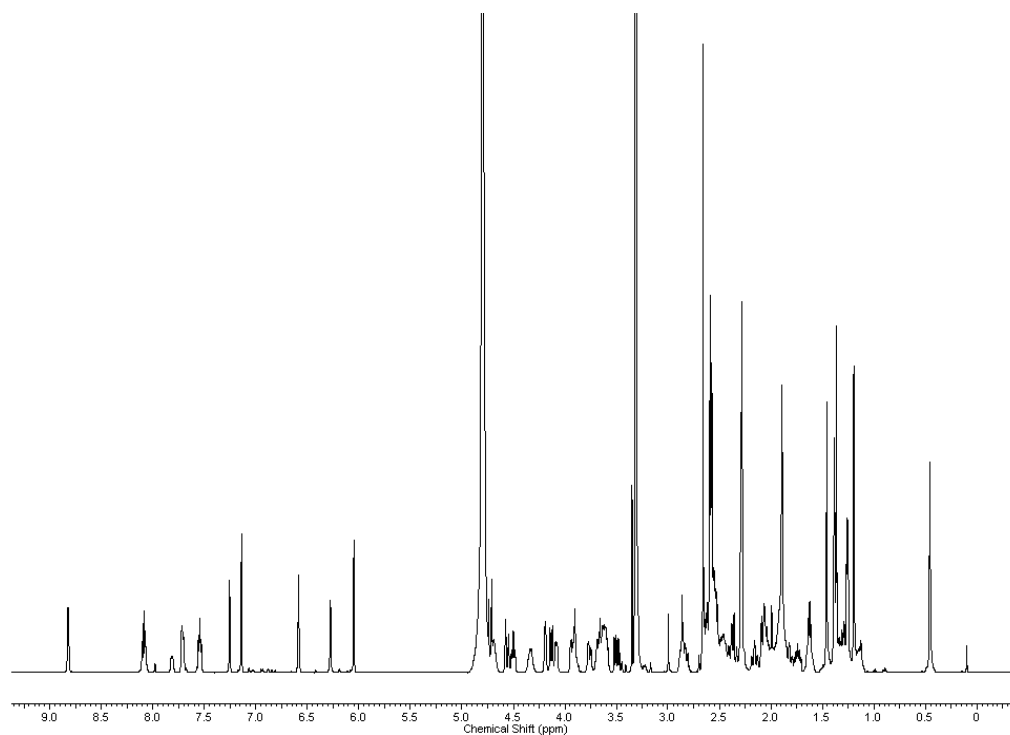
$^1\text{H}$  NMR from ribose,  $\beta$ -conjugate of  $\text{B}_{12}$ , Re-chelate, and cisplatin **17**.



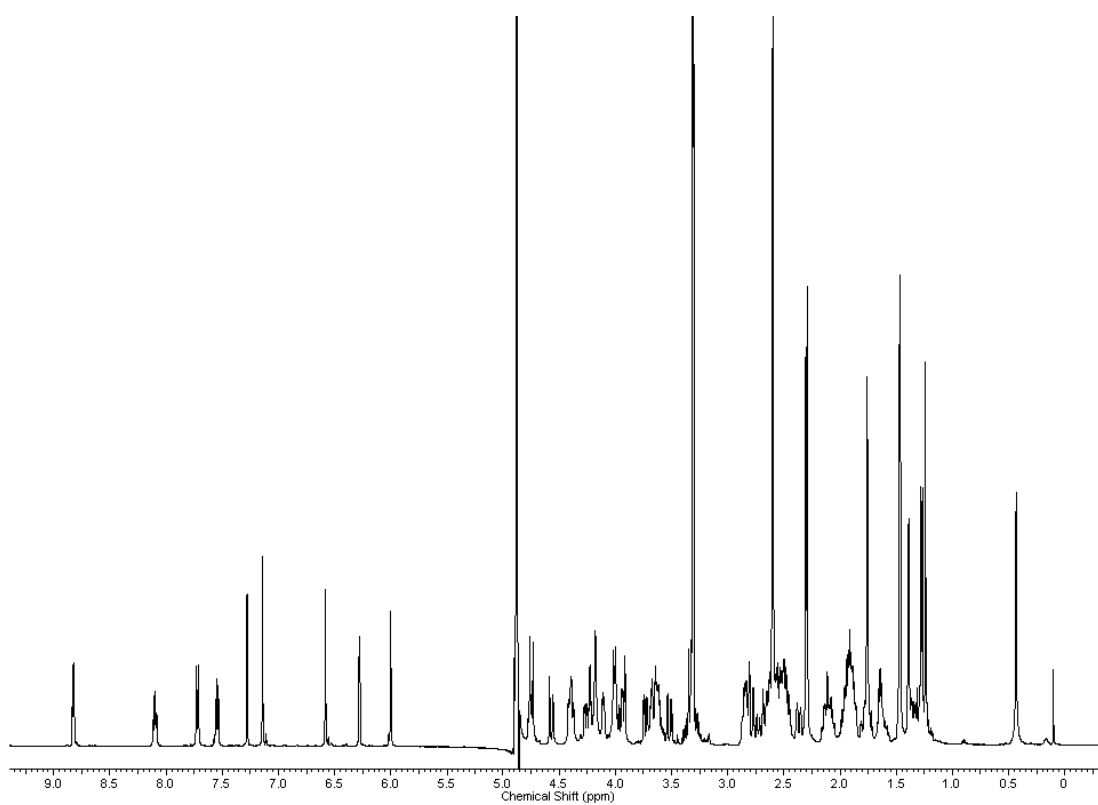
$^1\text{H}$  NMR from b-conjugate of  $\text{B}_{12}$  and tridentate ligand **26**.



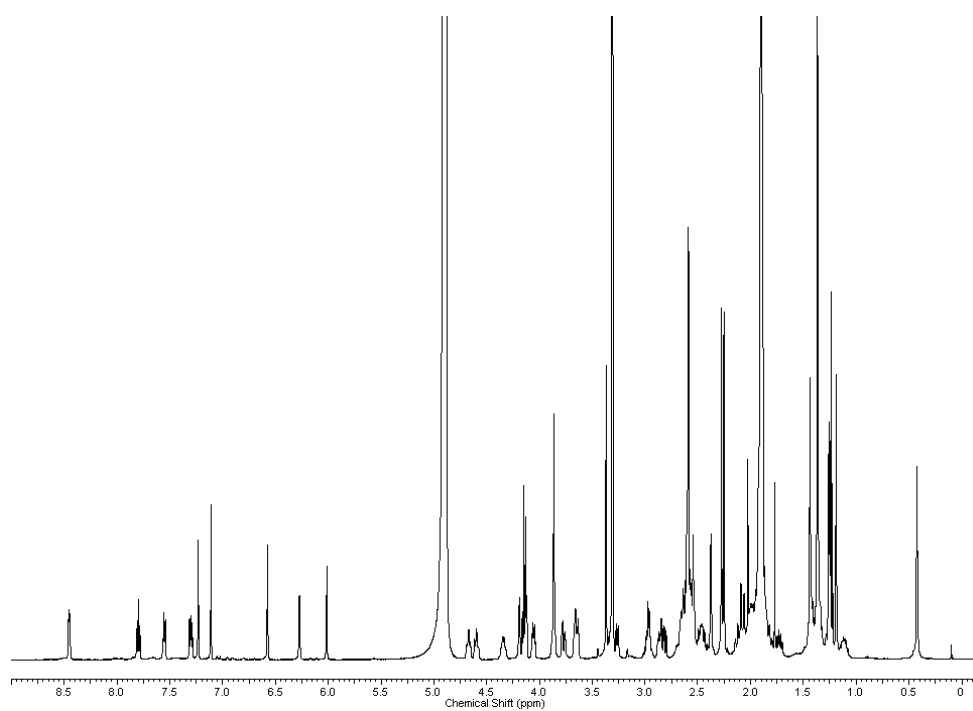
$^1\text{H}$  NMR from b, $\beta$ -conjugate of  $\text{B}_{12}$ , tridentate ligand, and cisplatin **27**.



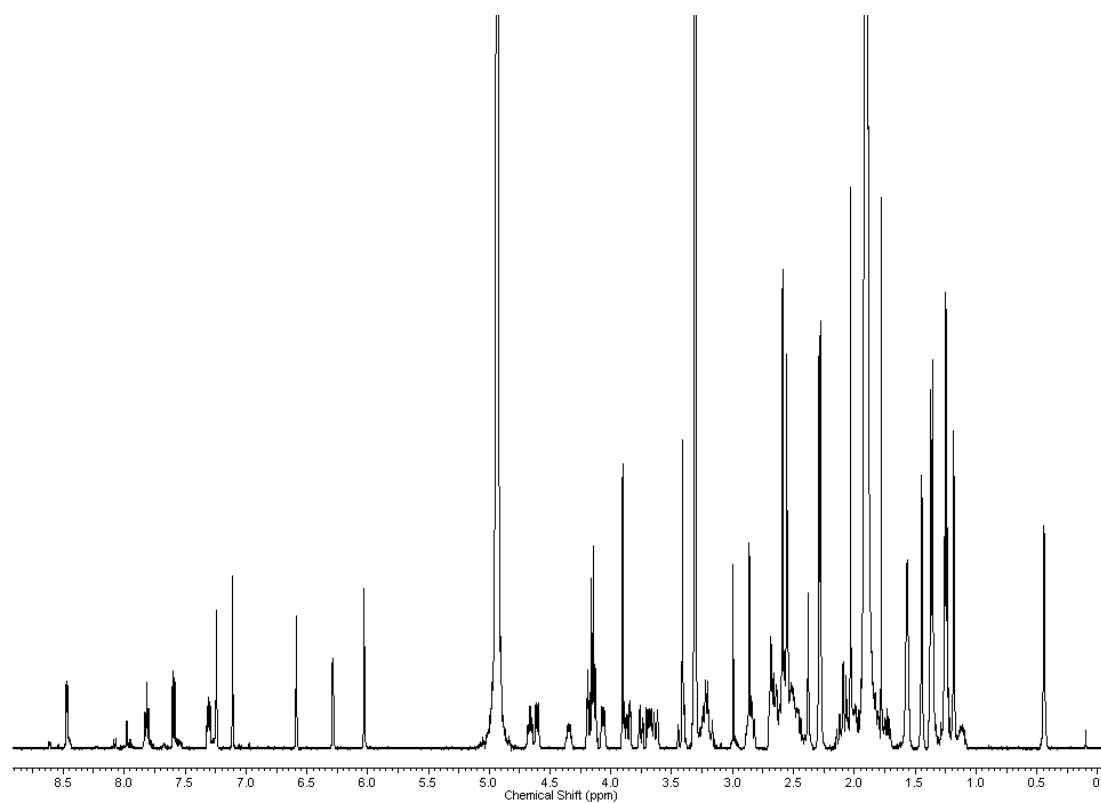
$^1\text{H}$  NMR from b-conjugate of  $\text{B}_{12}$  and Re-chelate **28**.



$^1\text{H}$  NMR from b, $\beta$ -conjugate of  $\text{B}_{12}$ , Re-chelate, and cisplatin **29**.



$^1\text{H}$  NMR from d-conjugate of  $\text{B}_{12}$  and tridentate ligand **31**.



$^1\text{H}$  NMR from e-conjugate of  $\text{B}_{12}$  and tridentate ligand **32**.



## IX Curriculum Vitae

### PERSONAL DATA

Full name        Tran Thanh Quynh-Mai  
Date of birth    31/03/1983  
Nationality      Vietnamese

### EDUCATION

2009-2013        Ph.D. Chemistry, University of Zürich, Switzerland  
                      Visiting Scholar, University of Copenhagen, Denmark (06/12, 11/11)  
                      Visiting Scholar, Paul Scherrer Institute, Switzerland (07-09/11)  
2007-2008        M.Sc. Chemistry, University of Umeå, Sweden  
2001-2005        B.Sc. Chemistry, University of Science, Vietnam  
                      Exchange student, University of Umeå, Sweden (09/04-06/05)

### PROFESSIONAL EXPERIENCE

2011-2012        Teaching assistant, University of Zürich, Switzerland  
2006-2007        Assistant Chemist, TÜV, Vietnam

### LANGUAGES

Vietnamese (native), English (fluent, IELTS 7/9), German (intermediate)

### PUBLICATIONS

Tran et al. "Increased cellular uptake of charged cobalamin prodrugs". *Manuscript*.  
Tran et al. "Two-step activation prodrugs: transplatin mediated binding of chemotherapeutic agents to vitamin B<sub>12</sub>". *Organic & Biomolecular Chemistry*, **2013**, 11, 3247-54.  
Tran et al. "Evaluation of cell lysis methods for platinum metallomic studies of human malignant cells". *Analytical Biochemistry*, **2010**, 396, 76-82.

### CONFERENCES & TALKS

2013                RheManTec Symposium (presentation), Switzerland  
2012                Guest Lecture (presentation), Department of Pharmacy,  
                          University of Copenhagen, Denmark  
2012                Advances & Controversies in B-Vitamins & Choline (poster),  
                          Germany  
2009-2012        Swiss Chemical Society Fall Meetings (posters), Switzerland